1. Report No. FHWA/TX-97/1370-3F	2. Government Accession No.	3. Recipient's Catalog No.
4. Title and Subtitle EVALUATION AND REPAIR OF IMPACT-DAMAGED PRESTRESSED CONCRETE BRIDGE GIRDERS		5. Report Date May 1996; Revised January 1997
		6. Performing Organization Code
7. Author(s) R. S. Zobel, J. O. Jirsa, D. W. Fowler, and R. L. Carrasquillo		8. Performing Organization Report No. Research Report 1370-3F
9. Performing Organization Name and Address Center for Transportation Research The University of Texas at Austin 3208 Red River, Suite 200 Austin, Texas 78705-2650		10. Work Unit No. (TRAIS)
		11. Contract or Grant No. Research Study 0-1370
12. Sponsoring Agency Name and Address Texas Department of Transportation Research and Technology Transfer Office P. O. Box 5080 Austin, Texas 78763-5080		13. Type of Report and Period Covered Final
		14. Sponsoring Agency Code

15. Supplementary Notes

Study conducted in cooperation with the U.S. Department of Transportation, Federal Highway Administration. Research study title: "Repair of Impact-Damaged Prestressed Concrete Girders"

16. Abstract

Impact damage of prestressed concrete bridge girders was studied through field inspections and laboratory tests of a damaged girder. Non-destructive techniques for evaluating the extent of damage and the quality of repairs were examined. Various materials and procedures for repairing damage to the concrete and the strands were considered.

A prestressed concrete bridge girder, damaged by impact from an overheight vehicle, was removed from a bridge in Austin, Texas. The damaged girder was transported to the laboratory for evaluation and repair. Several non-destructive methods were studied to evaluate the effectiveness of each in assessing the extent of concrete damage resulting from overheight vehicle impact. The surface hardness of the damaged girder was measured using a rebound hammer. Impact echo and spectral analysis of surface waves techniques were used to assess the extent of damage. All three methods were also used to evaluate the effectiveness of the concrete repairs that were undertaken.

Several classes of premanufactured patch materials were used to repair the damaged concrete girder. Materials consisted of cast-in-place concrete and hand-applied mortars. Cast-in-place materials were either magnesium-phosphate based or portland-cement based. The mortars were either latex-modified or fiber-reinforced, silica fume modified. Preload was applied to the girder, the damaged concrete was replaced and allowed to cure, and the preload was removed. Static loads were applied to investigate the flexural characteristics of the repaired girder.

Internal prestressing strand splice techniques were used to repair intentionally damaged strands of the same prestressed girder. Four different types of splice hardware were installed and evaluated. Each splice was tested to failure separately in a test machine to evaluate the strength and critical components of each assembly.

Finally, the results were used to suggest a procedure for rapid initial assessment of damage. The procedure should allow field personnel to distinguish between various types and locations of impact damage and to determine the course of action to be taken regarding the evaluation, repair, or replacement of an impact-damaged girder.

17. Key Words Prestressed concrete girders, impact damage, repair, evaluation	18. Distribution Statement No restrictions. This document is available to the public through the National Technical Information Service, Springfield, Virginia 22161.		
19. Security Classif. (of this report) Unclassified	20. Security Classif. (of this page) Unclassified	21. No. of Pages 209	22. Price

Form DOT F 1700.7 (8-72)   Reproduction of completed page authorized

EVALUATION AND REPAIR OF IMPACT-DAMAGED PRESTRESSED CONCRETE BRIDGE GIRDERS

by

R. S. Zobel
James O. Jirsa
D. W. Fowler
R. L. Carrasquillo

Research Report Number 1370-3F

IMPLEMENTATION

The State of Texas has a large number of prestressed concrete bridges. Impact damage occurs routinely, and may lead to serious traffic delays or detours unless the extent of the damage can be evaluated quickly and appropriate action taken to repair or replace severely damaged girders. In the past, replacement has been the preferred action, but construction costs of replacement, as well as costs of traffic interruption, may preclude replacement in all but the most severe cases.

The results obtained in this program will help personnel of the Texas Department of Transportation to assess the severity of damage and to formulate repair procedures applicable to the damage and the site. Non-destructive techniques have been evaluated and can be used to assist in assessing the severity of damage and the quality of repairs.

Prepared in cooperation with the Texas Department of Transportation
and the U.S. Department of Transportation, Federal Highway Administration

DISCLAIMERS

The contents of this report reflect the views of the authors, who are responsible for the facts and accuracy of the data presented herein. The contents do not necessarily reflect the official views or policies of the Federal Highway Administration or the Texas Department of Transportation. This report does not constitute a standard, specification, or regulation.

There was no invention or discovery conceived or first actually reduced to practice in the course of or under this contract, including any art, method, process, machine, manufacture, design or composition of matter, or any new and useful improvement thereof, or any variety of plant, which is or may be patentable under the patent laws of the United States of America or any foreign country.

NOT INTENDED FOR CONSTRUCTION,
BIDDING, OR PERMIT PURPOSES

James O. Jirsa, P.E. (Texas No. 31360)
David W. Fowler, P.E. (Texas No. 27859)
Ramon L. Carrasquillo (Texas No. 63881)
Research Supervisors

TABLE OF CONTENTS

LIST OF FIGURES

LIST OF TABLES

SUMMARY

Impact damage of prestressed concrete bridge girders was studied through field inspections and laboratory tests of a damaged girder. Non-destructive techniques for evaluating the extent of damage and the quality of repairs were examined. Various materials and procedures for repairing damage to the concrete and the strands were considered.

A prestressed concrete bridge girder, damaged by impact from an overheight vehicle, was removed from a bridge in Austin, Texas. The damaged girder was transported to the laboratory for evaluation and repair. Several non-destructive methods were studied to evaluate the effectiveness of each in assessing the extent of concrete damage resulting from overheight vehicle impact. The surface hardness of the damaged girder was measured using a rebound hammer. Impact echo and spectral analysis of surface waves techniques were used to assess the extent of damage. All three methods were also used to evaluate the effectiveness of the concrete repairs that were undertaken.

Several classes of pre-manufactured patch materials were used to repair the damaged concrete girder. Materials consisted of cast-in-place concrete and hand-applied mortars. Cast-in-place materials were either magnesium-phosphate based or portland-cement based. The mortars were either latex-modified or fiber-reinforced, silica fume modified. Preload was applied to the girder, the damaged concrete replaced, allowed to cure, and the preload removed. Static loads were applied to investigate the flexural characteristics of the repaired girder.

Internal prestressing strand splice techniques were used to repair intentionally damaged strands of the same prestressed girder. Four different types of splice hardware were installed and evaluated. Each splice was tested to failure separately in a test machine to evaluate the strength and critical components of each assembly.

Finally, the results were used to suggest a procedure for rapid initial assessment of damage. The procedure should help field personnel distinguish between various types and locations of impact damage and to determine the course of action to be taken regarding the evaluation, repair, or replacement of an impact-damaged girder.

CHAPTER 1

1.1 INTRODUCTION

A special type of damage to prestressed concrete bridge structures is caused by the impact of over-height vehicles and loads. In 1979, the National Cooperative Highway Research Program sponsored Project 12-21 "Evaluation of Damage and Methods of Repair for Prestressed Concrete Bridge Members". The main focus of Project 12-21 was first to identify and quantify the number of occurrences of damage to prestressed concrete bridge structures and to identify the methods of assessment and repair that were being used. Secondly different methods of correcting structural damage were to be investigated. A survey of the state departments of transportation in the United States and of the provinces of Canada determined that nearly 200 bridges were damaged per year and 80% of the damage occurred as a result of over-height vehicle impact (26, 27). Since the findings of this research were published, very little other research has been performed that is directly concerned with over-height vehicle impact. However, technological advances in nondestructive evaluation techniques and development of new repair materials and methods since the 1979 study can be used for the assessment and repair of impact damage of prestressed bridge members and provide an impetus for the study reported herein.

In 1992, the reusability and impact damage repair of twenty-year-old prestressed concrete bridge girders was studied at the University of Minnesota. Full-scale specimens were subjected to fatigue test programs in order to investigate the fatigue life of repaired girders. Analytical methods were also developed to evaluate the fatigue life of girders containing repaired prestressing tendons. Two different repair methods were studied: 1) internal strand splices, and 2) external post-tensioning. Both of these repair methods were found to be very sensitive to fatigue loading. Due to the repetitive nature of highway and railroad bridge loading it was recommended that these methods be used only to provide durable repairs by introducing precompression into the repaired zones in order extend the usable life of the structure, not to restore ultimate strength to a damaged member (22). When the remaining cross section and loss of prestressing reinforcement are not sufficient to provide the required ultimate strength of the member, it was recommended that repairs should not be used to increase the ultimate load capacity of the member due to the sensitivity to repetitive loading.

In 1992, Project 1370 ("Repair of Impact Damaged Prestressed Concrete Bridge Girders") was initiated. In the first phase of this research project, a comprehensive survey of damage occurrence and current practice in the assessment and repair of impact damaged girders was conducted. In the 12 to 15 years that have lapsed since Project 12-21 was completed, the occurrence of impact damage within the state of Texas alone has risen to 241 incidences over a five-year period, or approximately 50 incidences per year (12). Several categories were established to classify the severity of impact damage to bridge members as defined below:

Minor Damage - concrete cracks, nicks, shallow spalls, and scrapes

Moderate Damage - large concrete cracks and spalls, exposed undamaged tendons

Severe Damage - exposed and damaged tendons, loss of significant portion of concrete section, distortion or misalignment of the girder (12).

From the survey that was conducted during the first phase of Project 1370, Figure 1-1 compares the incidence of impact damage within the state of Texas to damage occurrences in all other surveyed states and provinces. In all, 241 girders were damaged within Texas during the five-year period and 1008 girders were damaged in all other participating states and provinces. Texas accounts for approximately one-fifth of all surveyed damage, reflecting both the large number of lane miles of highway in Texas as well as the high percentage of prestressed bridge girders used on the Texas highway system (12).

Figure 1-1   Impact damage between 1987 and 1992

The second phase of Project 1370, which is the subject of this report, involved laboratory and field investigations to examine several nondestructive assessment techniques, the use of several proprietary patching materials for repairing concrete damage, and methods of repairing damage to prestressing strands. Based on survey results, nondestructive techniques are very seldom used in assessing the extent of damage that occurs as a result of vehicle impact. Figure 1-2 reveals that visual observation is, in most instances, the preferred method of assessing the extent of damage due to vehicle impact. The ratio of using visual observation to nondestructive assessment methods was exactly the same for the state of Texas as for all other surveyed states and provinces. It is evident that utilization of nondestructive evaluation is not the preferred method of damage assessment. However, as technological advances in nondestructive assessment are continually being made, new techniques might be more useful where they may not have been in the past not only for initial damage assessment, but also for evaluating the quality of the repairs that are performed.

1.2   OBJECTIVES AND SCOPE OF INVESTIGATION

The overall research objectives for the investigation of repair of impact damaged prestressed bridge girders are:

1. To survey types of damage and repair techniques undertaken by the Texas Department of Transportation. Report 1370-1 provides a detailed description of the results of the survey that was conducted during the first phase of Project 1370.

Figure 1-2   Field procedures used to determine extent of damage

2

2. To develop procedures for estimating the degree of damage to girders and to assess the strength and expected performance of a bridge containing damaged and/or repaired elements. The evaluation procedure includes consideration of current nondestructive techniques which can provide data necessary for conducting analytical studies prior to making a decision regarding repair or replacement. Report 1370-2 provides information pertaining to nondestructive techniques that have been used in the past to evaluate loss of prestress as well as the development of a new method which could also be used to monitor the stressing of strands during repair.

3. To develop repair procedures which do not impair the appearance, durability, or maintenance of the bridge.

4. To develop procedures for field implementation of evaluation and repair techniques which seem most promising.

This report concerns the final phase of laboratory and field investigations performed for this project. Included for background purposes only are brief descriptions of current materials and techniques for repairing damage to both concrete and prestressing strands, as well as a brief overview of some of the many nondestructive techniques that are available for evaluating material quality in concrete structures.

CHAPTER 2

DESCRIPTION OF IMPACT DAMAGE

2.1 PROBLEM DESCRIPTION

As a result of vehicle impact, damage can occur to concrete, prestressing strands, and ordinary reinforcement. The damage to concrete is usually characterized by one or more of the following: small nicks and scrapes, small and large fractures, spalled regions, delaminated zones, crushed areas, and large loss of concrete section. When concrete is damaged, prestressing strands and ordinary reinforcement can be exposed to the elements, and to corrosion. Individual wires on strands could be nicked, the strand could yield during impact, or even completely sever, reducing the strength and stiffness of the girder.

It is important to determine the extent of the damage so that a proper assessment of the structure can be made. For the sake of standardizing the assessment procedure, several categories have been established to classify the severity of impact damage to bridge members as defined previously and repeated below (12).

Minor Damage - concrete cracks, nicks, shallow spalls, and scrapes

Moderate Damage - large concrete cracks and spalls, exposed undamaged tendons

Severe Damage - exposed and damaged tendons, loss of significant portion of concrete section, distortion or misalignment of the girder

Several girders can be damaged in the same structure when an over-height vehicle or load strikes a bridge. One or more of the damage classifications can be seen in a damaged structure. In addition to the above damage classifications, there is another possibility; complete collapse of a structure due to impact. Collapse of the structure precludes repair; however, it does help to convey the magnitude of the problems associated with over-height vehicle impact. In order to provide the reader with a better perspective of the occurrence and extent of impact damage, the following sections describe several damaged structures in the state of Texas.

2.2 SITE INVESTIGATIONS

Several damaged bridges were visited to gain better insight to the type and severity of damage resulting from over-height vehicle impact. Three different bridge structures were visited with damage ranging from minor to total collapse.

2.2.1 Damaged Bridge Structure at College Station, Texas

In early 1993 a bridge in College Station, Texas was damaged by over-height vehicle impact. The bridge carries traffic on FM 60 over FM 2818; the posted minimum vertical clearance of 15 ft. 8 in. (4.78 m) occurs at the northern exterior girder, and increases to 16 ft. 3 in. (4.95 m) at the center of the bridge. A

schematic of the transverse section of the bridge is shown in Figure 2-1 along with a girder numbering scheme used for inspection purposes. In April of 1993 the research team visited the site and found that seven girders were damaged as a result of impact from an unknown vehicle traveling north under the bridge.

Visual inspection revealed that the first girder struck was the southern exterior girder (girder 1 in Figure 2-1). The damage to girder 1 was classified as moderate; the spalled region along the lower flange was approximately 2 ft. (0.61 m) long, cracking extended into the web of the member, and approximately 10 in. (0.25 m) of prestressing strand was left exposed. A small piece of metal was embedded between two wires of the seven wire strand (refer to Figure 2-2), however, inspection of the strand indicated no apparent damage to the strand. The second girder was not damaged, girders 3 and 4 sustained several nicks and scrapes, classified as minor damage. Girders in the center portion of the structure were not damaged due to the increased vertical clearance at these locations.

Girders 11 through 14 were also damaged from the impact. The damage to girder 11 consisted of a 1 ft. (0.30 m) spalled region as well as evidence of cracking extending into the web on the nonimpacted side of the girder. One tendon was exposed in this region for approximately a 6 in. (0.15 m) length as shown in Figure 2-3. The damage sustained by girder 12 consisted of a 6 ft. (1.83 m) length of lost cover on the impacted face and exposure of two tendons as shown in Figure 2-4. Girder 13 also sustained damage similar to girder 12; a 6 ft. (1.83 m) spalled region as well as evidence of cracking extending outward from the spalled region and an 18 in. (0.46 m) length of three exposed undamaged tendons as shown in Figure 2-5. Girder 14, the exterior north side girder, sustained damage resulting in exposure of three tendons over a 2 ft. (0.61 m) length as well as an extensive region of side cover concrete splitting over an 11 ft. (3.35 m) length as shown in Figure 2-6. The damage sustained by girders 11 through 14 was classified as moderate, since exposed tendons appeared to not have been damaged by the impact.

2.2.2 Bridge Superstructure Collapse at Interstate Highway-35 and County Road 312, Jarrel, Texas

In April of 1995, impact of an over-height vehicle caused total collapse of a single span of the superstructure of a four-span, simply supported bridge structure. The bridge carried County Road 312

Figure 2- 1   Transverse section of College Station Bridge

Figure 2- 2   Girder 1 — College Station Bridge

Figure 2- 3   Girder 11 — College Station Bridge

Figure 2- 4   Girder 12 — College Station Bridge

Figure 2- 5   Girder 13 — College Station Bridge

Figure 2- 6   Girder 14 — College Station Bridge

over Interstate Highway 35 (IH-35) near Jarrell, Texas. An elevation and transverse section of the structure is shown in Figures 2- 7 and 2-8, indicating the approximate location of impact. The boom of a truck-mounted crane loosened during transit causing the crane arm to rise upwards as the truck traveled north on IH-35. As a result, the overall height of the vehicle increased above the minimum vertical clearance of the bridge structure without the knowledge of the driver and resulted in impact.

In order to lend perspective to the collapse, both the collapsed and remaining spans are shown in Figure 2-9 viewed from the south. Closer inspection of the collapsed span revealed that as the vehicle impacted the structure, all of the supporting girders were completely sheared off at the upper flange-web interface thereby destroying all structural support for the deck as shown in Figure 2-10. Further inspection revealed that the impact and collapse of the span caused misalignment of other sections of the structure as evidenced by rigid body rotation of the adjacent spans. This was clearly observed at the joints between spans. The joint width between railings of adjacent spans on one side was found to be narrower than on the opposite side. Figure 2-11 shows one joint on the south side of the bridge, while the north side of the same joint is shown in Figure 2-12.

As the structure collapsed, it dropped and lodged against the center pier structure as seen in Figure 2-13. Closer inspection of the columns at the center of the bridge revealed extensive damage . The bottom of one column sustained a shear failure through the entire cross section as shown in Figure 2-14, and at mid-height of another column flexural cracking occurred as shown in Figure 2-15. Shoring was placed beneath the intact structure near this damaged support until repairs could take place in order to stabilize the structure.

9

Figure 2- 7   Evaluation of bridge structure at Jarrell, Texas

Figure 2- 8   Transverse cross section of bridge at Jarrell and IH-35

Figure 2- 9   Southern view of collapsed structure at Georgetown, Texas

Figure 2- 10   Loss of structural support for superstructure at Georgetown, Texas

Figure 2- 11   South side of joint in railing — Georgetown collapse

Figure 2- 12   North side railway joint — Georgetown collapse

Figure 2- 13   Shear failure of column due to impact of falling structure

Figure 2- 14   Lodging of collapsed structure against central pier

Figure 2- 15   Flexural cracks at mid-height of supporting column

The collapse of this bridge and the extent of the damage that resulted to the remaining portions of the structure provide vivid evidence of the possible severity and consequences of over-height vehicle impact. Lives were endangered during the collapse. The crane vehicle passed completely underneath the structure prior to collapse; however, an automobile struck the collapsed bridge head-on just after the superstructure fell. Had the truck been moving at a slower speed or the automobile been traveling at a higher speed it is possible that either or both vehicles and their occupants could have been crushed beneath the structure. The disruption to traffic flow due to the collapse was also of concern; therefore, by the day after the accident, all debris was cleared from the roadway, the remaining structure stabilized, and the highway was opened to traffic.

2.2.3   Damaged Bridge Structure at Waelder, Texas over Interstate Highway 10

In February of 1993 a bridge over Interstate Highway 10 (IH-10) near Waelder, Texas was struck by a vehicle with an over-height load traveling west. As-built drawings in Appendix B indicate that the structure was built in 1969 and consists of exterior spans 65 ft. (19.8 m) long and interior spans 95 ft. (29 m) long and at a 5 ° 30 ' right forward skew angle. A schematic of the bridge elevation and transverse section of the structure are shown in Figures 2-16 and 2-17, respectively.

Figure 2- 16   Elevation   of   Waelder Bridge over I-10

Girders 1, 2, and 4 were damaged, with the most severe damage at girder 1. Impact occurred near the north strand draping location at the hold-down point. Four tendons were completely severed by the impact and almost all of the remaining strands in the section were exposed over approximately a 16 ft. (4.88 m) length just south of the centerspan location as shown in Figures 2-18 and 2-19. The damage to girder 1 was classified as severe.

Figure 2- 17   Transverse   section   of Waelder Bridge over I-10

The second girder also sustained damage as evidenced by cracking of the concrete extending outward from the point of impact on the bottom flange as shown in Figure 2-20. It appeared that the south diaphragm served as a reaction point for the transverse impact load as evidenced by the path that the cracking of the section followed: outward from the point of impact, down the side of the bottom flange, and across the bottom surface of the girder to the nonimpacted face near the diaphragm location. Since there did not appear to be any damage to tendons or loss of prestress, the damage sustained by girder 2 was classified as moderate. The damage that occurred to girder 4 consisted of several scrapes and spalled areas and was classified as minor damage. The extent of the damage to girder 4 can be seen in Figure 2- 21.

2.2.3.1 In-Situ Nondestructive Load Testing of Waelder Bridge

The Waelder bridge is symmetric with respect to both interior and exterior spans and is used very little (refer to Figure 2-22). On the south side of the bridge there is a small structure which is load rated for

Figure 2- 18   Impact damage of Girder 1 — Waelder Bridge

Figure 2- 19   Close-up view of damaged strands of Girder 1 — Waelder Bridge

Figure 2- 20   Damage to Girder 2 — Waelder Bridge

Figure 2- 21   Damage to Girder 4 — Waelder Bridge

16

Figure 2- 22   Superstructure of Waelder Bridge

very light vehicles; therefore use of the Waelder bridge is limited to automobiles, light trucks, and farm vehicles. As such, it presented an excellent opportunity to study the effects of overheight vehicle impact damage by in-situ nondestructive load testing. The load-deflection response of both the damaged and the undamaged spans could be directly compared due to the symmetry of the structure; both interior spans have the same dimensions. The differences in load-deflection response of the two identical interior spans were studied in order to evaluate the overall effects of impact damage.

Load Test Vehicle

In order to perform in-situ load tests, a vehicle slightly longer and heavier than an HS-20-44 design vehicle was used (Refer to Figure 2-23 for description of standard American Association of State Highway and Transportation Officials (AASHTO) HS-20-44 design vehicle) (28). Prior to placing the test vehicle on the bridge, each axle was weighed, the individual axle loads were recorded, and the total vehicle weight was determined. A schematic of the test vehicle showing individual axle loads, number and location of wheels and axles, and gross loaded vehicle weight is shown in Figure 2-24 for comparison to standard H-20-44 design vehicle. The test vehicle was provided by the maintenance division of the Texas Department of Transportation in Gonzalez County and was loaded with dense fill material.

The front axle of the test vehicle weighed 11,900 lb. (52,933 N) and the combined weight of the rear axles was measured to be 41,560 lb. (184,868 N) which was assumed to be distributed evenly between the two rear axles; the combined weight of front and rear axles measured 53,460 lb (237,800 N). The gross vehicle weight was also measured and determined to be 53,510 lb. (238,024 N), a negligible difference of 50 lb. (222 N).

17

Figure 2- 23   Schematic of AASHTO H-
                20-44 design vehicle

Figure 2- 24   Test vehicle for in-situ load
                testing of Waelder Bridge

Instrumentation of Waelder Bridge

In order to evaluate the overall effects of the damage, deflections at the quarter points and midspan locations for each span were measured by two different methods. In the first method, two automatic levels located at opposite ends of the loaded span were used for measuring differences in elevation as load was applied to the structure; however, the precision and repeatability of measurements by this method was found to be insufficient for the purposes intended. Measurements taken by level, therefore, will not be presented.

Deflections were also measured using a taut piano wire stretched across the interior spans along the sidewalls of the superstructure. Both interior spans were loaded and deflections were measured by using scales graduated in 0.01 in. (0.25 mm) increments. The concept is simple; as load is applied to the bridge between supports, the profile of the wire remains unchanged while the profile of the bridge deflects (Figure 2-25). The scales were mounted over mirrors so that readings would be made at right angles to the scale thereby reducing errors in measurements due to parallax (Figure 2-26). The two wires were attached to the sidewalls at the north end of the north span and at the south end of the south span by means of an angle bulkhead fitted with an eye bolt used to apply tension to the wire as shown in Figure 2-26. The wire was supported as shown in Figure 2-27 in between the interior spans over the central pier to reduce vibration from wind.

Displacements using the stretched wire method were measured only along the siderails, not directly over each girder. It would have been possible to place wires longitudinally over each girder as well as transversely across the bridge to develop a displacement contour for the entire bridge; however, placement of so many wires would have made movement of the test vehicle very difficult, if not impossible, and would have required that the bridge be closed to traffic. For this reason only the side displacements were measured for each span. A plan view of the two interior spans locating instrumentation, girders, and sidewalls is shown in Figure 2-28.

18

Figure 2- 25 *Wire displacement measurement con-*
cept for in-situ load tests of Waelder
Bridge

Once instrumentation for displacement measurements was in place, zero readings were taken at each scale location. The test vehicle was weighed as previously mentioned and the stationary test positions for the vehicle were marked on the bridge deck. In order to locate the vehicle, overall dimensions of the test vehicle were measured and are shown in Figure 2-29. Vehicle test positions for the north interior span are shown in Figure 2-30 and in Figure 2-31 for the south span. The vehicle was placed in four symmetric locations on the damaged span and in two symmetric locations on the undamaged span. Four locations were used for the damaged span in order to determine if the load-deflection response was unsymmetrical due to the severity and unsymmetrical location of the damage. On the undamaged span, however, only two vehicle test locations were needed for comparison purposes.

Results of In-Situ Load Test - Waelder Bridge

The measurements taken for all six vehicle positions (four for the north span and two for the south span), are shown in Figures 2-32 through 2-37.

Concerning only the damaged span (north interior span), several observations can be made about the results of the in-situ load testing. The most interesting observation is that very little difference in centerspan displacement was observed for the different vehicle locations (load tests 1 through 4). The magnitude of this displacement ranges from 0.21 in. (5.3 mm) to 0.22 in. (5.6 mm). Since the most severe damage occurred for girder number 1 just north of centerspan, it might be expected that the centerspan displacement would be largest for load tests 2 and 4. This is not the case, as is shown in Figures 2-33 and 2-35. There was very little difference in the load-deflection response at centerspan even though the damage was much more severe on the east side at girder 1. Comparing the displacements at the north and south quarter points, again very little difference in response was measured when the load was placed at the northwest and southwest locations (load tests 1 and 3, Figures 2-32 and 2-34, respectively). However, when the vehicle was placed at the northeast and southeast locations (load tests 2 and 4, Figures 2-33 and 2-35, respectively), there does appear to be a slight unsymmetric response with respect to the quarter point displacements, a maximum difference of 0.02 in. (0.51 mm). When the load was placed at the southeast location (load test #2, Figure 2-33) the displacement at the northeast quarter point was observed to be larger than at the southeast quarter point where the load was located. It appears that the unsymmetric nature of the observed displacements is consistent with the

Figure 2- 26   *Angle bulkhead for tensioning piano wire and mirrored scale for displacement measurement*

Figure 2- 27   *Interior support for piano wire displacement measuring device*

Figure 2- 28 Plan and transverse sections of Waelder Bridge showing locations for deflection measurements

Figure 2- 29 Overall dimensions for load test vehicle — Waelder Bridge load test

In-Situ Load Test of Damaged Interior North Span - Waelder Bridge

Test # 1

2 ft. 7 in. (0.79 m)

Test # 3

Test # 2

N

4 spaces @ 23 ft. 9 in. (7.24 m)

Test # 4

8 ft. 2 in. (2.49 m)

Test Vehicle Shown In Fourth Position - All Positions Are Symmetric
Locations 1 and 2 Vehicle Faces South
Locations 3 and 4 Vehicle Faces North

Figure 2- 30   Vehicle test locations for damaged north interior span — Waelder Bridge

In-Situ Load Test of Undamaged Interior South Span - Waelder Bridge

2 ft. 7 in. (0.79 m)

Test # 1

N

4 spaces @ 23 ft. 9 in. (7.24 m)

Test # 2

8 ft. 2 in. (2.49 m)

Test Vehicle Shown In Second Position - All Positions Are Symmetric
Locations 1 and 2 Vehicle Faces North

Figure 2- 31   Vehicle test locations for south interior span — Waelder Bridge

In-Situ Load Test # 1- Interior North Span - Waelder Bridge

Figure 2- 32   Results of north span Load Test #1 — Waelder Bridge

In-Situ Load Test # 2- Interior North Span - Waelder Bridge

Figure 2- 33   Results of Load Test #2 — Waelder Bridge

In-Situ Load Test # 3- Interior North Span - Waelder Bridge

Figure 2- 34   Results of Load Test #3 — Waelder Bridge

In-Situ Load Test # 4- Interior North Span - Waelder Bridge

Figure 2- 35   Results of Load Test #4 — Waelder Bridge

In-Situ Load Test # 5 - Interior South Span - Waelder Bridge

Figure 2- 36   Results of Load Test #5 — Waelder Bridge

In-Situ Load Test # 6 - Interior South Span - Waelder Bridge

Figure 2- 37   Results of Load Test #6 — Waelder Bridge

unsymmetric nature and location of the damage; the girder that was most severely damaged was girder 1 and this damage occurred north of centerspan where the observed quarter point displacements were largest. It should be noted, however, that the measured displacements were on the order of 1/5000th of the span, well within acceptable limits for servicability and functionality of the structure even in the damaged state.

Comparison load tests performed on the undamaged south interior span revealed that a very slight difference in response was evident. The maximum centerspan displacement measured on the undamaged span was 0.16 in. (4.1 mm), compared to the displacement of the damaged span of 0.22 in. (5.6 mm), a difference of 1/16th inch. To summarize the results of the in-situ load tests performed on the Waelder Bridge, it is apparent that although severe damage occurred as a result of vehicle impact, the overall servicability of the structure remained intact, and therefore repairs could be performed to extend the service life of the structure.

2.3 STECK GIRDER DAMAGE, REMOVAL, AND REPAIR

An exterior girder of a prestressed concrete railroad bridge in Austin, Texas, was struck and severely damaged by an unknown overheight vehicle or load (Figure 2-38). The girder was eventually removed and replaced. Although the damage did not threaten the integrity of the bridge, the girder provided an excellent specimen for investigating assessment and repair techniques in the laboratory on field damage. The girder was removed from the south span of a two-span simply supported bridge which carries the Missouri Pacific Railroad over Steck Avenue in Austin, Texas.

Structural as-built drawings of the superstructure of the Steck Avenue bridge which were obtained from the Texas Department of Transportation and are included in Appendix A. In order to remove the girder, a pneumatic hammer was used to break through the slab along its length. The side railing and supporting slab were also removed, all attached reinforcement was cut to free the girder, and it was then lifted from the bridge with a crane. The cross section remaining after removal from the structure is shown in Figure 2-39. It was transported to Ferguson Structural Engineering Laboratory at the University of Texas at Austin.

Once the girder was removed and brought to the laboratory, visual observations were made and research plan was devised. Laboratory investigations were divided into three phases to address different areas related to impact damage: 1) assessment of damage, 2) concrete repair, and 3) strand repair.

Figure 2- 38   Transverse section of Steck Bridge structures

Damage Assessment

The assessment phase consisted of using nondestructive techniques of varying complexity to locate and characterize the extent of damage to the concrete. Based on the interpretation of tests, the flexural and

Dimensions of Birder Section Removed From Steck Bridge

Girder Dimension	Inches	Centimeters
A	18	45.72
B	7	17.78
C	5.5	13.97
D	2.75	7
E	14	35.56
F	5.75	14.61
G	6	15.24
H	18	45.72
I	12	30.48
J	14	35.56
K	8	20.32
L	7.5	19.05

Figure 2- 39   Girder cross section after removal from Steck Bridge

shear strengths of the member were assessed. Analytical methods were used to evaluate the structural behavior of the damaged girder, and nondestructive load tests were then performed.

Concrete Repair

During the concrete repair phase several classes of patching materials were applied to damaged areas of the girder. Low pressure epoxy injection was used in conjunction with cast-in-place and hand-applied repairs. In order to evaluate the quality of the repairs, the same nondestructive methods were used. Nondestructive testswere run after the concrete was patched, after injection with epoxy, and after the repair was complete. Following repair, static load tests were conducted to assess the performance of the repair by measuring the girder stiffness and tendon deformations. The measured values were then compared to those of the damaged girder and theoretical values for an undamaged girder. Proprietary overhead and vertical, non-sag patch materials were used to evaluate the effectiveness of a pull-off test for compliance or prequalification of field repairs. Materials were applied to a concrete substrate in varying thickness both vertically and overhead. Pull-off tests were then performed on the patch materials to quantify interfacial bond strength.

Prestressing Strand Repair

Following the concrete repair studies, strand splice investigations were undertaken. Tendon damage was simulated by intentionally severing strands in the bottom flange of the girder. Repair of the girder was accomplished by internal strand splice techniques. In a series of tests each of four identified splice assemblies was installed, the strands retensioned, and the girder load tested for comparison with original (post-concrete repair) condition. Splice performance was evaluated based on ease of installation and tensioning, reliability of installation, time required for installation, ability to restore nearly full prestress to the repaired strand, and ability of repair to restore the girder to near original condition. A final repair of the girder was also performed which consisted not only of repairing the damaged strands, but also repairing the concrete that

was removed to expose the strands. After splicing the severed strand, the concrete was replaced using a cast-in-place, rapid-setting, proprietary patch material, and remaining cracks or voids were injected with epoxy.

The four splice assemblies were also evaluated for their respective ultimate load carrying capacities by static load testing each to failure in tension. Each assembly was used to splice together two pieces of prestressing strand, and the entire specimen then loaded in direct tension. The failure mode and ultimate strength were used to evaluate the performance of each splice.

CHAPTER 3

EVALUATION AND REPAIR OF DAMAGED PRESTRESSED CONCRETE GIRDERS

3.1 INTRODUCTION

In order to determine the most effective method of repairing impact damage to both concrete and prestressing strands, it is important to recognize that there are many different repair methods, and also many evaluation techniques, as well as an abundance of different materials that can be used. In this chapter the characteristics of some materials and methods that have been used to repair impact damaged members are described. Several different methods of evaluating both damaged and repaired concrete are discussed.

3.2 METHODS USED TO REPAIR IMPACT DAMAGE TO CONCRETE

Loss of prestressing force occurs during impact by severing of strands or single wires of strands, by yielding of strands, and/or by loss of concrete in the precompression zone. Loss of prestress results in lower stiffness, lower strength, and higher stress ranges in remaining strands. There are several methods which can be used to strengthen a prestressed girder with tendon damage, however, only those methods that restore prestress will be considered.

External Post-Tensioning

One of the most obvious and widely used methods of strengthening structures is by the addition of external post-tensioning. Post-tensioning can be accomplished using prestressing tendons or high strength steel bars. Transfer of prestress force occurs through the addition of concrete or steel corbels placed along the sides or above the bottom flange of an I-shaped girder. An example of this type of repair is shown in Figure 3-1. While the method may not be as desireable for aesthetic reasons as internal strand splices, the integrity of a damaged member can be restored, and the patched zone is subjected to compression to provide a more durable repair. External strengthening procedures were described in the NCHRP report on Project 12-21(26, 27).

Internal Strand Splices Combined with Application of Preload

Internal strand splices that enable restressing of the damaged strand at the splice location restore prestress to the member internally (Figure 3-2). However, unlike external post tensioning, the material used to repair the surrounding damaged concrete will not be compressed. By using a combination of internal strand splice techniques along with application of preload to the structure, it may be possible to restore prestress both internally and to the patch material. The concept of preloading prior to repair is shown schematically in Figure 3-3. By applying dead weight to the structure, or preloading,

Figure 3-1 *Repair of impact-damaged prestressed girder by external post-tensioning*

Figure 3-2 *Repair of impact damage using internal strand splices*

compression on the concrete in the precompressed tensile zone is relieved, cracks open, and tension in tendons below the centroid of the section increases. A patch material can then be allowed to cure while the preload is applied. When the preload is removed after the repair material has cured, the new patch will be precompressed, improving the durability of the repair by reducing cracking under traffic load or shrinkage of the repair materials.

Figure 3- 3   Example of applying preload to damaged girder to produce durable repair

Concrete Repair Methods

The repair of damaged concrete can be accomplished in many different ways. The most common method is to place formwork around the damaged zone, and cast new concrete in place. An example of a cast-in-place repair is shown in Figure 3-4. The damaged material is removed, the remaining concrete surface cleaned, and forms placed around the damaged area. Patch material is then placed from above and must be adequately consolidated to ensure proper filling of voided areas. Another repair method that makes use of forms is to preplace aggregate into the formed areas and pressure grout the repair. An example of this type of repair is shown in Figure 3-5. The main advantage of pressure grouting is that interior voids will be filled more effectively than with cast-in-place methods as the nature of this type of repair may involve small, narrow regions that are difficult to fill using vibration. A disadvantage of the method is the large amount of grout required to fill the large voids which may have a lower modulus and strength. If a polymer grout is used, it may significantly increase the coefficient of thermal expansion.

As an alternative to cast-in-place or pressure grouting methods of repair, concrete materials can also be pneumatically applied. This can be done with either high pressure application such as shotcreting, or it can be performed with low pressure application of the patch material. The main advantage of either of these methods is that overhead work can be performed quickly and easily without the use of formwork.

Figure 3- 4   Cast-in-place repair of impact-damaged concrete girder

29

Figure 3- 5   Repair of impact-damaged girder by pressure grouting with or without preplaced aggregate

Patch materials can also be formulated for hand application on vertical and overhead surfaces without the use of formwork. Most of the materials used for this type of application are commonly known as non-sag repair mortars. These will be discussed in greater detail in the following sections. The greatest advantage of using a non-sag repair material is that forms do not have to be erected, and the materials can be placed by hand-packing or with a trowel. However, these materials do have practical limitations on the thickness of the patch that can be repaired.

Low viscosity epoxy can be used to inject cracks and fractured zones within damaged areas. This is accomplished by either high or low pressure injection. In order to inject epoxy into cracks in concrete, injection ports are placed at the surface or internally, the crack is sealed at the surface, and the epoxy is injected from the low to the high point as shown schematically in Figure 3-6.

When undertaking any repair using one or a combination of the methods described, it is important to evaluate the extent of damage and also have a means of evaluating the quality of the repair that was undertaken. The following sections describe different strength assessment and condition assessment techniques.

3.3 CONCRETE EVALUATION METHODS

Evaluation of concrete in a damaged structure can be performed to assess the strength or condition of the original concrete, or it can be used for quality assurance or compliance purposes after repair. Whatever the reason for evaluation, nondestructive or destructive techniques can be utilized. The following sections describe some of the more common strength and condition assessment techniques.

3.3.1   In-Situ Strength Assessment of Concrete

In-situ strength assessment of concrete has been performed by both destructive and nondestructive methods. The simplest and

Figure 3- 6   Schmatic of epoxy injection using internal and surface mounted injection ports

30

Figure 3- 7   *Schematic of surface hardness testing of concrete using a rebound hammer*

probably most traditional method is to remove a core of the concrete from the structure and test it for compressive or splitting tensile strength. Coring is costly and time consuming. In the case of prestressed concrete there may be very little possibility of removing a core without severing tendons or other reinforcement. An indirect method of evaluating the compressive strength of concrete is by measuring the surface hardness. Two of the more common surface hardness tests are the Rebound Number of Hardened Concrete (ASTM C805) (5) and the Penetration Resistance of Hardened Concrete (ASTM C803)(5).

Surface Hardness Procedures for Compressive Strength

A rebound hammer (Figure 3-7) is a simple device that quantifies the surface hardness of concrete. As the instrument is pushed against the concrete surface, an internal compressed spring is released imparting a known or fixed amount of energy to a sliding mass. This mass glides along a guide bar and strikes the plunger which is in contact with the concrete surface. As the mass strikes the plunger, it rebounds along the slide bar a certain measurable distance, and this distance is recorded as the rebound number. In this application the rebound number gives an indication of the strength or soundness of the material being sampled.

Surface Hardness by Penetration

Figure 3- 8   *Schematic of surface hardness testing of concrete using penetration resistance*

The penetration resistance test quantifies the surface hardness by using a standardized powder charge and gun to fire a probe into the concrete. The penetration of the probe is then measured (Figure 3-8) and the depth of penetration is correlated with the compressive strength of the concrete.

Both surface hardness methods are very simple and take very little time to perform or interpret the results. The amount of damage to the concrete surface may be significant with the penetration resistance test if the probe must be removed from the concrete. The rebound hammer leaves only a small, barely noticeable circular indentation on the surface. The ASTM specification for both methods state that neither should be used in place of normal methods of strength determination, but rather to assess damage, deterioration, or changes of the structure. With respect to impact damage, the rebound hammer appears to be a simple, relatively quick method of globally

assessing the extent of damage from impact and identifying areas of damage that may require more detailed investigation.

Bond Tests

In order to evaluate the tensile strength of the bond between a repair material and the original concrete substrate, in-situ bond strength tests can be performed. There are two simple bond tests: the pull-off and the push-off tests.

Figure 3- 9   Schematic of pull-off bond strength tests by direct tensionz

Pull-off tests (11) can be performed a variety of ways. In the case of quantifying bond strength between a repair material and original concrete, the test is performed in one of two ways. One method is to core through the patch material into the original concrete to isolate the test core from the surrounding concrete as shown in Figure 3-9. A hydraulic or mechanical apparatus then pulls the core in tension to break it away from the concrete. The force required to pull-off the core is measured. Another method is to preplace a ring into the patch material down to the bonding surface to isolate the sides of the core from the surrounding material as shown in Figure 3-9. The specimen is then pulled from the surface as before and the force required to fail the interface is measured. An indirect method of determining tensile or bond strength is to apply torque to the sample from the surface (Figure 3-10). The torque required to break the sample from the surface is a function of the tensile or bond strength.

The push-off or flexural test (11) test is similar to the pull-off, but direct tension is not used to break the sample from the substrate. For in-situ testing a core can be drilled into the concrete surface and the opening at the top widened to accept a loading device. The core is loaded transversely near the top and the resulting flexural tensile stress at the base eventually leads to failure (Figure 3-10). This test can also be used for evaluation of bond between two materials by coring to the interface between the two materials.

3.3.2 In-Situ Condition Evaluation of Concrete

Sounding Methods

The simplest form of evaluating near surface damage to concrete structures is by sound. Striking the concrete surface with a hammer will produce a hollow or blunt sound if there a shallow delamination.

Figure 3- 10   Schematic of torque bond test and push-off flexural bond test

Another means of globally assessing part of a structure such as a bridge deck is by dragging a heavy chain across the surface. Again, near surface damage will result in a different sound than when the chain is dragged over undamaged areas. Both of these methods are very simple and provide enough information to determine if there are other areas that may require more detailed investigation. One step above these simple sounding methods would be to globally investigate near surface damage using the rebound hammer as mentioned earlier.

Wave Propogation Techniques

In contrast to the simple tests already described, there are sophisticated techniques based on the principles of wave propagation through elastic solids. Some techniques introduce sound into the test object and then record the resulting echo of the signal. These echoes, when interpreted, reveal information about the condition of the object. An example of this type of test procedure is the Pulse Velocity through Concrete test (ASTM C597)(5).

Although ultrasonic pulse velocity (UPV) has been used for strength assessment, it is considered to be a viable method to detect cracks and voids and for estimating the thickness of concrete elements (4). The method is fast, straightforward, and not expensive to perform. High energy ultrasonic sound is introduced into the concrete specimen using a pulse generator and a transmitter (Figure 3-11). Using a time measurement and display device the amount of time for the sound wave to travel from the transmitter, through the specimen, to the receiver is recorded. In order to test concrete which has a rough, porous surface, a coupling agent must be applied to provide acoustic coupling between the receiver/ transmitter and the concrete. Using the known thickness of the specimen and the time of travel, the wave velocity can be calculated and related to the compressive strength. For evaluation purposes, the transit time can be measured at an undamaged location, and compared to transit times at other locations to detect voids, cracks, and other defects or

Figure 3- 11   Schematic of ultrasonic pulse velocity tests of concrete

Energy Source

Signal Analyzer

―――― Propogation of stress wave

∧⁄ Surface Wavefront

Figure 3- 12   Schematic of concrete evaluation by spectral analysis of surface waves

damage.   For quality assurance measures, the method can also be used to monitor filling of cracks and voids in concrete (4).

Another wave propagation technique is that of Spectral Analysis of Surface Waves (SASW). Surface velocity measurements have been used extensively in geotechnical engineering. However, SASW has also been shown to be an effective means for flaw detection in concrete members (13).   In SASW testing, energy is imparted to the surface by impact, and receivers record particle motion in the time domain (Figure 3-12). An exponential window is typically applied to each time record in order to attenuate later arriving reflected energy in contrast to the direct arrival of surface wave energy (7). Fourier analysis is used to transform each windowed record to the frequency domain where the phase difference between the receivers is determined at each frequency. Phase differences are used to calculate surface wave velocities as a function of frequency, and wavelength is the velocity divided by the frequency. A dispersion curve of surface wave velocity versus wavelength is then constructed and used to evaluate the quality of the concrete.

impact device

Induced stress wave   ―――

Reflected wave   ‑‑‑‑‑‑

Figure 3- 13   Schematic of concrete evaluation by the impact ech method

The impact-echo technique of flaw detection is a nondestructive, noninvasive method whereby cross-sectional vibration characteristics of an object can be used as an indication of the material quality or soundness. A mechanical impactor strikes the test object introducing a stress wave that propagates through the material.   As the waves are reflected from surface boundaries, and/or internal cracks and flaws, they travel through the material back to the impacted surface.   Here they are again reflected, resulting in a transient stress wave that reverberates back and forth within the test object (Figure 3-13). This vibration results in small displacements of the surface of the object which are recorded and analyzed to give an indication of the condition of the material from which the object is made.

The compression wave velocity for the selected member must first be determined by sampling an area of the structure that is known to be sound and where the thickness of the element can be measured. Using the known thickness and measured dominant frequency, the wave velocity can be determined. Once the compression wave velocity for the material has been determined, damaged zones can be evaluated by

sampling the impact-echo response, measuring the dominant frequency of the vibration, and determining the thickness of the member or the depth to a crack or void.

Another method of evaluating the condition of a structure is by Acoustic Emissions(AE). Acoustic sensors are placed on a structure, and by monitoring the strength of the acoustic signals at various stages of the loading history, the condition of the structure can be analyzed. In this way the onset of cracking can be determined as well as differences in response to load application over time. It appears that AE could be used for monitoring the long-term performance of new or repaired structures by taking periodic AE measurements and comparing changes of the AE signals over time.

Selection of Procedures

There are many different types of evaluation techniques ranging from very simple to extremely complex, and methods at each end of the spectrum have advantages as well as inherent problems. Care should be taken that the correct method is chosen for the intended application. For example, when evaluating the extent of damage that a prestressed concrete bridge girder sustains from a vehicle impact, extremely detailed information may not be required in order to assess the reduction in load carrying capacity of the member. In this instance it may not be warranted or even cost effective to carry out a detailed condition assessment of the structure, but rather a global assessment to determine which areas might require more detailed investigation. In any event, there are so many different types of nondestructive tests available, that care needs to be exercized in selecting the right tool for the right job. Factors that may influence the decision to use one method over another include cost, amount of time required to perform the test, the reliability with which data can be obtained, the amount of detailed information that is needed, and familiarity with the test method.

3.4 MATERIALS FOR REPAIRING DAMAGED CONCRETE

Not only are the cause and extent of damage important to ascertain prior to choosing a material for repair, but the application and service conditions for the repair must also be determined. Once the application and service conditions have been determined, a material can be chosen to fit the conditions of the intended repair. However, there are so many different types of materials available, some knowledge is required in order to choose the best material for the intended application. First of all, the desirable material characteristics for a repair project should be known. Table 3-1 lists some of these characteristics (6, 15, 19, 23, 33, 36).

Patch materials fall into two major categories, cementitious and polymeric. These groups can be further subdivided. Cementitious materials use either a portland cement base or a magnesium phosphate base as a binder in concrete or mortar products. Polymer materials, on the other hand, generally use either an acrylic monomer or an epoxy as the binder and are known more typically as polymer concrete or polymer mortar.

3.4.1 Cementitious Patch Materials

Portland cement-based patch materials can include many different additives which enhance specific performance characteristics of the final repair. Modifiers for these products can be placed into three main categories: 1) polymer modifiers, 2) specially blended cements, and 3) admixtures.

Table 3- 1   Desirable characteristics of a concrete repair material

From a usability point of view, concrete repair materials may need to:	From a material point of view, a concrete repair material may need to:
be readily available in both small and large quantities	exhibit good adhesion
be easy to mix	be non-injurious to the parent material
be able to be placed easily at low water cement ratios	exhibit low permeability
be capable of curing quickly	have similar modulus to the parent material
be relatively self-curing	have similar thermal properties
be cost effective	exhibit low shrinkage
require a minimum of site preparation	have compressive strength at least equal to the original concrete
preferably similar in color and texture to the parent material	
have a wide range of placement temperatures and working times	

The most commonly found polymer modifiers for portland cement based materials are acrylic latex and styrene butadiene rubber (SBR); however, epoxy emulsions and polyvinyl acetates (PVA) have also been used. PVAs should not be used in moist environments as water tends to cause breakdown (34). Patch materials that are modified with acrylic or SBR additives are more commonly known as latex-modified concrete or latex-modified mortar. Latex modification is accomplished by using a liquid dispersion of latex which is added to concrete to replace a portion of the mixing water. It is usually added at a rate of approximately 15% by weight of solids to cement. Typically latex modifiers for cementitious materials are used in one of two ways. First, for smaller repairs they are used as a repair mortar. Latex mortars are usually obtained in one of two forms: a single or a two component system. The two-component system consists of prepackaged dry materials (sand, cement, water reducers) and a liquid component containing the latex mixed with water, while the single-component system contains the latex in a dry powder form premixed with other dry components; water is added to activate the cement and latex. The other way latex might be used is as an additive to concrete for larger or deeper repairs, resulting in latex modified concrete (LMC). Latex modification results in higher tensile and flexural strengths, increased or decreased compressive strength, increased adhesion and cohesion, and a lower modulus than that of normal concrete.

The second category of modifiers for cementitious materials are specially blended cements. Manufacturers use blended cements to achieve a combination of specific rates of strength gain and specific setting times. These blended cements typically have a high alumina content combined with gypsum. The high alumina content provides very fast strength gain while the gypsum is added to control

Table 3- 2   Admistures for Portland Cement-Based Products

Classification	Additive	Properties Enhanced
Chemical Admixture	Water Reducers	workability, durability, strength
	Superplasticizers	workability, durability, strength
	Accelerators	strength gain, setting time
	Retarders	strength gain, setting time
Mineral Admixtures	Pozzolans(Fly Ash)	workability, durability, strength
	Slags (Silica Fume)	workability, durability, strength
Misc. Admixtures	Air entrainers	workability, durability
	Expansive agents	shrinkage
	Corrosion inhibitors	durability
Misc. Additives	Glass Fibers	durability, non-sag characteristics
	Lightweight aggregate	non-sag characteristics
	Pigments	aesthetics

against flash set.   Quite often specially blended cements are used in conjunction with other additives to provide workable, durable, rapid strength gaining repair materials.

Many different admixtures can be used to enhance specific properties of portland cement-based products. Table 3-2 summarizes some of the admixtures that can be used with portland cement-based materials and the properties which each effect.

Magnesium phosphate based materials are also cementitious in nature, and are found as the binder for many proprietary patching products.   They exhibit excellent bond to dry substrates and very rapid strength gain;   however, they are extremely sensitive to small changes in water content and may be susceptible to sulfate attack.   The rapid rate of strength gain causes high heat of hydration which can result in thermal stresses building up within the patch if it is too large.   As the patch cools and contracts tensile stresses result and can cause microcracking eventually leading to durability problems.

3.4.2 Polymer Materials

Polymer repair materials typically are made with acrylics and epoxies, although other polymers are sometimes used.   Both acrylics and epoxies have been used in concrete repair in two different ways; first, as a crack filler and sealer, and second as the primary binder for polymer concrete or mortar.   The use of acrylics for repairing cracks and patches is generally limited to horizontal surfaces.   The material can fill the void by gravity and does not require pumping.   Therefore in most instances of girder impact damage, acrylics will have limited potential as polymer repair materials.   The exception may be in filling or sealing resulting cracks in the slab or railing components above damaged girders.   Epoxies, on the other hand have been shown to be very useful for many types of concrete repair.

Epoxies can be obtained with very different physical and mechanical properties.   The main uses for epoxies in the construction industry are as adhesives, binders for patching mortars or polymer concrete, and for crack repair by injection.   The discussion will be limited here to the use of epoxies for repair mortars and for crack injection in repairing impact damage.

Epoxy mortars can be formulated to different consistencies depending on the application.   For flatwork, they can be formulated to flow into voids, and for vertical or overhead work they can be formulated into non-sag gels allowing hand placement on vertical or overhead surfaces without the use of forms.   The

non-sag properties of epoxy mortars are ideally suited to the type of overhead repair that might be required for repairing girder impact damage.

Epoxy injection has proven on numerous occasions to be a very cost effective means of repairing cracks in concrete structures, in some instances offering the only viable alternative other than complete replacement of the structure. Low viscosity epoxies can be pressure injected into cracked regions in concrete to bond the surfaces together and seal the cracks from moisture and corrosive agents. It is often very difficult to ensure that the cracks to be repaired by epoxy injection are free of moisture. For this reason the type of epoxy that is used for this type of repair should be insensitive to moisture. Epoxy injection is meant for crack widths ranging from 0.25 mm (0.01 inches) up to about 6 mm (0.25 inch), however cracks as small as 0.125 mm (0.005 inches) have been successfully injected (30). If the cracks are larger than about 6 mm (0.25 inch), then the epoxy, extended by aggregates in the form of a mortar, can be injected in a similar manner. It is usually more practical to preplace aggregate followed by epoxy resin or acrylic monomer injection.

CHAPTER 4

TECHNIQUES USED TO EVALUATE DAMAGE

4.1. *INTRODUCTION*

Assessing the condition of a structure after it has been damaged is an integral part of the overall process of preparing a repair scheme. Plans, material specifications, and, if possible, as-built drawings should be obtained to become familiar with the structure prior to visiting the site. An initial site inspection is usually required in order to rapidly assess the extent of the damage; size and location of cracks, spalls, delaminations, loss of concrete cross section, exposure of and damage to prestressing tendons and ordinary reinforcement. If the structural capacity of the member or the structure is in question and further investigation is warranted, nondestructive methods might be employed to more clearly assess the extent of damage. It may also be possible to perform nondestructive load testing of the structure to evaluate the performance and remaining load capacity of the damaged structure. In this phase of the research, techniques that could be used for assessment of impact damage were evaluated using the Steck girder described previously.

As-built drawings of the Steck bridge are included Appendix B. The girder dimensions and tendon arrangement are shown in Figure 4-1. Specified concrete compressive strength for the girder at release (3 days) was 4,500 psi (31.0 MPa), and 28-day strength was specified as 6,400 psi (44.1 MPa). Cast-in-place concrete had a specified 28-day compressive strength of 4,500 psi (31.0 MPa). All ordinary reinforcement had a specified yield strength of 60 ksi (414 MPa), and all prestressing strand was specified as 270 ksi (1862 MPa), low relaxation strand.

4.2. *VISUAL OBSERVATIONS OF IMPACT DAMAGE*

Visual observations of the impact damaged girder from the Steck bridge located all visible areas of extensive loss of cross section, cracking, misalignment, and exposure of prestressing tendons. This was done both in the field as well as after the girder was removed from the bridge and brought to the laboratory. The photograph in Figure 4-2 shows an overall view of the damaged bridge. It is evident from this photograph that the impact also caused damage to the sidewall portion of the rail bed located above the exterior girder. The sidewall sustained damage near midspan as evidenced by three cracks extending through the full height and thickness. The cracks in the sidewall all exhibited extensive staining and efflorescence at the concrete surface.

This zone of cracking is more clearly visible in the photograph shown in Figure 4-3 which was taken after the girder was removed from the bridge and brought to the laboratory. The damage on the impacted face of the girder was difficult to observe in the field; a steel angle guard, still in place after the impact, covered most of the fractured zone. Once the angle guard was removed at the laboratory, the zone of fractured concrete surrounding the direct area of impact was clearly visible as shown in Figure 4-4. Figure 4-5 shows damage on the bottom of the girder revealing exposure of several tendons on the nonimpacted side of the girder. It is quite evident from these photographs that the impact damage was very extensive.

End Span   Center Span

15" (38.1 cm)

W

3" (7.6cm)

28 - 270 ksi Low-Lax Strands Total
Strands Depressed at 5' (1.52 m) Each Side of Center Span

Girder Dimension	Inches	Millimeters
A	12	305
B	18	457
C	6	152
Depth	34	864
E	5.75	146
F	14	356
G	2.75	70
H	5.5	140
W	7.5	191

Figure 4- 1   Steck girder dimensions and prestressing details

Figure 4- 2   Overall view of Steck girder in-situ

Figure 4- 3   Overall view of Steck girder after removal from the bridge structure

41

Figure 4- 4   Close-up view of Steck girder after removal — direct area of impact

Figure 4- 5   Schematic of impact damage of Steck Girder

For the purposes of this discussion, the damaged areas have been grouped into two distinct zones. Figure 4-5 shows a schematic of both sides and the bottom of the girder, illustrating the observable damage as well as the station numbering used for nondestructive tests. Severely damaged and spalled regions are indicated by hatching and the zone of direct impact is indicated by a large black dot.

The first damaged zone is located in the area of direct impact and consists of a group of concentric cracks extending from the lower flange up to the interface between the web and upper flange. There were several large spalled areas as well as several exposed prestressing tendons on both sides of the member on the bottom flange (refer to hatched zones in Figure 4-6). On the nonimpacted side a large delaminated zone of the web was located directly opposite the zone of impact. It appears that the impact resulted in a shear failure whereby a D-shaped region of the web and lower flange cracked completely through the member and the lower flange was horizontally offset approximately ½ to 1 in. (13 to 25 mm). The exposed tendons appeared to be undamaged, however, it was not known if yielding of any of the strands occurred during impact

The second zone of damage also appeared to be the result of a shear failure where the center span diaphragm acted as a reaction point for the transverse impact loading (Figures 4-6 and 4-7). The impact resulted in several cracks originating on the impacted side and propagating along and across the bottom flange. The extent of this zone of damage was not obvious, but some of the cracks appeared to extend into the web of the girder. Following visual inspection both in the field and at the laboratory, nondestructive methods were used as a means to further assess the extent of impact damage.

Figure 4- 6   Steck girder — damage to bottom flange and exposure of tendons

Figure 4- 7   Damage of bottom flange with diaphragm acting as reaction for impact load — Steck girder in-situ

4.3.   NONDESTRUCTIVE EVALUATION

In an attempt to determine the usefulness of nondestructive investigative techniques for damage assessment, three different methods were studied. The methods chosen are representative of both very simple procedures and those that are more complex investigative techniques. The first method used was to evaluate the surface hardness of the damaged girder using a rebound hammer. The other methods investigated were the Impact Echo (IE) method and the Spectral Analysis of Surface Waves (SASW) technique.

4.3.1.   Rebound Hammer Measurements

Rebound hammer measurements were taken using a type-N digital Schmidt hammer. Before testing began, and after approximately every 500 measurements, the hammer was calibrated using a calibration anvil. If the hammer was not within specified calibration parameters, it was disassembled, cleaned, lubricated, reassembled, and the calibration checked again. Measurements were taken at stations spaced at 6-in. (15-cm) along the length of the girder. At each station eight locations were tested on each side of the girder as shown in Figure 4-8, for a total of sixteen locations per station as follows: one at mid-height of the top flange, one at mid-height of the top haunch, two locations vertically spaced 6-in. (15-cm) apart on the web, one at mid-height of the bottom haunch, and three vertically spaced 1-in. (2.54-cm) apart on the bottom flange. For each test location eight measurements were taken, and the mean value computed. Since a major portion of the damage was concentrated in the bottom flange, the three bottom flange test locations were located very close together in order to obtain more detail.

44

Rebound Hammer Sampling Locations

34 in.

79

6 in.

15

7 Sampling Locations Per Station
Both Sides of Girder Evaluated

(1 in. = 2.54 cm)

Station Numbers
Along Girder

*Figure 4- 8   Schematic of rebound hammer testing
locations for damage assessment of Steck
girder*

The rebound hammer is a more elaborate and perhaps a less subjective evaluation procedure than a simple hand-held hammer to assess soundness by listening to the hollowness of the impact. A skilled inspector can probably obtain nearly the same results as can be obtained using the rebound hammer.

4.3.2.   Impact Echo Measurements

Impact echo measurements were taken using the DOCter Field Impact Echo Flaw Detection System, manufactured by German Instruments. This system consisted of a portable computer equipped with data acquisition hardware which was connected to the hand-held impact and sensing instrument. The instrument provides a choice of six different sizes of spring loaded impactors enabling selection of different contact times and sampling frequencies. An electronic displacement transducer is coupled to the concrete surface using a lead disc which is placed between the concrete surface and the displacement transducer. As the unit is placed against the concrete surface and the plunger is pushed down, the spring activated impactor strikes the surface of the concrete. The resulting surface displacements are recorded by a very sensitive piezoelectric displacement transducer, and the time-displacement history measured at the concrete surface is stored by the computer. The software that is used to set testing parameters and record results also performs a Fourier transformation of the data from the time domain to the frequency domain to facilitate interpretation. The user then evaluates the amplitude spectrum rather than the time-displacement record at each individual test location.

Data acquisition parameters for all tests taken on the damaged girder were left at the default settings which are recommended for structures less than about 20-in. (50-cm) thick. For each location tested 1,024 sampling points were taken at an interval of 2μsec for a total sampling duration of about 2 milliseconds. In order to evaluate the data quantitatively, the compression wave velocity of the concrete had to be determined. At several locations on each side of the web of the member that were assumed to be undamaged, samples were taken with the DOCter™ instrument. The normalized amplitude spectrum at each location was used to determine the dominant peak corresponding to the solid thickness frequency of the web. By measuring the actual thickness, and using the experimentally measured dominant frequency, an average compression wave velocity of 15,800 ft/sec (4800 m/sec) was determined. Using this experimentally determined compression wave velocity, the actual thickness of other locations could then be evaluated.

Once the compression wave velocity was determined at undamaged sections of the web, the same 6-in. (15-cm) station numbering was used for impact echo tests as for the rebound hammer; however, sampling at mid-height of the top haunch location was not performed. Figure 4-9 shows the sampling locations at each station that were used for impact echo measurements.

45

In order to evaluate the results of individual impact echo tests, the normalized amplitude spectrum at each location was plotted (normalized amplitude versus frequency). Each amplitude spectrum was then evaluated to determine the dominant mode of vibration at each test location. Individual normalized amplitude spectra were combined to form a contour of amplitude spectra along the length of the member. By evaluating individual and contour plots both local and global assessment at all test locations was made possible.

4.3.3. Measurements for Spectral Analysis of Surface Waves

Measurements for the SASW method were recorded using each pair of adjacent station intervals as shown in Figure 4-10. Again, the same 6-in. (15-cm) stationing was used for SASW evaluation of the damaged girder. Only grid points located along the haunch of the bottom flange were used for SASW evaluation. Sampling was performed by placing accelerometers at adjacent stations (points A and B in Figure 4-10), and impacting the concrete surface at stations X and Y one interval from opposite ends of the A-B interval shown in Figure 4-10. Five acceleration records were taken at each location on each side of the test interval, and the results averaged.

Individual dispersion curves showing the variation of surface wave velocity with respect to sampled wavelength were generated for each interval on the impacted side of the girder. Combining the individual dispersion curves from each interval, a contour of surface wave velocity versus wavelength was generated along the entire length of the haunch of the member. In this way individual dispersion curves were evaluated for localized damage assessment purposes, and then the contour of surface wave velocities was evaluated for global assessment of girder impact damage.

Rebound Hammer Sampling Locations

7 Sampling Locations Per Station
Both Sides of Girder Evaluated

(1 in. = 2.54 cm)

Figure 4- 9   Schematic of impact echo test locations for damage assessment of Steck girder

Indicates plane of material sampled by SASW tests

A,B = Test Interval
X,Y = Impact Points

(1 in. = 2.54 cm)

Figure 4- 10   Schematic of SASW testing locations for damage assessment of Steck girder

46

Damage Assessment Using Rebound Hammer
Steck Girder (Impacted Face)

Figure 4- 11   Results of damage assessment by rebound hammer - impacted face - Steck girder

Damage Assessment Using Rebound Hammer
Steck Girder (Non-Impacted Face)

Figure 4- 12   Results of damage assessment by rebound hammer - nonimpacted face - Steck girder

4.3.4. Results of Assessment by Rebound Hammer

The results of rebound hammer tests on both the impacted and nonimpacted faces of the girder are shown in the contour plots in Figures 4-11 and 4-12 respectively. Shown on each plot is the approximate location of impact. Plotted horizontally are the station numbers used for evaluation and the distance from the bottom of the girder is plotted vertically. The contour indicates the variation of rebound numbers on each face of the girder.

By direct comparison, it can be seen that damage on one side of the girder is not detectable when readings are taken on the opposite side. For example, at a height of 2-in. (5-cm) from the bottom of the girder, damage on the impacted face appears from station 21 to station 31, indicated by rebound numbers below 40. However, at the same location on the other side of the girder, much of the lower flange was intact in this region and the rebound numbers, all between 40 and 80 in this region, do not reflect the damage on the opposite side of the member.

On both sides of the girder the zone of delaminated and fractured material is very clearly defined by rebound measurements; however, damage that occurs deeper in the member or on the opposite side cannot be detected (refer to zone 1 in Figure 4-6 and Figures 4-11 and 4-12). Comparing the rebound values with the photographs in Figures 4-2 through 4-5, it appears that with the rebound hammer it is possible to delineate between sound and unsound material. The cross section at station 26, for example, based on visual observation, is shown in Figure 4-13. However, detailed information about damage that was not visible from the surface of the member was not able to be clearly defined using the rebound hammer.

4.3.5. Damage Assessment by Impact Echo

Rather than discuss the detailed process of data reduction for the impact echo method, only the results of testing will be presented. Figure 4-14 shows the normalized amplitude spectra obtained from the

Figure 4- 13   Cross section at sampling station 26 - based on rebound measurements and visual inspection

impacted side of the girder at stations 38 and 39 generated from impact echo sampling along the web. The peak amplitude at these locations occurs at a frequency of 12.2 kHz. Based on the measured compression wave velocity of 15,800 ft/s (4820 m/s) and measured frequency at peak amplitude, the corresponding thickness of the web at stations 38 and 39 was determined to be 7.77-in. (20-cm). The actual thickness of the web at the ends and center of the girder varied from 7.5 to 8.5-in. (19 to 22-cm).

It is obvious when comparing the spectra in Figure 4-14 and Figure 4-15 that damage is clearly indicated by a shift in the peak amplitude from a frequency of 12.2 kHz (the solid thickness response in Figure 4-14) to lower dominant frequencies (Figure 4-15). It should be noted that the most dominant frequency of 0.97 kHz in each case (the largest peak at the left end of each spectrum with an amplitude of 1.0) is the resonant frequency of the displacement transducer of the instrument, and, hence, is a false reading. However, the other high amplitude peaks that are evident in each normalized amplitude spectrum are meaningful and require further explanation. At station 18 there are three other dominant peaks; one at a frequency of 4.88 kHz and a normalized amplitude of 0.63 which corresponds to a thickness of 19.4-in. (49.4-cm), a second peak at a frequency of 7.32 kHz and normalized amplitude of 0.32 corresponding to a thickness of 12.9-in. (32.9-cm), and a third peak at a frequency of 13.18 kHz and normalized amplitude of 0.63 corresponding to a thickness of 7.2-in. (18.3 mm). At station 19 there are three dominant peaks other than the one corresponding to the resonant frequency of the instrument: one at a frequency of 3.91 kHz and a normalized amplitude of 0.74 which corresponds to a thickness of 24.3-in. (67.1-cm); a second peak at a frequency of 4.88 kHz and normalized amplitude of 0.80 corresponding to a thickness of 19.4-in. (49.4-cm); and a third peak at a frequency of 13.18 kHz and a normalized amplitude of 0.63 corresponding to a thickness of 7.2-in. (18.3-cm). In comparison to the actual web thickness of 7.5 to 8.5-in. (19.1 to 21.6-cm), all of these peaks correspond to a thickness greater than the web with the exception of the peaks occurring at a frequency of 13.18 kHz, very close to the solid thickness frequency of the web (12.21 kHz). The lower frequency vibration responses are indicative of a delaminated concrete. The impact echo response of samples taken over a

Figure 4- 14   Damage assessment by impact echo - upper web undamaged locations

Figure 4- 15 *Damage assessment by impact echo - upper web damage location*

delamination behaves much like a plate restrained at its edges undergoing flexural vibration. The flexural vibrations are characterized by lower frequencies than the solid thickness mode of vibration and, hence, are an indication in some instances that a delamination is present at the sampling location (24,25).

In order to assess the extent of damage on a global rather than local basis, a contour of the amplitude spectra along the length of the member for the upper web area on the impacted side of the girder is shown in Figure 4-16. The most evident observation is that the web of the entire beam is damaged from stations 15 to 42 and exhibits varying degrees of delamination as characterized by low frequency flexural modes of vibration.

When sampling locations along the bottom flange of the girder care must be taken in evaluating the results since the geometry of the flange is unlike that of the web. The vibrational response in the web behaves much like that of a flat plate where the stress waves will reflect off the two outer surfaces of the web, whereas the geometry of the flange of an I-shaped member has more surfaces which the stress

Figure 4- 16 *Global damage assessment using impact echo - upper web location*

49

Normalized Amplitude Spectrum
Bottom Flange Location - Undamaged

Solid Thickness
Frequency = 5.27 kHz

Figure 4- 17   Damage assessment by impact echo - undamaged bottom flange locations

waves can reflect from causing difficulty in interpretation of results. With this in mind several test locations along the bottom flange will be discussed.

Figure 4-17 shows the results of impact echo sampling at stations 41 and 42 on the impacted face of the member for a bottom flange sampling location. The frequency which corresponds to the solid thickness of the flange was calculated to be 5.27 kHz. As shown in Figure 4-17 the most dominant peaks of each normalized amplitude spectrum appear very near this solid thickness frequency. The actual response at each of these locations results in a dominant peak at a frequency of 4.39 kHz which corresponds to a thickness of 21.6 in (54.9-cm). Although this is not exactly the solid thickness frequency, interpretation of these tests reveals that there is relatively no damage in the bottom flange at this location which was also confirmed by visual inspection. It is possible that the geometry of the flange itself causes the response to contain some flexural modes of vibration which could account for the discrepancy between measured and expected frequencies.

n contrast to the undamaged flange locations at stations 41 and 42, Figure 4-18 shows the results of impact echo sampling of the bottom flange at stations 46 and 48 on the impacted side of the girder. It was evident by visual inspection at these locations that there was a crack running through the bottom flange of the member; however, it was not known how deep into the member the cracks extended. Between stations 46 and 48 this crack was very near the surface of the member. The response at these locations is dominated by low frequency flexural modes of vibration indicative of a delamination. In this instance, where the crack is near the surface, it is reasonable that the response is dominated by flexural frequencies indicating delaminated concrete. At station 46 the dominant frequency is 2.93 kHz and at station 48 the dominant frequency is 1.95 kHz, both of which are much less than the solid thickness frequency of 5.27 kHz, indicating near surface damage.

Normalized Amplitude Spectrum
Bottom Flange - Damaged- Impacted Face

Solid Thickness
Frequency = 5.27 kHz

Figure 4- 18   Damage assessment by impact echo - damaged bottom flange locations

The results of impact echo testing at stations 46 and 48 on the nonimpacted face of the girder were taken for comparison to the tests performed on

50

the impacted side of the girder. On the impacted face the response was interpreted as a delamination; the crack was very near the surface. Visual observations revealed that the crack was closer to the side face of the flange at station 48 than at 46. Referring to Figure 4-6, zone 2, the crack propagated from the nonimpacted face to the impacted face across the bottom flange and also up the face of the flange on the impacted side of the member. Again, the extent of this crack was not clearly evident, but impact echo results will show that the damage is clearly detectable from either side; however, interpretation of the results is simpler from the nonimpacted face.

Figure 4- 19   Damage assessment by impact echo - damaged bottom flange location - nonimpacted face

Figure 4-19 shows the results of impact echo testing at a bottom flange location for stations 46 and 48 on the nonimpacted side of girder. Again the frequency corresponding to the solid thickness of the flange was calculated to be 5.27 kHz. An interesting comparison to the solid thickness frequency can be made for the results at stations 46 and 48 on the nonimpacted face of the member. The dominant frequency response at station 46 was found to be 6.84 kHz with a corresponding calculated thickness of 13.89-in. (35.3-cm). The dominant frequency response at station 48 was found to be 5.37 kHz with a corresponding calculated thickness of 17.68-in. (44.9-cm). Remembering that the actual thickness of the bottom flange of the girder was measured to be 18-in. (45.7-cm), several observations can be made regarding the results of impact echo tests on both the impacted and nonimpacted face of the member.

First, in order to lend perspective to the location of these measurements, a more detailed schematic of Figure 4-6, zone 2 is shown in Figure 4-20. This schematic shows that measurements locating the crack in the bottom flange at stations 46 and 48 were very close to the results obtained from impact echo sampling on the nonimpacted face of the member. At station 46, the crack was measured to be approximately 11.5-in. (29.2-cm) from the nonimpacted face. Impact echo results indicated that the crack was 13.89-in. (35.3-cm) from the edge. It should be noted, however, that measurements for this sampling location

Figure 4- 20   Detailed schematic of Zone 2 damage of Steck girder

51

were taken approximately 3-in. (7.6-cm) from the bottom of the member, while exact location of the crack was measured on the bottom surface of the girder. It is likely that the crack did not extend perpendicularly from the bottom surface, but rather at an angle, and may account for the discrepancy between impact echo results and actual measurements. At station 48, where the crack was very near the surface on the impacted face, measurements located this crack to be 17.25-in. (43.8-cm) from the nonimpacted face, while impact echo results located the crack at 17.68-in. (44.9-cm) from the nonimpacted face. The results in this instance were easily verified due to the proximity of the crack to the surface of the member. It is much easier to interpret the vibrational response when flexural modes are not present as is the case at stations 46 and 48 on the nonimpacted face of the member. Delaminations are not as easily or confidently identified using the impact echo method; however it is possible to detect both visible and hidden damage in concrete using the impact echo technique.

For global assessment purposes a contour of the normalized amplitude spectra along the bottom flange on both sides of the member was constructed using the results from each individual sampling location. These contour plots shown in Figures 4-21 and 4-22 reveal the nature of the damage to the flange on a global basis. It should be noted that on the impacted face between stations 19 and 35 and on the nonimpacted face between station 33 and 43 there was such severe damage to the concrete in the bottom flange that no data were able to be recorded. This lack of data is evident in each the contour plot. No clear pattern of response exists in the contour plots for the bottom flange on each side of the girder which is an indication on a global level that there appears to be damage within the flange of the member throughout the entire sampling range with the exception of a few locations that exhibit peak amplitudes near the solid thickness frequency of 5.27 kHz as already discussed (Figure 4-17).

Figure 4- 21   Global damage assessment using impact echo - bottom flange location - impacted side of girder

Normalized Amplitude Spectrum Contour

Bottom Flange Location - Damage Assessment

Solid Thickness
Frequency = 5.27 kHz

Figure 4- 22   Global damage assessment using impact echo - bottom flange location - nonimpacted side of girder

4.3.6.   Damage Assessment Using SASW Method

Figure 4-23 shows the dispersion curves generated from SASW testing between stations 10-11, 18-19, and 21-22.   These three cross sections represent zones of varying degrees of visible damage on the impacted side of the girder.   The dispersion curve over the station 10-11 interval corresponds to undamaged concrete.   It shows relatively constant velocity as a function of wavelength varying from about 7,100 ft/s (2,150 m/s) to about 8,200 ft/s (2,500 m/s). Comparison of this dispersion curve with the cross section in Figure 4-24(a) shows that even though some damage exists on the non-impacted side of the girder, it is not directly beneath the array axis, and therefore does not affect the observed surface wave velocities.

Dispersion curves over the 18-19 and 21-22 station intervals show reductions in surface wave velocity (Figure 4-23). These reductions in velocity occur at longer wavelengths (deeper in the

Figure 4- 23   Damage assessment using SASW Method - bottom haunch location - impacted side of Steck girder

53

(a) Station 10-11   (b) Station 18-19   (c) Station 21-22

*Figure 4- 24   Interpretation of SASW test results for damage
assessment of Steck girder*

member) for the 18-19 interval, but affect shorter wavelengths (shallower) for the 21-22 interval. Figure 4-24(b) and ©, based on visual observation, indicate deep damage between interval 18-19 and shallow damage between interval 21-22 respectively. Comparing visual observations with SASW results over these station intervals shows how the dispersion curves can be used qualitatively to evaluate the extent and relative depth of damage.

Individual dispersion curves generated from SASW tests, like individual amplitude spectra from impact echo tests, provide detailed information which allow localized assessment of damage. However, if the individual dispersion curves are combined to form a contour of surface wave velocities, global assessment of the damage is made possible in much the same way as was shown using impact echo test results. Figure 4-25 shows a contour of surface wave velocities along the bottom haunch of the impacted side of the damaged girder.

Figure 4- 25   Global damage assessment using SASW Method

The trends observed in the contour plot (Figure 4-25) reveal how the SASW method, like the impact echo method, is capable of delineating between sound and unsound material. The apparent decrease in surface wave velocities between stations 17 and 21 correspond to a transition from sound concrete to the beginning of severely fractured material. The low surface wave velocities present between stations 22 and 36 represent the severely damaged zone in the region nearest the impact, and another transition zone from damaged to more sound material exists from station 37 to 46. Between stations 46 and 48 another zone of low surface wave velocity exists, which correlates very closely with impact echo measurements taken in the same region (Figures 4-18 and 4-21).

4.4.   DAMAGE EVALUATION OF STECK GIRDER BY NONDESTRUCTIVE LOAD TESTING

Following the initial damage assessment by both visual observations and nondestructive methods as herein described, instrumentation and nondestructive load testing were performed on the damaged girder.

Applied Load

Transverse
Post-Tension
Force

☐ Existing Cross Section

■ New Concrete

*Figure 4- 26   Schematic of Steck Girder Cross Section
Showing Additional Concrete Placed to
Facilitate Loading*

The load-deflection response of the girder and the load-deformation response of several exposed prestressing strands were studied in order to evaluate the effects of impact damage.

Because the combined cross section of the precast girder and the cast-in-place railing was not symmetric, additional concrete was cast at the locations where load was to be applied in order to minimize load eccentricity. The additional concrete was held in place by external transverse post-tensioning through the new concrete and existing sidewall as shown in Figure 4-26.

4.4.1.   Test Setup

In order to facilitate load testing of the girder, support blocks were placed such that the centerline between bearings near the ends of the member was 36.4 ft. (11.1 m) apart. Even though the length of the girder was 39 ft. 4 in. (12 m), one end sustained considerable damage during transport and the span length had to be shortened to prevent further damage or premature failure during load testing. Figure 4-27 shows the test setup schematically identifying the support locations as well as the locations of load application and lateral bracing for the specimen.

4.4.2.   Girder Instrumentation

Linear Voltage Displacement Transducers (LVDT's) were located at the load application points and at centerspan to monitor the deflections of the girder during load testing. The hydraulic pressure was monitored using a 5,000 psi (34.5 MPa) electronic pressure transducer. All LVDT's and the pressure transducer were monitored by computerized data acquisition hardware and software.

Deformations of individual wires of several exposed strands were measured by using electrical resistance strain gages. Figure

(1 ft = 0.3048 m)

*Figure 4- 27   Schematic of Test Setup and Loading Frame for
Steck Girder Load Tests*

55

Figure 4- 28   *Location of Electronic Resistance Strain Gage Instrumentation*

4-28 illustrates the approximate locations where tendons were instrumented with strain gages. Three gages were applied to different wires of each instrumented strand to provide redundancy if the rather fragile gages became damaged or loosened during loading of the girder. Difficulty arose in the application of the gages to a rounded wire rather than a flat surface. As the tendon elongated, the tendency for individual wires to move relative to one another also caused problems with adhesion of the gages to the surface of the strand.

4.4.3. Test Procedure

Static load was applied to the girder using the hydraulic jacks as described. Hydraulic pressure was maintained using a hand-actuated pump. At each load increment deflections, tendon strains, and pressure were monitored using the computerized data acquisition system. The load test consisted of a single static load cycle and in order not to damage the girder excessively, the maximum load that was applied to the girder was 85 kips (378 kN). This load was originally intended to produce a midspan moment approximately equal to the live load service level moment based on E-80 design loads distributed to three of the four interior girders without consideration of impact (17).

4.4.4. Results of Nondestructive Load Tests

Experimental Load-Deflection Response. The measured load-deflection response at the load application points and center span locations are shown in Figure 4-29. It should first be noted that the locations at the south load point and center span were both damaged, whereas the location at the north load point remained relatively undamaged. Several observations can be made regarding the experimentally measured load-deflection response at each of the instrumented cross sections.

The slope of the load-deflection curve, or member stiffness, for the south load point, based on least squares regression of experimental data was found to be 167 kips/in. (29,250 kN/m). The stiffness at the

Experimental Load Deflection Response

Figure 4- 29   Experimentally   Measured   Load-Deflection   Response   of Damaged Steck Girder (1 kip = 4.45 kN)

north load point was experimentally determined to be 215 kips/in. (37,650 kN/m), while at center span, the stiffness was measured to be 152 kips/in. (26,620 kN/m). It is evident when comparing the response at the north and south load application points that the difference in measured stiffness reflects the unsymmetrical nature of the damage to the girder; the south location was severely damaged resulting in a lower stiffness than the essentially undamaged north cross section. The stiffness at the center span location was less than that found at both north and south cross sections as expected. The center of the girder should experience more deflection than at either load point, and this was reflected in the experimental response. It should be noted, however, that the stiffness of a damaged girder does not appear to be an extremely important factor when assessing the extent of damage. In this instance comparison of stiffness is made to distinguish the unsymmetrical nature of the response. When in-situ nondestructive load testing was performed on the Waelder bridge, stiffness did not play a major role in the overall performance of the damaged structure. The measured displacements were on the order of $1/5000^{th}$ of the span length, while for the Steck girder, after removal from the bridge, the displacements were on the order of $1/1000^{th}$ of the span length, still within acceptable limits. While the girder from the Steck Avenue bridge was still in place, displacements of the damaged girder were measured as a train passed over the bridge, but deflection of the girder was barely perceptible. It is evident that when a damaged girder is removed from a bridge, the damage effects are more pronounced in terms of load-deflection response than when the load is able to be shared by other parts of the structure by load transfer through the slab and diaphragms. It is reiterated that reduction in stiffness alone should not be a deciding factor as to repair-in-place or replace damaged girders, but rather the decision should be based in part on remaining and repaired load capacity as well as durability of the repair.

Using an elastic analysis procedure, the theoretical load-deflection response at center span was determined and compared to the experimentally measured response at the same location in order to evaluate the reduction in stiffness due to impact damage. Figure 4-30 compares the theoretical and experimental behavior at the center span location. The theoretical stiffness of the center span section was determined by analysis to be 455 kips/in (79,680 kN/m), and, as previously shown, the

Comparison of Theoretical and Experimental Load-Deflection Response

Figure 4- 30   *Comparison of Theoretical Load Deflection Response of Damaged Steck Girder at the Centerspan Location (1 kip = 4.45 kN)*

experimentally observed stiffness at center span was only 152 kips/in (26,620 kN/m). It is obvious that the extent of impact damage incurred was quite severe and that the experimentally derived stiffness is only 33 % of the theoretical value. Again, stiffness should not be considered as the deciding factor for repair or replacement of a damaged girder.

Load Deformation Response of Instrumented Tendons. The deformations of tendons, as previously mentioned, were measured at slightly different locations than deflections. Tendons were exposed at cross sections one and two, and concrete side cover was removed at cross section three in order to expose and instrument tendons at this location. Figure 4-31 shows the average measured changes in strain of instrumented tendons. Again, each tendon had three individual wires with strain gages applied, and the average of the three gages for each instrumented tendon is shown in Figure 4-31.

Several observation can be made regarding the measured tendon deformations. First and foremost, the relative magnitudes of the tendon deformations at each cross section correlate closely with the extent of damage based on both visual observations as well as the measured girder displacements. Cross section one appeared visibly to have sustained the most severe damage, and this is reflected in the measured tendon deformations at this location; the maximum changes in elongation of the tendons were between 1600 and 1800 microstrain. Cross section two sustained less damage than cross section one, and cross section three sustained little damage with the exception of cracking of the concrete near the bottom on the impacted side of the girder. Again, the magnitude of the tendon deformations at cross sections two and three correlate well with the observed visible damage of the girder.

It would normally be expected that if a tendon is below the centroid of the cross section, the strain due to applied loading should be higher than a tendon with smaller eccentricity from the centroid (for a simply supported girder). However, this was not the case for the measured tendon strains at each cross section. Although the results appear perplexing, the reason for this behavior became evident upon further

Experimental Load-Deformation Response of Instrumented Tendons

Figure 4-31   Experimentally Measured Deformations of Instrumented Tendons - Steck Girder - Damaged (1 kip = 4.45 kN)

inspection of the girder especially at cross section three. At this location, as previously mentioned, it appeared that the concrete surrounding the tendon was cracked, and upon application of load on the girder this zone of cracking increased, signifying an increased length along which the bottom tendon became debonded. Debonding would cause the measured strains in the bottom tendon to be less than for the top as was the case. The same could be said for the tendon behavior at cross section one; however, the damage was so extensive that visual observations were not sufficient to determine exactly where this debonded zone occurred. The observed tendon strains at cross section two, center span on the nonimpacted face of the girder, exhibited the expected response where the lower tendon became more highly stressed as the load on the girder increased. The following chapter describes in detail the materials, methods of application, and evaluation of concrete repair of the damaged girder.

CHAPTER 5

REPAIR OF IMPACT DAMAGED CONCRETE AND EVALUATION OF REPAIRS

5.1 INTRODUCTION

Once the initial damage assessment for the Steck girder was completed, repair of the damaged concrete was initiated. Several different materials were used for the concrete repair in order to assess their individual performance so that the most appropriate materials can be selected for use in the field. The laboratory environment provided an excellent opportunity to evaluate several different classes of concrete repair materials as well as different methods of placement. Repair materials and methods of placement, nondestructive load testing of the repaired girder, and evaluation of the concrete repair (using the same nondestructive techniques that were used for damage evaluation described in Chapter 4) are presented in this chapter.

5.2 CONCRETE REMOVAL AND SURFACE PREPARATION

The damaged girder had more camber than it had prior to impact because the bottom flange had several areas of extensive damage and shortening. To prepare the girder for repair, a preload was applied to restore the profile of the girder, to facilitate removal of loose, delaminated, and fractured material in the bottom flange and web regions by relieving compression in the concrete, to open existing cracks prior to injection of epoxy, and to allow precompression of the patch material after removal of the preload. Following application of preload, all of the damaged concrete was removed using either a chipping hammer or with a hammer and chisel for areas where damage to the strands was likely. After most of the damaged concrete was removed, a bush hammer was used where possible to roughen the surface and to remove any remaining fractured material. Once the concrete surface was prepared using the bush hammer and a wire brush, dust was removed by flushing with water and then by blasting the surface with compressed air.

Figures 5.1 through 5.3 show the impacted side, the bottom, and the nonimpacted side of the girder respectively after concrete removal and surface preparation were complete. Also visible in each of these photographs are the preparations for placing internal epoxy injection ports. Figure 5.4 shows how the damaged regions were divided to permit trial uses of various patching materials.

5.3 REPAIR MATERIALS AND METHODS

Cast-in-Place Prepackaged Repair Materials

The portions of the beam that required large volume of concrete replacement were repaired with two cast-in-place prepackaged materials, each extended 60 % by weight with 3/8-in. (10-mm) river gravel. Both materials were recommended by their suppliers for horizontal and formed repairs. The first

Figure 5- 1   Impacted side of Steck girder following removal of damaged concrete.

Figure 5- 2   Bottom of Steck girder after removal of damaged concrete

Figure 5- 3   Non-impacted side of Steck girder following removal of damaged concrete

material, Set 45 HW, manufactured by Masterbuilders Incorporated, is a magnesium phosphate-based single-component system that has a flowable consistency upon mixing and does not require wet curing . The second material, Patchroc 10-61, manufactured by Fosroc Industries, is a portland cement-based prepackaged repair material. It is a single-component system and has been modified by other blended cements to achieve a rapid setting time and very rapid strength gain. Both of these cast-in-place materials were special hot weather formulations with extended working times, since the repairs were performed during the summer. Figure 5.4 shows schematically the regions on the bottom flange where

Figure 5- 4   Placement of patching materials for repair of concretein Steck girder

63

these two materials were placed. Plywood forms were placed in a sleeve around the girder as shown schematically in Figure 5.5, and in the photographs in Figures 5.6 and 5.7.

Prepackaged Vertical/Overhead Repair Mortars

Areas on the web that consisted mainly of severely fractured or delaminated material were repaired using non-sag or vertical and overhead (V/O) repair mortars. The repair materials were placed without forms, either by troweling, hand-packing, or a combination of both. The materials chosen were either single- or two-component repair mortars specifically designed for vertical and overhead application.

Figure 5- 5   *Schematic of formwork for cast-in-place concrete repairs of Steck girder*

The first two mortars used were two-component latex-modified repair mortars, from different manufacturers. One was Burke V/O, manufactured by Burke, and the other was Renderoc HB2, manufactured by Fosroc Industries. Each consisted of a premeasured 55 lb. (24.9 kg) package of dry

Figure 5- 6   *Placement of formwork for bottom flange concrete repair using set 45 HW of Steck girder - impacted face*

64

Figure 5- 7 Placement of formwork for bottom flange concrete repair of Steck girder using Patchroc 10-61 - impacted face

components, and one gallon of a liquid dispersion of acrylic latex used in place of mixing water. Both of these materials were used to repair web damage on the impacted side of the girder. The patched areas were approximately 3 or 4-in. (7.5 to 10-cm) deep by 8-in. to 18-in. (20 to 46-cm) in plan.

Both of these materials were also used to repair portions of the lower flange where patch depth was in excess of 6-in. (15-cm) (Figure 5.4). The web repairs were hand-packed and then shaved smooth, while the flange repairs were performed with partial formwork in one location and without any forms in the other location. Prior to placing the two-component latex-modified materials, a slurry coat of thinned latex mortar was applied to the surface, and then the mortar was either troweled or hand-packed into the damaged area.

The second type of V/O material chosen was a single-component acrylic latex-modified repair mortar. Acrylic Patch, manufactured by Burke, is described as a blend of dry acrylic polymer, portland cement, silica aggregate, plasticizer, water reducers and other admixtures. It was used on the nonimpacted face for repair of a large delaminated zone on the web (Figure 5.4). The patch size ranged from 1/2 to 3-in. (1.3 to 7.5-cm) in depth and was approximately 60-in. by 8-in. (152-cm by 20-cm) in plan. Initial presaturation of the surface for approximately 4 hours was required as well as an application of a thinned slurry coat.

The third type of V/O material that was chosen for the repair, EMACO S88CA, manufactured by Masterbuilders Incorporated, was a silica fume, fiber-reinforced, cementitious repair mortar. EMACO S88CA was used to complete the repair of the web on the nonimpacted face of the girder (Figure 5.4). The patch depth ranged from 1/2 to 4-in. (1.3 to 10.2-cm) and was approximately 60-in. by 8-in. (150-cm by 20-cm) in plan. In contrast to the two-component latex-modified mortars, this material did not require a slurry bond coat; however, prewetting of the surface for 24 hours prior to placement was required in addition to a 7-day moist cure.

Figure 5- 8   Installation of polyethylene tubs for internal injection ports

Epoxy Injection Materials and Apparatus

Epoxy injection is normally performed prior to patching the concrete; however, in this case, patching was performed first. The extreme fracturing and loss of the concrete precluded surface sealing which is required to effectively pressure inject epoxy. Polyethylene tubing was adhered to the interior fractures at intervals between 6 and 12-in. (15 to 30-cm) to facilitate injection (Figures 5.1 through 5.3 and Figure 5.8). The concrete was then patched, leaving the tubes protruding from the patch surface. The tubes were then ground smooth with the patched surface and injection ports were placed over the exposed tube ends. Finally, remaining cracks and patches that exhibited shrinkage cracking were sealed at the surface and injection ports were placed (Figure 5.9).

Epoxy injection can be performed by either high pressure equipment or using prepackaged, proprietary, low pressure injection apparatus. The prepackaged kits have the advantage that the two components, the resin and hardener, are premeasured, reducing the possibility of errors in proportioning.

Low pressure, hand-held epoxy injection equipment (a modified caulking gun), furnished by HILTI, was selected for the epoxy injection repairs. Each epoxy injection kit contained 12 cartridges with premeasured amounts of resin and hardener. The two components were separated by a glass barrier which, when broken, allowed mixing of the resin and hardener. The kit also contained 30 surface mounted one-way injection ports, 6 one-way valve connection hoses, and 4 air relief stoppers. The epoxy surface sealer, injection gun, additional ports, hoses, and air relief stoppers were also furnished by HILTI.

5.3.1 Girder Instrumentation and Test Setup for Post-Repair Nondestructive Load Test

Displacements were monitored in the same locations as in load testing during the damage assessment phase. The girder was not moved during repair; therefore, the identical test setup was used for

Figure 5- 9   Sealing of surface cracks and placement of surface mounted injection ports

measurements of load, displacement, and tendon deformations as was used for nondestructive load testing during damage assessment (Chapter 4 Section 4.4.2).

5.3.2 Girder Repair Procedures and Quality Assurance by Nondestructive Methods

The concrete repair of the impact damaged girder was performed in several phases. The process was organized as follows:

Phase A

1. Preload Girder

2. Concrete Removal and Surface Preparation

3. Placement of Tubes for Internal Epoxy Injection Ports

4. Erection of Forms

5. Placement of Cast-in-Place Materials

6. Placement of V/O Mortars

7. Nondestructive Evaluation

Phase B

1. Sealing of Surface Cracks and Placement of One Way Valve Injection Ports

2. Perform Epoxy Injection

3. Nondestructive Evaluation

4. Removal of Preload

5. Nondestructive Evaluation

6.

Phase C

1. Post-Repair Nondestructive Load Test

2. Injection of Cracks in the Sidewall

3. Post-Repair Nondestructive Load Test

After different phases of the repair were completed, the repairs were evaluated with the same three nondestructive techniques used for damage assessment: 1) surface hardness using the rebound hammer, 2) impact echo method, and 3) spectral analysis of surface waves technique.

Evaluation by nondestructive methods was performed after the concrete and mortar materials were placed and cured, after epoxy injection, and following the removal of preload. The nondestructive techniques were used to evaluate the quality of the repairs that were undertaken, and the effectiveness of each nondestructive method for quality assurance.

5.4 OBSERVATIONS AND PERFORMANCE OF EACH REPAIR MATERIAL

5.4.1 Observations for Cast-In-Place Repairs

Set 45 HW, the magnesium phosphate-based horizontal patching material, was mixed using a drum mixer and then placed into forms by conventional means. Form vibration and tapping with a rubber mallet were required to consolidate and place the material. It had a flowable consistency and appeared much darker than the original concrete (Figures 5.10 and 5.11). Prewetting of the substrate was not required; the manufacturer's recommendations indicated that surface moisture and moist curing would be deleterious to the performance of the material due to extreme sensitivity to water content. Complete saturation of the forms with form oil was required to keep the material from bonding to the forms.

The Set 45 HW gained sufficient strength within 30 minutes to allow removal of forms (Figure 5.12). Two 4-in. by 8-in. (10-cm by 20-cm) cylinders were tested for compressive strength at 24 hours. The cylinder strength was approximately 4600 psi (31.7 MPa). The fracture plane went through the matrix, not the aggregate, and resulted in a very abrupt, almost explosive failure. Considerable heat was generated during initial set. If Set 45 were to be used for large volume replacement of damaged concrete, even if extended with coarse aggregate, the high heat of hydration combined with the rapid setting time of the material could eventually lead to durability problems. When a large volume of the material is placed and extreme heat is generated during initial set, it is likely that tensile stresses could develop as the material cools and sets causing microcracks to develop within the repair. Such microcracking could

Figure 5- 10   Placement of set 45 HW for cast-in-place bottom flange concrete repair

Figure 5- 11   Consolidation of set 45 HW

69

Figure 5- 12   Completed repair of bottom flange using set 45 HW

eventually lead to poor durability for a repair of this nature. Furthermore, only an amount of material that can be placed within about 5 minutes of mixing should be batched, because the working time of the Set 45 and Set 45 HW is extremely short (approximately 10 minutes in hot weather (HW) conditions). For several days after placement, the Set 45 emitted an objectionably strong odor of ammonia.

The Patchroc 10-61 was also mixed using a drum mixer, placed by conventional means, and mechanical vibration was used to consolidate the material into the void space. Because this was a cementitious product, the consistency and appearance was much closer to that of original girder concrete (Figure 5.13). Sufficient strength was gained within one hour of placement to remove forms (Figure 5.14). Two 4-in. by 8-in. (10-cm by 20-cm) cylinders were tested for compressive strength at 24 hours. The average cylinder strength was 3970 psi (27.4 MPa). The combination of the longer working time of this material, approximately 15 minutes, and the ability to use mechanical vibration, made placement of the Patchroc 10-61 much easier than the Set 45 HW.

Some difficulty was noted with placement of both materials resulting in voids within the repaired zone.. As the spaces to be patched became narrower, it was difficult to completely consolidate the voids by conventional methods of placement. Consolidation might be improved by using pressure grouting rather than casting from above and relying on hydrostatic pressure to force the material into the voids. The remaining voids were later repaired using two of the latex modified mortars.

5.4.2 Observations for Latex-Modified V/O Mortars

Two-Component Latex-Modified Mortars. The physical appearance, consistency after mixing, and application of the Renderoc HB2 and Burke V/O were identical. At first, each material appeared very dry, but as liquid acrylic was slowly added and mixed with the dry components in a 5-gallon (18.9-liter) pail using a paddle mixer, the consistency changed to a very sticky, cohesive mixture that could be placed

70

Figure 5- 13   Placement and consolidation of Patchroc 10-61

Figure 5- 14   Completed repair of bottom flange using Patchroc 10-61

Figure 5- 15   Application of slurry coat prior to placement of Renderoc HB2

and shaped by hand. The surface of the damaged concrete was presaturated for approximately 4 hours before placement of the repair materials. A 2-to-1 slurry coat of liquid latex to dry powder was scrubbed into the surface between lifts prior to material placement (Figure 5.15).   Both materials had approximately 30 minutes of working time.

An attempt was made to finish the first portion of the web repair in one lift using the Renderoc HB2; however, the weight of the patch caused it to pull away from the concrete substrate. Some of the patching material was removed to leave a thickness of about 2-in. (5-cm). The surface was roughened, and the material was allowed to cure overnight. A slurry coat was applied prior to placement of the second lift of about 2 to 3-in. (5 to 8-cm) to complete the patch. The patch area was overfilled, and the excess material shaved flush with the concrete surface. Figure 5.16 shows the completed zone of web repaired using Renderoc HB2.

Renderoc HB2 was also used to repair an area of the bottom flange using partial formwork. A single sheet of plywood was placed on the bottom surface of the girder, a slurry coat scrubbed into the concrete surface, the patching material hand-packed, and the vertical surface shaped with a trowel (Figure 5.17). An attempt was made to complete this repair in one lift; however, the patch began to sag even with the use of a bottom form from below. The material was removed to a depth of 2-in. (5-cm), the repair allowed to cure overnight, and a second lift of about 3-in. (8-cm) placed to complete this portion of the repair.

Burke V/O was mixed and placed in the same manner as the Renderoc HB2. Two lifts were required to completely fill the 4-in.-deep (10-cm) damaged zone of the web, and three lifts were required to finish the repair of the bottom flange on the nonimpacted side of the girder (Figures 5.18 and 5.19). The main difference in terms of application between the Renderoc HB2 and Burke V/O was that the Renderoc HB2 tended to pull away from the surface more readily than the Burke V/O, resulting in slightly less build per lift. Even though each material seemed to be nearly identical in appearance and consistency, extensive

Figure 5- 16   Completed web repair using Renderoc HB2

Figure 5- 17   Partially formed bottom flange repair using Renderoc HB2

73

Figure 5- 18   Repair of web damage on impacted side of girder using Burke V/O

Figure 5- 19   Repair of the bottom flange on the nonimpacted face of girder using Burke V/O

shrinkage cracking was observed in the thinner web patches using the Burke V/O whereas the Renderoc HB2 exhibited none.

Both materials were also used to repair the overhead voids that remained unfilled from the cast-in-place repair (Figure 5.20). Even though the depth of the void was approximately 6-in. (15-cm), the entire void could be filled with a single lift. A higher material build was possible than for web repairs because the shape of the voids was deep and narrow, allowing more surface area around the sides of the voids to be in contact with the patching materials, thereby providing more surface for adhesion and a smaller volume of material to be supported by adhesion (Figure 5.20).

Figure 5- 20   Overhead repair of bottom flange using Burke V/O

Single-Component Latex-Modified Mortar

Burke Acrylic Patch was used to repair part of the large delaminated zone on the nonimpacted face of the web. The consistency of this material was much thinner and less cohesive than the two-component mortars. A thinned slurry coat was applied to the prewetted surface prior to placement. Figure 5.21 shows the material being placed on the web in the damaged zone on the nonimpacted face of the girder.

The working time was much shorter than either of the Latex-Modified mortars which severely hindered placement. Cold mixing water was used to offset the short working time (less than 10 minutes) and the material could only be placed to a maximum thickness of approximately 1/2-in. (1.3-cm) per lift. Moist curing was required, however this proved difficult on a vertical surface, and considerable shrinkage cracking was observed around the perimeter and throughout the entire patched zone. The excessive shrinkage cracking might have been lessened by use of a curing compound eliminating the need for moist curing.

Figure 5- 21   Placement of burke Acrylic Patch on nonimpacted side of girder
for repairing damaged area of the web

Fiber-Reinforced, Silica Fume Modified Mortar

EMACO S88CA required 24-hour presaturation of the repair substrate as well as a 7-day moist cure. Unlike the other V/O mortars, EMACO did not require the use of a slurry coat. It was very stiff and much darker than the original concrete due to the addition of silica fume as part of the material formulation (Figure 5.22). When applied thicker than 1-1/2-in. (38 mm), the material tended to sag, precluding single-lift repairs. Fine aggregate consisted of rounded silica beads which made the material difficult to finish, however use of a finishing agent proved beneficial. Because curing the vertical surface was extremely difficult, cracking was observed throughout the patch during the first 24 hours. However, when the cracked surface was struck with a hammer the patch appeared very sound.

Low Pressure Epoxy Injection. After all of the concrete patching was complete, low pressure injection equipment was used to inject epoxy into remaining cracks and voids to complete the concrete repair (Figure 5.23). Several problems arose with the use of this injection system. The most evident problem associated with the premeasured cartridges of resin and hardener was that complete mixing of the components was not always accomplished, and, as a result, some of the epoxy that was injected did not cure properly. Instructions provided by the manufacturer specifically stated that once the glass barrier between the resin and hardener was broken, vigorous mixing of the cartridge was to be avoided. Without vigorous shaking of the cartridge the two components were not always completely mixed, and therefore did not cure properly.

The use of one-way injection ports was necessary if the applied pressure was to be maintained. However, there were instances where the ports did not completely seal, and pressure was not able to be maintained after removal of the injection hose. When this occurred, the epoxy that had been injected

76

Figure 5- 22   Placement of MasterBuilders Emaco S88CA for web repair of nonimpacted side of girder

Figure 5- 23   Epoxy injection using low pressure injection system

simply seeped out of the ports where it had been injected. In this instance, injection hoses were left in place thereby providing a secondary one-way valve to maintain the pressure.

Workers had to take precautionary measures to insure against prolonged exposure of the epoxy with the skin. In one instance, one of the workers developed a severe allergic reaction to the epoxy and as a result any contact of the material with the skin caused irritation.

Even though some problems were encountered with the low pressure injection system, the overall effectiveness of the system proved adequate in sealing cracks and internal voids. Without epoxy injection, the integrity of the repair would have been questionable.

5.5 EVALUATION OF REPAIR BY NONDESTRUCTIVE METHODS

5.5.1 Monitoring Concrete Repair with the Rebound Hammer

It was found that there was no difference in surface hardness measurements after each phase of the repair; therefore, only the final rebound hammer measurements will be presented for comparison with those taken for damage assessment purposes. A contour of post-repair rebound hammer results was plotted for each face of the girder showing the variation of surface hardness over the repaired zones. Results of damage assessment rebound measurements are repeated for comparison to post-repair results (Figure 5.24). Comparison of the measurements reveals that the surface hardness of the damaged girder clearly indicated the damaged zones; however, post-repair rebound numbers indicated a sound repair had been accomplished. It should be emphasized that the rebound hammer is not sensitive enough to distinguish internal flaws with any degree of accuracy, and therefore, as a means of providing quality assurance, the rebound hammer cannot detect areas where internal damage remains after the repair is complete. The rebound hammer should not be used for quality assessment of repaired concrete for this reason alone; however, it may be possible to detect patched areas that have not sufficiently adhered to the concrete substrate with the rebound hammer.

5.5.2 Monitoring Concrete Repair Using the Impact Echo Method

Impact echo measurements were taken during and after the repair. The normalized amplitude spectrum for each location was generated and used for qualitative comparison. As an example, Figure 5.25 shows a comparison of pre- and post-repair impact echo responses for a web location at station 18. The normalized amplitude spectrum for the upper web location on the impacted side is shown. In the damaged state delaminated concrete is detected at this location (refer to Figure 4.15 and discussion of damage assessment). After patching the damage, there was an evident shift in the response to a peak amplitude at a frequency of 12.21 kHz, the web solid thickness frequency. The response following injection at this location did not change significantly between the patched and injected phase; both reveal a peak amplitude at the solid thickness frequency.

The amplitude spectra at each web location were then used to generate a contour of spectra along the web for the impacted side. Figures 5.26 and 5.27 show the spectral contours for the impacted side of the girder in the damaged state and after concrete patching and epoxy injection, respectively. It should be noted that these contours do not differentiate between the maximum peak amplitude at each location, but instead are meant to be interpreted in a qualitative fashion by showing relative changes in the impact-echo response as the member underwent repair.

Impacted Face of Girder   Nonimpacted Face of Girder

(a) Damage Assessment   (b) Damage Assessment

(1 in. = 2.54 cm)

(c) Post-repair assessment   (d) Post-repair assessment

Figure 5- 24   *Comparison of rebound measurement before and after concrete repair*

Normalized Amplitude Spectrum

Solid Thickness
Frequency = 12.21 kHz

Figure 5- 25   *Quality assessment of concrete repairs using impact echo — upper web location — Station 18 — impacted face*

79

Normalized Amplitude Spectrum Contours

Solid Thickness
Frequency = 12.21 kHz

Amplitude

☐ 0.75-1.00
■ 0.50-0.75
☐ 0.25-0.50

Figure 5- 26   Global damage assessment using impact echo - upper web location

Figure 5.26 indicates that stations 15 through 42 are dominated by peak amplitudes composed of low frequency response or delaminated areas. The dark zones indicating frequency responses at amplitudes from 0.75 to 1.0 are observed at low frequencies which were interpreted as delaminated zones. The interpretation of the impact echo response was substantiated by visual inspection as discussed in Section 4.3.5. When the epoxy was injected after the concrete was patched using various materials, a shift towards a solid vibrational mode of response was indicated for the most dominant peaks in the 0.75 to 1.0 range (Figure 5.27). There is a distinct decrease of what appears to be low frequency vibration indicating that partial restoration of member integrity has occurred over its length at the upper web sampling location.

Normalized Amplitude Spectrum Contours

Approximate Shift in
Frequency Response

Solid Thickness
Frequency = 12.21 kHz

Amplitude

▦ 0.75-1.00
■ 0.50-0.75
☐ 0.25-0.50

Figure 5- 27   Global assessment of epoxy injection phase - upper web area - impacted face

80

Normalized Amplitude Spectrum
Bottom Flange Location - Station 46 - Impacted Face

Solid Thickness
Frequency = 5.27 kHz

Figure 5- 28   Localized assessment of concrete repair using impact echo - bottom flange - impacted face

In terms of localized assessment of the repair, station 46 only required epoxy injection, not any patching of the concrete. Figure 5.28 shows the results from pre- and post-repair impact echo results for the bottom flange location at station 46. It is evident that the epoxy injection improved the integrity of the member at this location as revealed by a shift in the peak amplitude towards the solid thickness frequency of 5.27 kHz. In the damaged state the maximum amplitude occurred at a frequency of 2.93 kHz and, once the girder was injected, the peak amplitude occurred at a frequency of 4.39 kHz. Again, as stated in the discussion of impact echo results for the bottom flange sampling locations (Section 4.3.5), there appears to be a discrepancy between the measured frequency and the calculated solid thickness frequency (5.27 kHz vs. 4.39 kHz). However, it is possible that the geometry of the flange itself causes the response to contain some amount of flexural vibration which could account for the discrepancy between measured and expected frequencies (refer to Figure 4.17 and the corresponding discussion of damage assessment results for stations 41 and 42 respectively).

Again, the individual spectra for each location along the bottom flange were combined to form a spectral contour along the length of the member for the damaged state and after the girder was both patched and injected. These are shown in Figures 5.29 and 5.30. As discussed in Section 4.3.5, the results of global damage assessment using the impact echo method revealed that no clear pattern existed in the spectral contour, and that damage was indicated throughout the length of the girder. The range of maximum normalized amplitude, or most dominant peak of the frequency response, was very large with a minimum frequency of 0.98 kHz to a maximum of 9.28 kHz indicating damage throughout the length of the member (Figure 5.29). However, as the repair progressed, impact echo data indicated a shift towards a solid vibrational mode of 5.27 kHz (compare high amplitude regions in Figures 5.29 and 5.30). Following concrete repair by patching and epoxy injection, the range of frequency content was drastically reduced as compared to the damaged state. The minimum dominant frequency measured 3.42 kHz and the maximum measured was 4.39 kHz, both of which are much closer to the solid mode vibrational frequency of 5.27 kHz (Figure 5.30). The shift in the peak amplitudes found from the

81

Normalized Amplitude Spectrum Contours

Figure 5- 29   Global damage assessment using impact echo - bottom flange area - impacted face

Normalized Amplitude Spectrum Contours

Figure 5- 30   Global assessment of epoxy injection phase - bottom flange area - impacted face

Figure 5-31   Assessment of concrete repair using SASW method - bottom haunch location (47-48)

injection assessment spectral contour indicated that along the length of the repaired girder integrity had for the most part been restored. The peak amplitudes for the bottom flange sampling locations along the length of the girder became much more uniform indicating a clear pattern of a solid vibrational mode of response.

5.5.3 Monitoring Repair Using SASW Technique

SASW measurements were taken after application of preload and patching of damage, after epoxy injection, and removal of preload. Dispersion curves were generated for each interval over the length of the beam for comparison. As an illustration, the dispersion curves for the different repair phases at interval 47 to 48 are shown in Figure 5.31. Prior to repair, surface wave velocities were less than 7,000 ft/s (2,130 m/s) due to damage beneath the surface of the beam. After the application of preload and patching of the concrete with various materials, surface wave velocities decreased and the integrity of the beam at this location appeared to deteriorate. This was most likely due to the development of additional cracking upon application of preload. Note that no new concrete was placed at this location. After epoxy injection, surface wave velocities were greater than 7,000 ft/s (2,130 m/s) at all wavelengths indicating that integrity had been restored.

The dispersion curves developed between each station interval were combined to generate a contour of surface wave velocity versus wavelength along the length of the girder for each phase as well as in the damaged state. Comparison of the contours in Figure 5.32 and Figure 5.33 give an indication of the ability of the SASW technique to monitor effectiveness of the patching and epoxy injection. In the damaged, state several zones of low surface wave velocity are evident (Figure 5.32-a) from stations intervals 17 to 18 (plotted at 17.5) through interval 37 to 38 (plotted at 37.5) and then again from intervals between stations 45 and 50. Once the patching phase was complete (Figure 5.32-b), there appeared to be a definite increase in surface wave velocities from station intervals between 17 and 33 (plotted at 17.5 through 32.5) indicating the effectiveness of the repair in this region. However, between station intervals 33 to 38 (plotted at 33.5 through 37.5) the zone of low surface wave velocity appears to have increased in size, and station intervals between 45 and 50 surface wave velocities appear to have

Damage Assessment

(a)

Impact
Location

After Patching

(b)

Impact
Station Along Beam

Surface Wave Velocities (ft/s)

| ■ 6000-7000 | ■ 7000-8000 | □ 8000-9000 |

(1 ft. = 0.3048 m)

Figure 5- 32   Global assessment of damaged and patched girder using SASW - lower haunch area - impacted face

Load-Deflection Response of Repaired Girder
After Concrete Patching and Epoxy Injection

Figure 5- 33   Load deflection response of Steck girder after concrete repair and epoxy injection

decreased. This is most likely due to the formation of additional cracking upon application of the preload. After epoxy injection was complete, very low surface wave velocity zones ranging from 4,000 to 5,000 ft/s (1,219 to 1,524 m/s) exhibited a velocity increase to 6,000 to 7,000 ft/s (1,830 to 2,130 m/s) range (Figure 5.33-a) and upon removal of the preload the few zones below 7,000 ft/s (2,130 m/s) surface wave velocity practically disappeared (Figure 5.33-b). This is more than likely due to the closing of any remaining cracks upon the removal of preload.

5.6 POST-REPAIR NONDESTRUCTIVE LOAD TESTS

Evaluation of the effects of concrete repair was made possible by nondestructive load testing of the repaired girder. The load tests consisted of two cycles of static loading. Removal of preload was monitored and followed by a single cycle of static loading to compare the stiffness of the girder and strains in the instrumented tendons after repair with measured values obtained prior to repair. After repairing the cracks of the siderail portion of the girder by epoxy injection, a second cycle of static loading was applied. Instrumentation for displacements of the girder, deformations of tendons, and monitoring of applied pressure were discussed previously.

5.6.1 Results of Post-Concrete Repair Load Tests

An elastic analysis based on the undamaged cross sectional properties of the composite girder was performed and compared with experimental results for the load-displacement response as discussed previously in Section 4.4.4.1.

Experimental Load-Deflection Response and Section Stiffness. Figure 5.33 shows the experimental results obtained for the load-deflection response at each of the three instrumented cross sections. Linear regression of experimental measurements revealed that the slope of the load-deflection response, or member stiffness, at the south load point was 250 kips/in. (43,800 kN/m), an increase of 18 % from the damaged state. The center span stiffness was measured to be 217 kips/in. (37,950 kN/m), an increase of 14 % from the damaged state, and at the north load point the measured stiffness was 292 kips/in. (51,000 kN/m), an increase of 17 %.

It is still evident from these results that even though the girder was repaired, the nature of the damage still resulted in unsymmetric displacement of the girder. However, as previously discussed, the stiffness of the member is not extremely important to the overall performance of the girder in terms of functionality.

Figure 5.34 shows the comparison of damaged, post-repair experimental and theoretical load-displacement response at the center span section. The theoretical center span displacement at an applied load of 82 kips (365 kN) per load point was 0.18 in. (5 mm) and the theoretical undamaged stiffness was found to be 455 kips/in. (79,700 kN/m). In the damaged state, a displacement of 0.55 in. (14 mm) was measured at 82 kips (365 kN), and the damaged stiffness based on linear regression of experimental results was found to be 152 kips/in. (26,600 kN/m), only 33% of the undamaged stiffness. Once the girder was repaired (patched and injected), the measured displacement was reduced to 0.38 in. (10 mm). The repaired member stiffness was found to be 217 kips/in. (37,950 kN/m), 48% of the undamaged stiffness, an increase of 15% from the damaged state.

After the initial post-repair load test was performed, the cracks in the top siderail portion of the girder were injected with epoxy. Once the epoxy cured, the girder was load tested for comparison with the damaged and repaired states. The displacement at the south load point reduced from 0.33 in. (8.4 mm) to

Load-Deflection Response of Repaired Girder
Comparison at Different Stages of Repair

Figure 5- 34   Experimental load deflection response of Steck girder after concrete repair and epoxy injection

0.28 in. (7.1 mm) at a load of 82 kips (365 kN), a 15 % decrease in displacement. The experimental stiffness at this location increased from 250 kips/in. (43,800 kN/m) to 289 kips/in. (50,600 kN/m). The midspan displacement decreased from 0.38 in. (9.7 mm) at a load of 82 kips (365 kN) to 0.32 in. (8.1 mm), approximately a 15 % decrease, while the stiffness increased from 217 kips/in. (37,950 kN/m) to 249 kips/in. (43,600 kN/m). The displacement at the north load point decreased from 0.28 in. (7.1 mm) to 0.25 in. (6.4 mm) at a load of 82 kips (365 kN), a decrease of approximately 10 %, and the stiffness increased from 292 kips/in. (51,000 kN/m) to 323 kips/in. (56,600 kN/m).

Measured Response of Instrumented Tendons. The measured strains in the bottom instrumented tendon at the south cross section are shown in Figure 5.35. Tendon strains are shown for the damaged state, the effects of preloading prior to repair, the repaired state, and after the final injection of the siderail cracks. The first observations that can be made concerning the experimental measurements of tendon deformations at this location, is that the slope of the load-deformation response in the damaged state is much less than after the initial repair was complete. It is possible to follow the history of the tendon response from stage 1(damaged state) up to a preload level of 54 kips (240 kN) per load point to stage 2 when the repair was performed. Once the concrete patching and epoxy injection were accomplished while maintaining the preload at stage 2, the preload was removed. The tendon strains then followed the unloading curve to stage 3 after removal of preload. Stage 3 identifies a very important effect of preloading the girder prior to repair. By applying preload it is shown here that the effective prestress in the tendon increases and, at the same time, the patch material in the bottom flange is compressed. Upon subsequent load application, the response of the tendon follows the loading curve beyond the level of applied preload (stage 4) until stage 5 is reached. Cracks form within the patch at stage 5 at an applied load of 78 kips (347 kN) per load point when both the precompression supplied by preloading as well as the tensile resistance of the patch material are eventually overcome. Following the loading history through stage 5, the response changes from uncracked behavior (prior to stage 5) through a transition to

86

Load-Deformation of Tendon at Section I
Steck Girder

*Figure 5- 35   Experimental load-deformation response of tendon at south
cross section following concrete repair*

cracked response, and eventually unloading through stage 6. Once the siderail cracks were repaired and the girder again loaded, the load history of the tendon follows through stage 7 where the transition from an uncracked to a cracked response is again experienced. However, it should be noted that this transition occurs very near the level of preload at approximately 54 kips (240 kN) rather than at the higher level of load when not only precompression needed to be overcome, but the tensile strength of the patch as well, which, after initial loading, had already experienced flexural cracking .

The measured response of the bottom instrumented tendon at the midspan cross section is shown in Figure 5.36. Here again a comparison is made between behavior in the damaged state, effects of preloading prior to repair, repaired state, and after final injection of the sidewall cracks. The behavior is very similar to the results shown for the south cross section. It is evident that the effects of preload lead to an obvious change in slope of the curve before and after the repair was performed. As the preload was applied deformations followed the same path as measured in the damaged state (refer to stage 1 in Figure 5.36). The repair was performed while the preload was sustained at 54 kips (240 kN) per load point (refer to stage 2 in Figure 5.36). After concrete patching and epoxy injection, the preload was removed and the unloading path defined between stage 2 and stage 3. Again the effects of preload are evident: increased stiffness, higher effective prestress, and precompression of the patched zone. The difference between the response at the midspan and the south cross sections was that the centerspan section was not stressed as highly as the severely damaged south cross section and therefore did not crack upon subsequent loading.

In comparison to the south and center span locations, the tendon behavior at the north cross section changed very little (Figure 5.37). It was shown in Chapter 4 that the north cross section sustained very little concrete damage. As a result, the effects of preload and concrete repair are not as significant as was shown for the other two cross sections. However, there does appear to be a slight change in the behavior

Load-Deformation of Tendon at Section II
Center Span - Steck Girder

Preload Level = 54 kips

Legend:
— Preloading/Removal
—∘— Top Injected
- - Repaired/Injected
··∘·· Damaged Section

Figure 5- 36   Load-deformation response of tendon at center span cross section following concrete repair

Preload Level = 54 kips

Legend:
- - - Preloading/Removal
········ Top Injected
—— Repaired/Injected
—— Damaged Section

Figure 5- 37   Experimental load-deformation response of tendon at north cross section following concrete repair

when comparing the damaged to the repaired state; the slope of the girder load versus change in tendon strain curve increases, signifying that the repair had a beneficial effect.

5.7   POST-REPAIR DESTRUCTIVE EVALUATION OF GIRDER CONCRETE REPAIR

Once the concrete and strand repair studies for Steck girder were complete, the girder was saw-cut through the entire thickness of the cross section at two locations in order to confirm the condition of the beam after repair (patching and epoxy injection). The girder was saw-cut while still in the laboratory as shown in Figure 5.38. The girder was braced to prevent movement during the sawing procedure. Figure 5.39 through Figure 5.41 are close up views of cross sections of the repaired girder.

The most evident observation from these photographs is that the low pressure epoxy injection system combined with the internal injection procedure was effective at sealing and filling the remaining internal cracks and voids following the concrete patching. Figure 5.40 and Figure 5.41 clearly reveal the depth of epoxy penetration when using the low pressure injection system and internal injection ports. The void space within the web of the member was completely filled with epoxy at this

Figure 5- 38   Photograph showing saw-cut section while girder is still in place

location (Figure 5.40). It is also evident from the close-up photographs that, for the most part, the hand-applied materials bonded to the concrete substrate around the perimeter of the patches. In some locations where the bond appeared questionable, the injected epoxy was able to penetrate and fill any spaces that existed around the patch perimeter.

Figure 5- 39   Photograph of interior of repaired girder showing cast-in-place, hand-applied, and injected repair materials

Figure 5- 40   Close-up detail of web section of repaired girder showing benefits of epoxy injection through internal injection ports.

Figure 5- 41   Photograph showing epoxy penetration at a bottom flange repair location

CHAPTER 6

PRESTRESSING STRAND REPAIR TEST PROGRAM

6.1 INTRODUCTION

In structures where impact damage to the bottom flange of a girder damages or severs prestressing tendons, the damaged tendons may need to be repaired. Strand splicing hardware will be needed to repair the strand and to restore prestress to the member internally. Used in combination with preloading, strand splicing may offer a means of restoring integrity and strength to a damaged girder. Laboratory tests of internal strand splice installations on severed strands were conducted. The Steck girder was used for these tests, and the strands were intentionally severed. In addition splice hardware was tested to ultimate load in a testing machine. Finally, the Steck girder was repaired using a combination of preloading, internal strand splices, and cast-in-place concrete to repair damaged areas and loaded to determine flexural characteristics.

6.2 IDENTIFICATION OF INTERNAL STRAND SPLICES

The first objective was to identify commercially available hardware for splicing damaged strands as well as splice hardware which might require fabrication. Several different types of strand splice hardware were identified, however not all were included in the test program.

A commercially available splice that has been widely used for repairing impact damage to prestressing strands was the Grab-It™ Cable Splice, supplied by Prestress Supply Incorporated. The Grab-It™ splice assembly consists of single usage wedge anchorages at each end of the splice to grip the strand, along with an integral threaded rod and a turnbuckle assembly as shown in the photograph in Figure 6.1. One side of the assembly has a left hand thread while the other side has a right hand thread to enable the anchorages to be held stationary while the turnbuckle in the center is torqued to induce tension in the repaired strand. Detailed drawings and material specifications for the Grab-It™ Cable Splice can be found in Appendix A.

Figure 6- 1   Exploded view of Grab-I™t cable splice

A splice manufactured by DYWIDAG International has strand grips that are offset to allow hydraulic stressing of the strand during repair. This splice assembly is used mainly for prestressed or post-tensioned concrete members where the spacing of strands is typically much greater than the standard 2-in. (5-cm) spacing found in most prestressed bridge girders. The DYWIDAG assembly was considered impractical for use in repair of impact damage of prestressed I-shaped bridge girders, and was not included in the experimental program.

An assembly that has been used for repair of impact damaged bridge girders in Canada was designed by The Alberta Transportation and Utilities Department. The assembly uses a combination of commercially available components along with components which must be fabricated. The assembly is fabricated from 2-in.- (5-cm-) diameter hex stock which is bored out to accept standard strand wedge anchorages. The anchorages have to be machined down to a 9/16-in. (1.4-cm) outside diameter, and a bolt is also fabricated from the same 2-in. (5-cm) hex stock. As the threads of the bolt or bored out nut are advanced, the wedge anchorages are brought closer together inducing tension in the strand. A half-size drawing of the assembly which was provided courtesy of The Alberta Transportation and Utilities Department can be found in Appendix A. An exploded view of the fabricated assembly is shown in the photograph in Figure 6.2 and detail drawings of the splice can be found in Appendix A.

Figure 6- 2   Splice hardware designed and used by Alberta Transportation and Utilities Department (fabricated at The University of Texas at Austin

Another splice included in the test program was a multiple bolt assembly with swaged end anchorages which is manufactured by Barsplice Incorporated. Due to the swaging process, this splice required partial fabrication. The swaging is carried out in a two stage process; first hydraulic dies press indentations into the tendon to provide anchorage for the swage sleeve. The swage sleeve is hydraulically squeezed or swaged onto the "deformed" tendon. The manufacturer can provide rental equipment for swaging tendons in the field rather than sending sections of strand for prefabricated swaged sections. A schematic of the swaging process is shown in Figure 6.3. A photograph of the multi-bolt splice assembly is shown in Figure 6.4, and a half-size drawing of the splice is found in Appendix A. Material specifications for the different components were not available from the manufacturer. As with other splice assemblies, bolts are advanced into the threads of the transfer plate and the ends of the strand are brought closer together to produce tension in the assembly.

Figure 6- 3   Schematic of two-stage swage process used by Barsplice Incorporated

Figure 6- 4   Multi-bolt swaged anchorage splice assembly manufactured by Barsplice Incorporated

Dual Tendons with Swaged Anchorages

2" Hex Turnbuckle

12" Long High Strength Bolt (LH/RH Threads)

Transfer Plate

Figure 6- 5   Schematic of dual tendon splice with swaged end anchorages

Barsplice Incorporated manufactures a splice very similar to the Grab-It™ splice which uses a single turnbuckle assembly to induce tension in the strand. The only difference between the two assemblies is that the Grab-It™ uses wedge anchorages whereas the Barsplice assembly uses swaged anchorages. The Barsplice turnbuckle assembly was not included in the test program.

The last splice assembly identified was described in NCHRP Project 12-21 and was modified for inclusion in this investigation. The assembly was originally a dual strand splice which was fabricated using an upset threaded rod in order to accommodate the larger dimensions of standard commercially available wedge anchorages while maintaining the 2-in. (5-cm) strand spacing. Rather than using an upset threaded rod, the splice was modified to utilize swaged end anchorages which were of much smaller diameter rather than commercially available wedge anchors. In this way an upset threaded rod was not required for clearance between the bolt and the strand anchorage. A schematic of the dual tendon swaged anchorage assembly is shown in Figure 6.5. The original design from NCHRP Project 12-21 along with the modified version of the dual strand splice can be found in Appendix A.

The splice assemblies that were included in the strand repair test program were as follows:

- 2-in. (5-cm) Hex Barrel Splice - Alberta Transportation and Utilities Department

- Multi-Bolt with Swage Anchorages - Barsplice Incorporated

- Dual Strand Splice with Swage Anchorages - Barsplice Incorporated

- Grab-It™ Cable Splice - Prestress Supply Incorporated

6.3   STRAND INSTALLATION TEST PROGRAM - STECK GIRDER

6.3.1   Modification of Girder Cross Section

The side rail portion of the girder was removed over a 2 ft. 6 in. (0.76 m) length at midspan (Figure 6.6). The midspan cross section was reduced so that higher tendon stresses could be achieved without moving the test frame to achieve the same stress levels. Once the side rail was removed to the level at the top of the cast-in-place slab, a single cycle of static load was applied to the girder to evaluate any changes in tendon deformations and member stiffness due to the reduced cross section. Results of this initial load test were used as a base level of response for comparison with the response following installation of each splice assembly.

(1 ft = 0.3048 m)

Figure 6- 6   Schematic of reduced cross section and strain gage placement

6.3.2 Girder Instrumentation and Preliminary Load Tests

Since the girder loading frame was not moved or modified for the strand tests, the location of deflection measurements remained the same as for all previous load tests. Deflections were measured at each load point and at the midspan location. Instrumentation of the tendons, however, was modified to accommodate measurement of deformations for each spliced strand. The six bottom corner strands on the impacted side of the girder were exposed for approximately a 6-in. (15-cm) length at three locations: midspan, and approximately 3 ft. (0.91 m) from each side of midspan as shown schematically in Figure 6.7. Each tendon had two strain gages applied to different wires at each of the end openings.

Following instrumentation with strain gages, the tendons were severed one at a time at the midspan opening.

6.3.3 Monitoring Stressing of Strand Splices

In order to assure that the correct level of prestress was applied to a strand undergoing repair, different methods of monitoring the stressing operations were investigated. Not all methods could be used for each splice assembly due to dimensional constraints, however, each method will be discussed.

Strand Elongation Measurements. Average strand elongations were measured using a dial gage apparatus developed by The Alberta Transportation and Utilities Department. This device was used for the Grab-It™ splice and the Alberta splice, but not for either of the swaged assemblies. The swage splices were longer than the others, and not enough length of exposed strand was available for installation of the dial gage assembly. The dial gage assembly was slightly modified from the original design by removing the pvc tubing, and is shown in the photograph in Figure 6.8. A detailed drawing of the Alberta splice in Appendix A includes a design for the dial gage assembly.

(1 ft = 0.3048 m)

Figure 6- 7   Instrumentation of strands for splice investigations

96

Figure 6- 8   Elongation measureing device (Design courtesy of The Alberta Transportation Utilities Department)

Strain Gages. Strain gages were also used to monitor elongations of individual wires of the repaired strands. Stresses were calculated based on measured strains and an assumed elastic modulus of the strand of 28,000 ksi (193 MPa). Since the length of strand that was removed from the girder was in excess of the length of each type of splice hardware, an additional length of strand was spliced into the damaged region. This new section of strand was also instrumented with strain gages to provide redundancy in strain measurements in case some gages were damaged.

Torque Measurement. Indirect measurement of tension using the applied torque was also investigated. A 600 lb.-ft. (813 N-m) torque wrench was used to measure the torque applied to the turnbuckle portion of the Grab-It™ splice assembly. Comparisons between manufacturer recommended and measured torque values were made. The available torque wrench could not be used on other splices due to dimensional constraints and the size of the open ended wrench attachment.

Tendon Stress Indicator. Part of the laboratory investigations for Project 1370 was to investigate different methods of evaluating the remaining prestress after the occurrence of impact damage. Several techniques were identified that have been used on exposed strands in the past. As part of this investigation a method based on the lateral stiffness of a stressed tendon was developed (9). The device that was developed was not only used for evaluation purposes, but also for monitoring the stressing of tendons during splice repairs. A photograph of the apparatus is shown in Figure 6.9. As transverse load is applied to the stressed tendon, the resulting lateral displacement of the tendon is recorded. The slope of the transverse load versus lateral tendon displacement based on calibration curves for a given tendon size provides an indication of the tendon tension, and the associated tendon stress.

6.3.4 Initial Evaluation of Strand Splice Hardware

Prior to using any of the splice hardware for strand repairs, tests were conducted for each splice assembly to ensure that each was capable of being used safely. The unexpected failure of any of these splices during stressing could lead to a very dangerous situation where fracture of a highly stressed tendon and/or splice could injure the operator.

Grab-It™ Cable Splice - Working Load Torque Tests. Prior to using the Grab-It™ splice to repair damaged tendons in Steck girder a series of tests were carried out to ensure that the splice was capable of safely inducing a tension of approximately 25 kips (111 kN) without failure. A tendon was placed in a stress bed equipped with a 50 kip (222 kN) load cell to monitor the tension of the strand as the splice was tightened. Recommended torque values were based on both lubricated and dry threads. For a tension of 25 kips (111 kN) the recommended dry torque was 313 lb.-ft. (424 N-m), and for lubricated threads the

Figure 6- 9   Tendon stress indicating device developed as part of Project 1370

recommended value was 234 lb.-ft. (317 N-m). The first test involved applying torque to the assembly without lubrication of the threads, and for the second test the threads were cleaned on a wire wheel and lubricated with grease.

Without using any lubrication the turnbuckle was very difficult to torque. The initial test was stopped when the applied torque reached 550 lb.-ft. (746 N-m) and resulted in an induced tension of only 17.5 kips (78 kN). The results varied significantly from the recommended torque value. The test was halted when the turnbuckle began to show signs of failure; cracks formed through the entire thickness of the turnbuckle and the torque wrench began to slip and strip the outside of the turnbuckle. Figures 6.10 and 6.11 show the interior and exterior of the turnbuckle respectively after removal from the stress bed.

Figure 6- 10   Grab-It^{TM} cable splice — cracks through interior threads - dry threads - torque proof test

When the external threads were cleaned with a wire wheel and then lubricated, the required torque was closer to the expected value; tensioning of the splice was more reliable and much safer to install when the threads were lubricated. At an applied torque of 250 lb.-ft. (339 N-m) the induced tension was measured to be 25 kips (111 kN). Figure 6.12 shows the exterior of the turnbuckle after the test with lubricated threads. It is evident from the

Figure 6- 11   Grab-It^{TM} cable splice — exterior of turnbuckle - dry threads - torque proof test

results that if the Grab-It™ splice assembly is to be used safely and reliably, the threads must be thoroughly cleaned and lubricated prior to stressing.

Alberta Transportation and Utilities Department Splice - Working Load Test. Using the same stress bed, tests were carried out for the Alberta splice. Although the applied torque was not measured, the installation and stressing of the splice was evaluated for safety and reliability. Based on prior experience with the Grab-It™ assembly, only lubricated thread tests were carried out. Four splices were fabricated for installation and repair of the severed strands in Steck girder, however, after initial evaluation of the splice was carried out, it became evident that there was a basic flaw with the modified design of the splice.

Figure 6- 12   Grab-It^{TM} cable splice — exterior of turnbuclke - lubricated threads, torque proof test

The thrust bearings that were intended to isolate the rotation of the splice from the strand did not work as intended. The bearings at each end of the splice sleeve did not work properly and therefore did not isolate rotation of the splice sleeve and bolt from rotation of the strand. As the bearing at the threaded end of the splice rotated, damage to the threads and the bearing resulted. As torque was applied to the assembly and the thrust bearings began to bind, the strand twisted such that it began to unravel. The only modification that was made to the original design of the splice more than likely caused this problem to worsen. The original design called for a buttress thread for the bolt and matching splice sleeve. Upon closer evaluation of the original design it appears that the intent of using the buttress thread was to alleviate the problem of binding of the thrust bearing by allowing the bearing to slide over the angled or buttress thread as the tendon was stressed. However, the laboratory machine shop did not have the capability to produce a buttress thread. Even though the bearings did not function properly this splice was able to be consistently, reliably, and safely tensioned to the desired working load of 25 kips (111 kN), and it was decided to attempt strand repairs with the splice. If the threads were damaged during installation, then they were machined a second time so that the splice could be reused for ultimate strength tests of the assembly.

Multi-Bolt Swaged Splice Assembly - Working Load Test. The swaged anchorages of this splice were only rated at 90 % of the ultimate strength of 270 ksi (1862 MPa) strand or approximately 37.2 kips (165 kN). The main reason for the reduction in strength was due to the swage process during which the effective cross sectional area of the tendon was reduced in order to prevent the strand from slipping through the swage sleeve (Figure 6.3). Prior to attempting installation of the swaged splice, a single torque test was carried out to determine if the splice could be installed safely. First, it was found that the bolts supplied with the splice (ASTM 193 B7) did not have enough thread length to sufficiently tension the assembly to the desired load. Threaded rods with double hardened nuts were cut to length and used instead of the bolts supplied with the splice. It was found that the multiple bolt assembly could be tightened to reach the required working load of 25 kips (111 kN) using the threaded rods, however, the strand tended to twist as torque was applied to the individual bolts because of difficulty in restraining the assembly during stressing. It was found that if a single bolt was tightened too much, uneven tension and bending of the bolts occurred. It was decided that the splice could be safely stressed and strand repairs using the multi-bolt swaged splice were attempted.

Dual Strand Swaged Splice Assembly - Working Load Test. The stress bed that was used for the previous working load tests on all other splice assemblies was built for only a single strand. The working load tests for the dual strand splice were carried out using a Tinius Olsen 120 Kip (534 kN) capacity displacement controlled test machine. The splice was installed between the platens of the machine, the transfer plates at each end of the splice restrained from rotating using crescent wrenches, and the turnbuckle torqued to induce tension in the strands. Using an open ended crescent wrench and a four foot length of pipe for additional leverage, the splice could be safely tensioned to a working load of 45 kips (200 kN) before the wrenches began to slip on the both turnbuckle and the transfer plates. It was decided to attempt strand repairs of Steck girder using the dual tendon splice.

6.4 STRAND REPAIRS - INSTALLATION OF INDIVIDUAL SPLICE ASSEMBLIES

Four series of strand repair tests were carried out, one for each splice assembly. Each test, with the exception of the dual strand swaged splice, consisted of installing splices on the four bottom corner tendons that were previously severed. Once all four tendons were spliced and stressed, a single cycle of static load was applied to the girder, the results evaluated, and the two outer splices were removed. A second static load cycle was then applied to the girder to evaluate the changes in member stiffness and

Numbering Sequence for
Repaired Tendons (1 - 4) and
Adjacent Intact Tendons (5 & 6)

Figure 6- 13   Numbering sequence for internal strand splice repairs of severed tendons (1 through 4) and adjacent tendons (5 and 6)

characteristics of tendon deformations with only two strands spliced. In order to summarize the results for each series of splice installations, the strand numbering scheme shown in Figure 6.13 was utilized. Strands one through four were individually stressed, the girder loaded, splices one and two were removed and the girder retested. The splices on strands three and four were then removed. This was the general procedure for all but the dual strand splice. For the dual splice assembly only tendons three and four were repaired. In addition a single cycle of static load was applied to the girder in between each series of installations to determine if the girder stiffness had changed significantly. The order in which the installations were carried out was as follows:

- Alberta Splice

- Multi-Bolt Swaged Splice (Barsplice Incorporated)

- Dual Tendon Swaged Splice (Project 12-21 and Barsplice Incorporated)

- Grab-It™ Splice (Prestress Supply Incorporated)

General observations of problems encountered during installation of each assembly will first be presented. Following a description of the general observations, results of static load testing and strand stressing for each splice assembly will be discussed.

6.4.1 Alberta Transportation and Utilities Department Strand Splice Installation

Observations During Splice Installation. Installation of the Alberta splice hardware was fairly simple and straightforward. In order to provide clearance for tightening the individual splices had to be staggered; splices for tendons one and four were placed at the north end of the repair zone, and splices for tendon numbers two and three were placed at the south end of the repair zone. Because the length of the splices was shorter than the length of tendon that was removed when each strand was severed, additional sections of strand were spliced into the repair as shown schematically in Figure 6.14. Each of the four splices were initially located to determine both the required stagger between the devices and the additional length of strand required for each splice. For ease of installation as well as wrench clearance, the individual splices were applied in the following order: 4, 3, 1, 2.

Zero readings for the strain gages were taken prior to the installation of each splice assembly in order to reduce errors in measurement due to bending of the tendon under the weight of the splice. The splice was installed and the slack removed by sliding the tendon through the wedge anchorages in both the

splice and coupling device. If this did not remove most of the slack, the splice was engaged until slack was removed. After the slack was removed, the elongation measuring device was placed over an 18 in. (45.7 cm) gage length either on the new section of tendon or on the original section of tendon, whichever would allow sufficient length for the device (Figure 6.15). If there was not enough room for an 18 in. (45.7 cm) gage length, the device was shortened accordingly.

Figure 6- 14   Schematic of installation of Alberta splice assembly

Rather than having one person hold one end of the splice (either the bolt or the sleeve) and the other person torque the assembly, a method was devised which only required one person to stress the tendon. A wrench was placed on one end of the assembly with a pipe extension and was either held down with weight keeping it from turning, or the extension was supported on the laboratory floor to react against rotation of the splice, depending on torque direction (Figure 6.15). In the field this could be done with a bracket attached to the girder. At different stages during stressing, both elongation measurements and individual wire strains were monitored. When the tension in the strand approached the working load, the Tendon Stress Indicating Device (Section 6.3.3) was used to evaluate the tension induced in the strand.

During installation of the splice on strand number two it was observed that the thrust bearing began to bind up to such an extent that the twist angle of the strand became almost horizontal as shown in the photograph in Figure 6.16. At this stage stressing of this spliced strand was stopped. Figure 6.17 shows the completed repair of all four severed strands using the Alberta splice.

Stressing of Splices. Due to twisting of the strand when stressing each splice assembly, elongation measurements were not possible because the axis of the dial gage assembly rotated off center. As rotation of the strands occurred, observed strain gage measurements were found to be unreliable as well. Table 6.1 summarizes both strain gage readings as well as the tension indicated using the lateral load-deflection method (Tendon Stress Indicator).

It is quite obvious that strain measurements of individual wires of each spliced strand were very inconsistent. The rotation of the strand consistently caused one side of the splice to have higher readings than the other with the exception of strand number one. Because of the inconsistencies in measurements with the strain gages when used with this splice, a series of stressing tests for the Alberta splice were conducted in the stress bed with the use of a 50 kip (222 kN) load cell in order to evaluate how the strand rotation affected the measured strains.

A single strand was spliced in the stress bed with two strain gages on each side of the splice and oriented as shown in Figure 6.18. First, the bolt was restrained and torque applied to the splice sleeve. Next the strand was stressed using a hydraulic ram to avoid twisting of the strand. Finally the splice sleeve was restrained while torque was applied to the bolt. Results of each test are shown in Figure 6.19 through Figure 6.21.

Figure 6-15   Installation of Alberta splice and measurement of average strand elongation to monitor stress level

It is obvious when evaluating the results from the additional stress monitoring tests of the Alberta splice that the effects of twisting of the strand are observed in the measured deformation response of the tendon.(Figure 6.19 and Figure 6.21). When torque is applied to one side of the splice while the other side is restrained against twisting, rotational energy is stored in the strand on the unrestrained side. As the direction of the applied torque is reversed (the splice unloaded), this energy is immediately released as evidenced by the flat portion of the unrestrained curves in Figure 6.19 and Figure 6.21. It is also evident that when the splice is stressed hydraulically, this twisting behavior is not observed as shown in Figure 6.20. These tests reveal more detailed behavior than was possible for splices that were installed in the girder as the load in the tendon could be directly monitored with a load cell.

Figure 6-16   Binding of thrust bearing causing extreme twisting of spliced strand

Load-Deflection Response of Repaired Girder. In order to evaluate the overall effects of repairing severed strands using the Alberta internal strand splice, the displacements at each load point and midspan locations were measured and comparisons made between the damaged and repaired specimen. The repair and load test procedures were as follows:

- Load test with four strands severed (no splices)

- Repair all four damaged strands

103

Figure 6- 17   Completed repair of severed strands using the Alberta splice

Table 6- 1   Summary of Stressing of Alberta Splices

Strand Number	Strain Gage 1 (10⁶)	Strain Gage 1 (10⁶)	Strain Gage 1 (10⁶)	Strain Gage 1 (10⁶)	Tendon Stress Indicator (values converted from load to strain)
1	5284	5302	5172	5639	N/A*
2	4825	4809	2633	1608	6135
3	1544	1699	4102	4416	4782
4	1820	3377	5692	5274	5249

*Tendon Stress Indicator not able to be used due to dimensional constraints

Right-Hand Threaded Splice

Restrained Against Rotation   Applied Torque
Test 1

Hydraulic Pressure   Test 2   Hydraulic Pressure

Test 3   Restrained Against Rotation

Strain Gages

Applied Torque   North

Figure 6- 18   Additional splice strtests for right-hand threaded Alberta splice

Figure 6- 19   Test of Alberta splice in stress bed — bolt restrained and torque applied to unrestrained sleeve

Figure 6- 20   Test of Alberta splice in stress bed — bolt and sleeve unrestrained - load applied hydraulically

Figure 6- 21   Test of Alberta splice in stress bed — sleeve restrained and torque applied to unrestrained bolt

106

- Load test girder with four tendons repaired

- Remove the two outer splices on tendons one and two

- Load test the girder with two tendons repaired

- Remove the two inner splices on tendons three and four

- Load test with four strands severed (no splices)

Results for the initial and final load test were nearly identical, but were performed to determine if any damage occurred during the test cycle for the Alberta splice. The load-deflection response of only the initial load test will be used for comparison since no change occurred.

Figure 6.22 shows the load-deflection response of each instrumented cross section when all four tendons were spliced. At a maximum applied load of approximately 83 kips (369 kN) the measured displacements at the north, midspan, and south cross sections were 0.39 in. (9.9 mm), 0.51 in. (13 mm), and 0.41 in. (10 mm) respectively. The member stiffness at these locations, based on least squares regression analysis of experimental measurements are shown in Figure 6.22.

When the two outside strand splices were removed and load applied to the girder, there was very little change in load-deflection response of the girder. Figure 6.23 shows the results of load testing carried out on the girder when the two interior strands were repaired and the two exterior strands were not. It is obvious in comparing the differences in load-deflection response that two or four tendons are repaired, that there is very little change.

Figure 6- 22   Load-deflection response of Steck girder with four strands repaired using the Alberta splice

107

Figure 6- 23   Load-deflection response of Steck girder with two strands repaired using the Alberta splice and two strands damaged

Figure 6- 24   Comparison of midspan load-deflection response of damaged and repaired girder using Alberta splice assembly

Figure 6.24 shows the midspan response for the damaged and repaired girder. When four strands were damaged and only two were repaired, there was little evidence of any benefit in performing the repair of only a portion of the damaged tendons. However, if comparison is made to the undamaged condition when all of the tendons remained intact, there was a definite change in member stiffness. When all tendons were undamaged, the midspan stiffness was measured to be 183 Kips/in. (32,050 kN/m). After four tendons were cut the stiffness was 144 kips/in. (25,200 kN/m), and when only two of the four damaged strands were repaired with the Alberta splice the midspan stiffness was 152 Kips/in. (26,600 kN/m). When all four tendons were spliced, the stiffness changed very little when compared to the case where only two tendons were repaired. Comparison of the midspan stiffness during different stages of the repair show that there is very little difference between repairing two or four strands out of a total of 28.

Strain Response of Repaired Tendons. There were six strands instrumented with strain gages and the results have been organized by location within the girder: results for lower tendons (tendons #1, #3, and #5) and results for upper tendons (tendons #2, #4, and #6). When tendon numbers 1 through 4 were not spliced, strains were measured for the undamaged tendons (5 and 6) for comparison with the strains measured when the damaged tendons were spliced. The measured strains of the intact tendons for the damaged state (none of the severed tendons were spliced) are shown in Figure 6.25. As might be expected the tendon with less eccentricity (number 6) experienced less strain than the tendon below (number 5). It is also evident that there was a very slight transition from an uncracked to a cracked response as the applied load approached 60 Kips (267 kN).

When the four severed tendons were repaired with the Alberta splice, the load-deflection response did not change much; however, the measured strains in the undamaged tendons were reduced. When repairing damaged strands with the Alberta splice, there did not appear to be any transition from an uncracked to a cracked section; there was a higher prestress in the section due to the tensioning the

Figure 6- 25   Load-deformation response of tendons 5 and 6 (intact tendons), strands 1 through 4 not repaired

damaged strands, and therefore more load was required to produce or open flexural cracks (Figure 6.26 and 6.27). Measured strains for both the upper and lower tendons reveal that anchorage losses occurred for the tendons which have splices installed, while the intact tendons exhibit none. In each plot (Figure 6.26 and Figure 6.27) both a gradual and sudden slippage within the anchorages of either the splice or the coupler are evident; the slope of each splice curve is less than the corresponding response of the intact tendon, and a very sudden decrease of strain was evident for three of the four spliced tendons. As the load was removed from the girder there was a residual negative strain for every tendon that had a splice installed, a further indication of anchorage seating.

Figure 6- 26   Load-deformation response of bottom tendons — four severed strands repaired with Alberta splice

When the splices were removed from the two outer tendons (1 and 2) and the girder retested, the strains in the spliced and undamaged tendons increased accordingly; there was less prestress and not as much reinforcement to share the tension due to applied loads. Figure 6.28 and 6.29 show the response of the spliced and undamaged lower and upper tendons respectively. Not as much anchorage seating was experienced during the second load cycle as was during the first; the residual strains are less than shown for the previous load cycle when most of the anchorage seating occurred. The repaired strands experienced higher strains than the undamaged tendons.

6.4.2 Barsplice Incorporated Multi-Bolt Swaged Strand Splice Installation

Observations During Installation. Prefabrication of the swaged assemblies was required in order to use the multi-bolt swaged splice. Swaged ends were attached to 4 ft. (1.22 m) lengths of strand by the manufacturer (refer to Figure 6.3). Installation of the multi-bolt swaged splice hardware was slightly

Figure 6- 27   Load-deformation response of top tendons - four severed strands repaired with Alberta splice

Figure 6- 28   Load-deformation response of bottom tendons — two strands repaired using the Alberta splice

111

Figure 6- 29   Load-deformation response of top tendons — two strands repaired using the Alberta splice

The modifications made to the dual strand splice design from Project 12-21consisted of using swaged anchorages and prefabricated 12 inch long high strength bolts, rather than standard wedge anchorages and a machined down threaded rod. The transfer plate was not modified.

Figure 6- 30   Schematic of multi-bolt swaged splice installation

different than for the Alberta splice. As with the previous splice, clearance for installing and stressing the individual splices was accomplished by staggering; splices for tendons one and four were placed at the north end of the repair zone, and splices for tendons two and three were placed at the south end of the repair zone. Rather than splicing in an additional section of new strand, the installation of the multi-bolt splice was accomplished by cutting the prefabricated swaged tendon sections to the appropriate length. Two strand couplers were used, one attached to the each end of the damaged strand. The installation is shown in Figure 6.30.

Each of the four splices was initially located without stressing the strand to determine both the required stagger between the devices and the length to cut each prefabricated swaged tendon. For ease of installation as well as wrench clearance, the individual splices were applied in the following order: 4, 3, 2, 1.

Zero readings were taken for the strain gages prior to attaching the splice assemblies in order to reduce errors in measurement due to bending of the tendon under the weight of the splice as was done previously with the Alberta splice. Each end of the swaged strand was first attached to the strand coupler, and then threaded rods with double hex nuts were inserted to tie the assembly together (Figure 6.31). Slack was removed from each assembly by sliding the ends of the spliced strand further into the wedges of the couplers and, if required, engaging the threaded rods into the transfer plates of the assembly.

Since a series of four bolts were used to stress the splice assembly, less effort was required to torque the bolts than for other splices. Two 3/8-in. (9.5-mm) socket wrenches equipped with a universal swivel joint were used to torque the bolts in order to stress the strand. Two bolts were tightened at a time at opposite diagonals in order to restrain the strand from rotating (Figure 6.32). As the tension in the strand

Figure 6- 31   Installation of multi-bolt swaged splice assembly

Figure 6- 32   Initial stressing of multi-bolt swaged splice assembly

Figure 6- 33   Final stressing of multi-bolt swged splice assembly

Figure 6-34   Photograph of out of shape swage installed on tendon #2.

increased, pipe extensions were used to increase the applied torque (Figure 6.33) to reach the working load of approximately 25 kips (111 kN).

Stressing of Splices. The two main problems encountered while stressing the strands with the multi-bolt assembly were rotation of the strands and uneven tension in the bolts. Although rotation of the strands was not nearly as severe as with the Alberta splice, twisting of the strand did occur. However, the twisting was immediately relieved because neither end of the splice was restrained. Torque was applied to two bolts at a time on opposite sides of the splice thereby providing restraint against rotation only when torque was being applied. Therefore twisting of the strand was relieved each time the socket wrenches were removed. If a single bolt was turned more than another bolt, the result was uneven loading in the bolts. When the engaged length of one bolt was different than another, the transfer plates rotated and caused uneven loading on the swage itself as well as flexure of the tendon.

One other problem became evident when installing the splice for strand number two. During the swaging process, the swage itself was pressed out of shape and became slightly bent. As the tension in the splice increased it was more difficult to torque the bolts than for the other strands, and, therefore, this strand could not be stressed to the same level as the others. It appeared that the bend in the swage caused flexural stresses in different portions of the splice assembly, and resulted in difficulty during installation. The photograph in Figure 6.34 shows the splice installed on strand number two.

Table 6.2 summarizes the tendon strains measured for all four spliced strands. It should be noted that not all strands had the same number of strain gages installed. As testing proceeded from one type of splice to another additional gages were installed to replace damaged gages and to provide additional redundancy. It is evident that the measured strains were much more consistent and reliable than those for the Alberta splice.

Table 6-2   Summary of Strain Gage Data During Stressing of Multi-Bolt Swaged Splice

Strand Number	Strain (10^6)	Strain (10^6)	Strain (10^6)	Strain (10^6)	Strain (10^6)	Strain (10^6)
1	5258	5057	4570	4935	3163	5756
2	3616	3065	3557	3919	-	-
3	4848	5122	4814	5355	5267	5388
4	5023	4345	5378	5736	5320	-

The average strain for strand 1 was 4800 x 10^{-6}, which corresponds to a stress of approximately 134 ksi (924 MPa) and a load of 20.5 kips (91 kN). Strand 2 had an average measured strain of only 3540 x 10^{-6} corresponding to a stress of 99 ksi (683 MPa) and a load of 15.2 kips (68 kN). Average measured strains for strands 3 and 4 were over 5200 x 10^{-6}. The stress in strands 3 and 4 was found to be 144 and 145 ksi (993 and 1000 MPa) respectively, and the corresponding tension of each strand was approximately 22 kips (98 kN) each. The results summarized in Table 6.2 substantiate the difficulty with stressing strand number 2 due to the bend in the swage. Consistency and reliability of strain measurements appeared to be better than for the Alberta splice, which can be attributed to the twisting behavior of the Alberta splice

Load-Deflection Response of Repaired Girder. The displacements at each load point and midspan location were measured and comparisons made between the damaged and repaired girder. The testing sequence was identical to that used for the Alberta splice. Results for the initial and final load test were almost identical, therefore only the results for the initial load test will be used for comparison.

Figure 6.35 shows the load-deflection response of each instrumented cross section when all four tendons were spliced. At a maximum applied load of approximately 83 kips (369 kN) the measured displacements at the north, midspan, and south cross sections were 0.40-in. (10-mm), 0.53-in. (13-mm), and 0.43-in. (11-mm), respectively. The member stiffnesses at these locations based on least squares regression analysis of experimental measurements were 206 kips/in. (36,000 kN/m), 153 kips/in. (26,800 kN/m), and 194 kips/in. (34,000 kN/m), respectively.
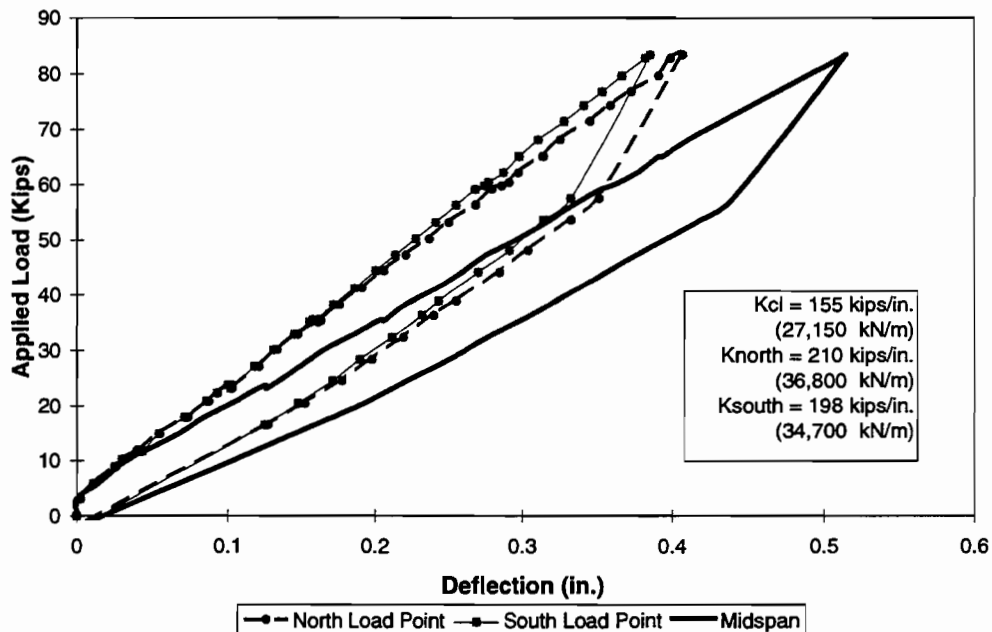

Figure 6- 35   *Load-deflection response of Steck girder with four strands repaired using the multi-bolt swaged splice*

116

Figure 6- 36   Load-deflection response of Steck girder with two strands repaired using the multi-bolt swaged splice

After the load test when all four strands were spliced, the two outside splices were removed from tendons 1 and 2 and the girder stiffness reevaluated. Figure 6.36 shows the results of the reevaluation. As with the Alberta splice, it is shown that there was very little change in the stiffness of the girder is compared. In Figure 6.37, the response at midspan for the damaged and repaired girder. Again the results are almost the same as with the Alberta splice. When only two of the four strands were repaired the midspan stiffness was 151 kips/in. (26,400 kN/m) as compared to 153 kips/in. (26,800 kN/m) when all four severed strands were spliced with the multi-bolt assembly.

Strain Response of Repaired Girder. Results for individual tendon strains will be presented for lower tendons (tendons #1, #3, and #5) and then for the upper tendons (tendons #2, #4, and #6) as was done for the Alberta splice. For the base level of damage when tendons 1 through 4 were cut, the strains for tendons 5 and 6 were measured. The strains of the undamaged tendons (5 and 6) with none of the tendons repaired are shown in Figure 6.25. The damaged state response showed no signs of any change as compared to corresponding tests before and after installation of the Alberta splice. Again there was a transition from an uncracked to a cracked response at a load level of approximately 60 kips (267 kN). The damaged response will again be used as a base level for comparison to different stages during the strand repair using the multi-bolt swaged tendon splice.

A reduction in the level of strain experienced by the undamaged tendons was observed when all four damaged strands were spliced with the multi-bolt splice mechanism. With the increase in internal prestress from strand splice installation, the transition to a cracked response was no longer observed (Figures 6.38 and 6.39). Even though there should be no anchorage losses within the swaged assembly, installation required usage of two strand couplers which have wedge anchorages. Anchorage losses did occur as observed by the residual strains of all four spliced strands, and it appeared that the losses occurred within the couplers rather than within the swages (Figures 6.38 and 6.39).

117

Figure 6- 37   Comparison of midspan load-deflection response of damaged and repaired girder using multi-bolt swaged splice assembly

Figure 6- 38   Load deformation response of bottom tendons — four severed strands repaired with multi-bolt swaged splice

Figure 6-39   Load deformation response of top tendons — four severed strands repaired with multi-bolt swaged splice

The strand splices on the outer strands (1 and 2) were removed and the deformation characteristics for the remaining two spliced strands (3 and 4) and the undamaged strands (5 and 6) were reevaluated by a second cycle of static load testing. Figures 6.40 and 6.41 show the results for the second stage of the repair where only two of the tendons were spliced with the multi-bolt swaged splice. The strains of the spliced and undamaged tendons increased as expected when compared to the first stage of the repair when all four damaged tendons were spliced. Figures 6.40 and 6.41 show the response of the spliced and undamaged lower and upper tendons respectively. As was observed for the Alberta splice tests most of the anchorage seating for the multi-bolt splice occurred during the first stage of static loading as well.

6.4.3 Dual Strand Swaged Splice Installation

Observations During Installation. The dual tendon swaged splice required fabrication of the swaged components as well as the transfer plates, the left- and right-hand threaded high strength bolts, and the turnbuckle. A specially designed swaged component was attached to the ends of 4-ft. (1.22 m) length sections of strand that were sent to Barsplice Incorporated. Installation of the dual tendon splice proceeded in much the same way as for the multi-bolt swaged assembly; however, unlike all single strand splices, staggering of the hardware was not required. Installation of the dual strand splice was accomplished by cutting the prefabricated swaged tendon sections to length as was done for the multi-bolt splices. Four strand couplers were used, one attached to the each end of the damaged strand. A schematic of the installation procedure is shown in Figure 6.42. The swaged tendons were placed through the 5/8-in.- (16-mm-) diameter outer holes in the transfer plates, the high strength bolts were then placed through the center holes of the transfer plates in the opposite direction as the strand (Figure 6.43). Once the swaged tendons and the bolts were in place through the holes in the transfer plate, the turnbuckle was engaged with approximately ½-in. (13-mm) of thread length for each bolt, and the
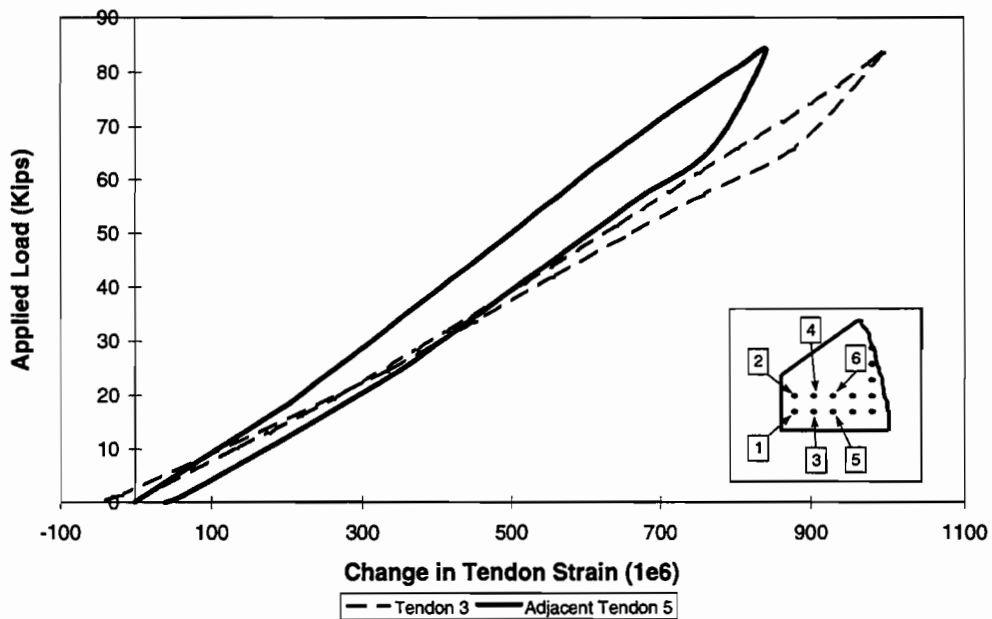
119

Figure 6- 40   Load deformation response of bottom tendons — two strands repaired using the multi-bolt swaged splice

Figure 6- 41   Load deformation response of top tendons — two strands repaired using the multi-bolt swaged splice

120

Figure 6- 42   *Schematic of dual tendon swaged splice installation*

swaged components were cut to the required length. After the swaged components were measured and cut to length, each side of the assembly was attached to the existing strands using couplers, the bolts slid backwards, the turnbuckle inserted, and the bolts engaged. Slack was removed by sliding the tendons further into the wedge anchorages of the couplers and then partially engaging the turnbuckle. Due to the weight and bulk of the assembly it was difficult to install the splice with all of the swaged components the exact same length, and spaces between the ends of the swages and the transfer plates resulted. As the turnbuckle was engaged, the transfer plates rotated until the ends of the swages came in contact with the surface of the plate (Figure 6.44) resulting in uneven load distribution between the splice components.

Zero readings were taken for the strain gages prior to attaching the splice assemblies in order to reduce errors in measurement due to bending of the tendon under the weight of the splice as was done previously with the other splices. A similar method of stressing the splice was used for this assembly as was for the Alberta splice in order to restrain the ends of the assembly from rotating as torque was applied to the turnbuckle. Open-ended crescent wrenches were used to restrain the transfer plates against rotation and

Figure 6- 43   *Installation of dual strand swaged splice assembly*

121

Figure 6- 44 Schematic of difficulties encountered installing dual tendon splice — unequal distribution of load between splice components

as the tension in the strands increased, a pipe extension was used to increase the applied torque (Figure 6.45). Only two dual tendon splices were fabricated. Rather than installing both splices in the girder and risking damage to more than one assembly, only one was installed in the girder. This ensured that one assembly would be available for later evaluation of the splice ultimate strength. A photograph of the completed installation of one dual strand splice is shown in Figure 6.46. Upon close observation rotation of the transfer plates is evident.

Stressing of Dual Strand Splice. There were problems encountered while installing the dual strand splice. The most evident difficulty was to assure equal distribution of load to all of the components of the strand splice. As previously mentioned, it was not possible to install all four swaged tendons such that the bearing ends of the swages were equidistant. This caused rotation of the transfer plates and uneven load distribution throughout the splice components. It was also difficult to restrain the ends of the splice assembly. Rather than having a bolt or nut which could be rotated to facilitate gripping with a wrench, the transfer plates had to be gripped to provide restraint against rotation while applying torque to the turnbuckle. The transfer plates had a fixed vertical position which made gripping with a wrench difficult and slippage frequent.

Figure 6- 45 Stressing of the dual tendon swaged splice assembly

122

Figure 6- 46   Completed installation of one dual strand splice assembly on strand 3 and 4

Table 6.3 summarizes the tendon strains measured for spliced strands. It is evident that the measured strains substantiate the uneven load distribution expected between the spliced strands. Upon close inspection of the completed installation of the splice, it was found that the bottom of the transfer plates were closer together than the top. This indicated that there was initially a space between the bottom swages and the transfer plate. Prior to load being transferred into the bottom tendons, the gaps needed to be closed in order for the swage surface to come into contact with the transfer plate. It should also be noted that torque was applied to the splice until the wrench slipped and no further increase in torque was possible.

The average strain for the bottom strand, number 3, on the south end of the splice, 2975 μstrain, corresponds to a stress of approximately 83.3 ksi (574 MPa) and a load of 12.75 kips (57 kN). While the average strain for strand number 3 on the north end of the splice, 3540 μstrain, corresponds to a stress of approximately 99.1 ksi (683 MPa) and a load of 15 kips (67 kN). The average strain for the top strand, number 4, on the south side of the splice was 4098 μstrain, corresponding to a stress of 115 ksi (793 MPa) and a load of 17.6 kips (78 kN). The north side of the splice, strand number 4, had an average strain of 4208 μstrain, with a corresponding stress of 118 ksi (814 MPa) and a load of 18 kips (80 kN). It appears that the load in the top tendon was consistent on both sides of the splice, however, this was not the case for the bottom tendon as shown in Table 6.3. This uneven load distribution can be further explained by the uneven bearing of the swaged end anchorages causing rotation of the transfer plates.

Table 6- 3	Summary of Strain Gage Data During Stressing of the Dual Strand Swaged Splice					
Strand Number	South Side of Splice			North Side of Splice		
	Strain (10^6)	Strain (10^6)	Average Strain (10^6)	Strain (10^6)	Strain (10^6)	Average Strain (10^6)
3	2884	3065	2975	3236	3844	3540
4	4105	4090	4098	4370	4047	4208

Load-Deflection Response of Repaired Girder. Only two of the four damaged tendons were spliced for this stage of evaluation. Comparisons are made between the damaged response with four tendons severed and the repaired response with only two of the four tendons repaired.

Figure 6.47 shows the load-deflection response of each instrumented cross section when tendons 3 and 4 were spliced. At a maximum applied load of approximately 83 kips (369 kN) the measured displacements at the north, midspan, and south cross sections were 0.41-in. (10-mm), 0.55-in. (14-mm), and 0.43-in. (11-mm), respectively.

Tendon Strain Response of Repaired Girder. Results for individual tendon strains will be presented for bottom tendons (tendons 3 and 5) and then for the top tendons (tendons 4 and 6) since only two of the four damaged strands were repaired using the dual strand splice. For the base level of damage when tendons 1 through 4 were cut, the strains for tendons 5 and 6 were measured. The strains of the undamaged tendons (5 and 6) for damaged state (no tendons repaired) are shown in Figure 6.25. As before there was a transition from an uncracked to a cracked response at a load level of approximately 60

Figure 6- 47   Load-deflection response of Steck girder with two strands
repaired using the dual strand swaged splice

124

kips (267 kN). The damaged response will again be used as a base level for comparison to the strand repair using the dual tendon splice.

Figure 6.48 and 6.49 show the measured strains for each side of the splice assembly for both the bottom and top strands respectively, as well as the adjacent strands 5 and 6. A reduction in the level of strain experienced by the undamaged tendons (5 and 6) was observed when two of the four damaged strands were spliced with the dual tendon splice. As shown with previous splices, there was an increase in internal prestress from strand splice installation and there was no longer a transition to a cracked response. Anchorage losses occurred within the strand couplers similar to that in the multi-bolt swaged splices.

6.4.4 Grab-It™ Cable Splice Installation

Observations During Installation. Installation of the Grab-It™ Cable Splice system was very straightforward. The individual splice assemblies were initially placed without stressing in order to make sure that the staggering of each assembly was sufficient to allow clearance for the torque wrench as well as open-ended wrenches to restrain the splice ends against rotation as torque was applied. After locating each splice within the repair zone, additional lengths of tendon were measured and cut to the required length. The additional section of tendon was cut to fit between the end of the severed strand at one end and the end of the splice hardware at the other end while allowing approximately 1-in. (2.5-cm) of thread to be engaged prior to stressing (Figure 6.50). As the splice was installed, the elongation measuring device was placed over an 18-in. (45.7-cm) gage length either on the new section of tendon or on the original section of tendon, whichever would allow sufficient length for the device. If there was not

Figure 6- 48   Load-deformation response of top tendons — two strands repaired with dual strand swaged splice

125

Figure 6- 49   *Load-deformation response of bottom tendons — two strands repaired with the dual strand swaged splice*

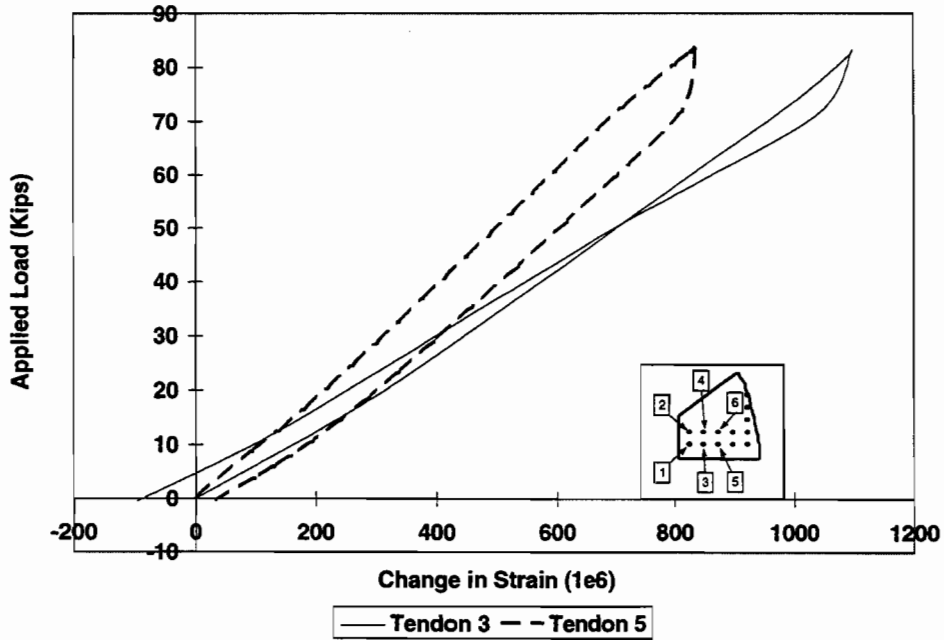Figure 6- 50   *Schematic of Grab-It^{TM} cable splice repair installation*

enough room for an 18-in. (45.7-cm) gage length, the device was shortened accordingly.

Zero readings for the strain gages were taken prior to the installation of the splice assembly as was done for all other splice installations. The Grab-It™ splice was installed and slack removed by sliding the tendon through the wedge anchorages in both the splice and coupling devices as was done for all other splice assemblies. If sliding the tendon into the anchorages did not remove most of the slack, the turnbuckle was engaged until slack was removed, and then the dial gage on the elongation assembly was set to zero. Photographs of the installation are shown in Figures 6.51 and 6.53.

In order to assure that this splice could be stressed in the field by one person a method was devised to restrain the ends of the splice assembly against rotation. Rather than bearing the open-ended wrenches on the floor, 2x4 blocking was installed against the web of the girder and the wrenches secured to the blocking in such a way that as torque was applied to the splice, the wrenches were restrained by the blocking against the web. In this way the stressing could actually be accomplished in the field by only one person. A photograph showing this method of restraining the splice against the web of the girder is shown in Figure 6.52. The main problem with using this method was that rotational energy builds up in the strand as torque is applied. Unless the splice is restrained against rotation in both directions, which it

126

Figure 6-51   Installation of Grab-It^{TM} splice assembly

is not when using the 2x4 blocking, the blocking must constantly be repositioned. For ease of installation of the remaining splices restraint was provided in both directions in the same way as for all other assemblies.

The most difficult part of the installation of the Grab-It™ splice was to ensure proper placement of the wedge anchorages. The wedges that were supplied with the first shipment of splices were made of two pieces rather than three pieces like most standard anchorages are manufactured. The two-piece wedges were not held together by any type of O-ring which made placement around the tendon very difficult (Figure 6.54). Furthermore, the two-piece wedge components did not grip the strand sufficiently, resulting in differential slippage of the two pieces when gripping the tendon. In some cases the ends of one or both wedges protruded out of the end of the anchorage. Once the difficulties encountered with installing and using the two-piece wedges were discussed with the manufacturer, the wedge details were modified to use a three piece system held together by an O-ring. The modified wedges were similar to standard anchorage details, but were smaller and not made of a hardened steel. Instead, the modified, as well as the original wedges, were specifically made for single rather than multiple usage, however; in retrospect all of the splice assemblies tested are meant for one-time usage.

Other than the problems associated with the anchorage details for the Grab-It™ splice assembly, installation on all four damaged strands proceeded very smoothly. As long as the threads of the splice were thoroughly cleaned and lubricated, the splice was able to be installed in a safe and consistent manner. It was observed that the machining of the threaded components was not of very high quality, and some of the threads did not allow free movement. Prior to installing any splice and after the threads

127

Figure 6- 52   Method of stressing splice by restraining ends against the web of the girder

Figure 6- 53   Completed installation of the Grab-It^{TM} splice

Figure 6- 54   Anchorage installation for Grab-It^{TM} splice assembly

were cleaned and lubricated, if the turnbuckle was able to be engaged with little resistance, the splice was used, otherwise it was not installed.

Stressing of the Grab-It™ Cable Splices. Stressing of strands using the Grab-It™ splice assembly was very simple. All of the methods of monitoring the tension in the splice were used and compared. It should be noted, however, that all of the splices were installed after the external threads were cleaned and greased. A summary of the results using each different method of monitoring the tension of each strand splice is shown in Table 6.4.

Table 6- 4   Comparison of Stress Monitoring Procedures

Strand Number	Dial Gage Kips (kN)	Torque lb.-ft. (N-m)	TSI Kips (kN)	Strain Gages and Corresponding tension	
				Strain (10^6)	Tension Kips (kN)
1	-	280	21.3 (94.7)	4728	19.9 (88.5)
2	28.6 (127)	250	23.4 (104)	5304	22.3 (99.2)
3	21.9 (97.4)	240	23.2 (103)	5219	22.0 (97.9)
4	23.8 (106)	240	26.2 (117)	5278	22.2 (98.7)

129

The results using the strain measurements appear to be reliable as long as the strands do not twist as was shown with the Alberta splice. The Tendon Stress Indicator (TSI) also appears to give consistent results. Measurement of the applied torque to indirectly determine the induced tension does not appear to give consistent results. The applied torque for tendon 1 was higher than all of the rest , 280 lb.-ft. (380 N-m); however, measurements of strain as well as with the TSI indicate that the tension in the strand was considerably lower than what was expected based on the applied torque. According to the manufacturer an applied torque of 280 lb.-ft. (380 N-m) corresponds to a tension of approximately 30 Kips (133 kN).

Perhaps one of the most important aspects of repairing damaged tendons is knowing when the required design tension has been reached. It has been shown here that several methods can be used to monitor the stressing operation, however, some are much more practical and consistent than others.

The strain gages provide reliable results, but they are costly and delicate, as well as time consuming to apply and use. Strand elongations measured by the dial gage assembly do not always produce consistent results. It is difficult to obtain a clear reference point as the weight of the splice assembly causes the tendon to sag until enough torque is applied to remove the slack. In addition, as torque is applied to the assembly, the strand tends to twist. This twisting, as well as slippage between the strand and the extensometer, results in errors in elongation measurements. The lateral load-deflection apparatus (TSI) not only produces consistent results, but is also a practical test method that could be used for monitoring stresses in exposed strands as well as for assessing loss of prestress. Use of direct torque measurements appears to be the least reliable of all methods in determining the level of tension in the splice. If the threads are not clean, free of flaws, and properly lubricated, then inconsistent measurements occur.

Load-Deflection Response of Repaired Girder. For comparison to all other splices used for repairing the damaged strands the displacements at each load point and midspan location were measured. The testing sequence was identical to what was used for the Alberta splice and for the multi-bolt swaged splice. Prior to repairing damaged strands and following load tests for repair evaluation, the girder base response was evaluated by load test. Repair evaluation was accomplished in the following manner: the four damaged tendons were repaired, the girder load tested, the two outer splices removed, and the girder reevaluated. Results for the initial and final base response load tests were almost identical, therefore only the results for the initial load test will be used for comparison.

Figure 6.55 shows the load-deflection response of each instrumented cross section when all four tendons were spliced. At a maximum applied load of approximately 83 kips (369 kN) the measured displacements at the north, midspan, and south cross sections were 0.40-in. (10-mm), 0.54-in. (14-mm), and 0.42-in. (11-mm), respectively.

After the two outside splices were removed from tendons 1 and 2 the girder stiffness was reevaluated. Figure 6.56 shows the results of the reevaluation. There was very little change in the stiffness of the girder. Figure 6.57 compares the response at midspan for the damaged and repaired girder.

Strain Response of Repaired Girder. The base level of response for the undamaged tendons did not change significantly, and with the reduction in prestress a transition from a cracked to an uncracked response was again observed. When the four damaged strands were repaired using the Grab-It™ splice, there was no longer a transition to a cracked response. The level of strain experienced by the undamaged tendons was reduced during both stages of repair when four tendons and two tendons respectively were spliced with the Grab-It™ assembly (Figures 6.58 through 6.61).

Figure 6- 55   Load-deflection response of Steck girder with four strands splicedusing the Grab-It^{TM} cable splice

Figure 6- 56   Load-deflection response of Steck girder with two strands spliced using the Grab-It^{TM} cable splice assembly

131

Figure 6- 57   Comparison of midspan load-deflection response of damaged and repaired girder using the Grab-It^{TM} cable splice assembly

Figure 6- 58   Load-deformation response of upper tendons — four strands repaired with Grab-It^{TM} cable splice assembly

132

Figure 6- 59   Load-deformation response of upper tendons — four strands repaired with the Grab-It^{TM} cable splice assembly

Figure 6- 60   Load-deformation response of lower tendons — two strands repaired with the Grab-It^{TM} cable splice assembly

133

Figure 6-61   Load-deformation response of upper tendons — two strands repaired with the Grab-It^{TM} cable splice assembly

Figure 6- 61   Load-deformation response of upper tendons — two strands repaired with the Grab-It^{TM} cable splice assembly

6.4.5 Summary of Strand Splice Installation Tests

Load-Deflection Response of Repaired Girder. The results for the experimental girder load-deflection response for each of the strand splice assemblies are summarized in Table 6.5. Comparisons are made of member stiffness and deflections at the three instrumented cross sections; the north and south load points as well as the midspan location. The different stages represented in Table 6.5 are as follows:

- Stage 1 - No Strands Spliced

  after the geometry of the cross section was modified by removing the top railing down to the slab level as well as removing the concrete surrounding the six corner strands in the tension flange over approximately a 6-ft. (1.8-m) length,

- Stage 2 - Four Strands Spliced

  the four strands that were severed (No. 1 through 4) are spliced

- Stage 3 - Two Strands Spliced

  two of the four severed strands are spliced (No. 3 and 4) and the other two (No. 1 and 2) are not

- Stage 4 - Four Strands Severed

  four severed strands

134

Table 6- 5   *Summary of Load-Deflection Results from Strand Installation Tests on the Steck Girder*

Splice Assembly	Stage	Applied Load kips (kN)	Stiffness kips/in. (kN/m)	Δ in. (mm)	Stiffness kips/in. (kN/m)	Δ in. (mm)	Stiffness kips/in. (kN/m)	Δ in. (mm)
Alberta Splice	No Strands Spliced	83.4 (371)	229 (40,100)	0.41 (10)	183 (32,000)	0.31 (7.9)	214 (37,500)	0.34 (8.6)
	4 Strands Spliced	83.4 (371)	210 (36,800)	0.39 (9.9)	155 (27,150)	0.51 (13)	198 34,700)	0.41 (10)
	2 Strands Spliced	83.6 (372)	208 (36,400)	0.41 (10)	152 (26,600)	0.56 (14)	196 (34,300)	0.44 (11)
	4 Strands Severed	82.4 (367)	199 (34,850)	0.41 (10)	144 (25,200)	0.56 (14)	188 (33,000)	0.43 (11)
Multi-Bolt Swaged Splice	No Strands Spliced	83.4 (371)	229 (40,100)	0.41 (10)	183 (32,000)	0.31 (7.9)	214 (37,500)	0.34 (8.6)
	4 Strands Spliced	83.6 (372)	206 (36,000)	0.40 (10)	153 (26,800)	0.53 (13)	194 (34,000)	0.43 (11)
	2 Strands Spliced	83.3 (371)	206 (36,000)	0.41 (10)	151 (26,400)	0.56 (14)	194 (34,000)	0.43 (11)
	4 Strands Severed	84.8 (377)	199 (34,850)	0.42 (11)	144 (25,200)	0.59 (15)	188 (33,000)	0.45 (11)
Dual Strand Splice	No Strands Spliced	83.4 (371)	229 (40,100)	0.41 (10)	183 (32,000)	0.31 (7.9)	214 (37,500)	0.34 (8.6)
	2 Strands Spliced	83.2 (370)	205 (35,900)	0.41 (10)	151 (26,500)	0.55 (14)	194 (34,000)	0.43 (11)
	4 Strands Severed	83.4 (371)	198 (34,700)	0.43 (11)	144 (25,200)	0.58 (15)	186 (32,600)	0.45 (11)
Grab It Cable Splice	No Strands Spliced	83.4 (371)	229 (40,100)	0.41 (10)	183 (32,000)	0.31 (7.9)	214 (37,500)	0.34 (8.6)
	4 Strands Spliced	83.3 (371)	204 (35,700)	0.40 (10)	151 (26,400)	0.54 (14)	193 (33,800)	0.42 (11)
	2 Strands Spliced	83.4 (371)	204 (35,700)	0.42 (11)	150 (26,300)	0.56 (14)	193 (33,800)	0.44 (11)
	4 Strands Severed	83.4 (371)	199 (34,900)	0.45 (11)	146 (25,600)	0.58 (15)	188 (33,000)	0.45 (11)

When the four tendons were cut there was a 21 % reduction in stiffness at midspan compared to the original state when all four tendons were intact. However, when these strands were spliced using the different splices the increase in the midspan stiffness relative to the case when the strands were severed varied from 4 to 6 %, not a very significant difference. When two of the four severed strands were spliced, the increase in the midspan stiffness relative to the case when the strands are severed varied from 3 to 4 %. In reality the effect on the stiffness of the member is not significantly different if the strands are damaged or repaired. This is not surprising since only 4 tendons were damaged out of 28 total in the tension flange (14 % damaged).

Strain Response of Repaired Strands. The results of strain measurements for the tests carried out on the different splice assemblies have been summarized in Table 6.6. The most important aspect of repairing damaged strands is the reduction of the portion of the load carried by undamaged tendons (tendon Number 5 and 6). Without repair of damaged strands, the remaining reinforcement will experience higher stresses. As shown in Table 6.6 repairing two of the four damaged strands resulted in a decrease of the measured strains for the undamaged strands when any of the splice assemblies were installed. A further reduction in the measured strains for the undamaged strands was also observed when four strands were spliced.

Perhaps the most important item to consider when repairing damaged strands is reduction of the level of strain in remaining strands. It was shown by other researchers (22) that the abrupt change in axial stiffness of a strand when repaired using a splice assembly contributes to lower fatigue strength for the repaired strands. The higher axial stiffness causes a repaired strand to attract a larger portion of the tension, and therefore, under external loading, a repaired strand will experience higher stresses than undamaged tendons in the same region. However, from the point of view of repairing impact damage, it is likely that a maximum of 10% of the total number of strands within a girder would be considered for repair. Most prestressed bridge girders are overdesigned with respect to strength, and even with a 10% reduction in prestressed reinforcement, the flexural strength of the damaged girder would not be of major concern. This is especially true for most instances of impact damage from overheight vehicles where usually an exterior girder is most severely damaged. The exterior girder carries a smaller portion of the applied loads than do interior girders. In most instances, repair of the exterior girder is extremely cost

Table 6- 6   Summary Comparison of Strains for Damaged and Repaired Tendons

Splice Assembly	# of Tendons Repaired	Tendon # 1 Strain (10^6)	Tendon # 2 Strain (10^6)	Tendon # 3 Strain (10^6)	Tendon # 4 Strain (10^6)	Tendon # 5 Strain (10^6)	Tendon # 6 Strain (10^6)
Alberta Splice	4	803	820	697	764	720	664
	2	-	-	998	962	841	771
	none	-	-	-	-	855	797
Multi-Bolt Swaged Splice	4	600	594	788	784	772	715
	2	-	-	1098	989	838	768
	none	-	-	-	-	979	873
Grab-It Splice	4	743	755	838	878	777	718
	2	-	-	1068	1039	849	783
	none	-	-	-	-	978	871
Dual Strand Splice		579	655	708	739	844	764
		-	-	-	-	975	867

effective. Repair of impact damage by a combination of preloading, concrete patching, and splicing damaged strands can provide a durable repair that could extend the service life of the structure.

6.5 ULTIMATE STRENGTH TESTING OF STRAND SPLICES

Evaluation of the ultimate strength of each of the strand splice assemblies was performed by direct tension tests. The location of failure for each assembly was noted as well as the ultimate load for each. The test setup for each different assembly and the test procedures are described.

Test Setup for Ultimate Strength of Splice Assemblies. A displacement controlled 120-kip (534-kN) tensile testing machine was used to test the ultimate strength of each strand splice assembly. Each splice along with two segments of strand, one attached to each end of the assembly, was placed between the loading platens of the testing machine. Schematics showing the test setup and location of strain gages for every test are shown in Figure 6.62 through 6.65. Dimensions for each test setup and the results for each test are summarized in Table 6.7 through Table 6.12.

Additional tensile tests were performed on six specimens of strand for comparison to the splice tests It was noted during the splice tests that the strand in all cases was not yielding. It was assumed that the splices were the cause of the premature failure, yet this was not the case in all instances. When the strand only tests were performed it was found that the type of wedge anchorages that were being used to secure the spliced sections of strand into the testing machine (American Multi-Use Strand Chucks) were causing premature failure of the strand in all cases. At the onset of strand yielding, the wedges pinched the strand and caused failure at the notches created by the wedge anchorage. When different anchorages were used to secure the strands for tensile testing (Supreme Multi-Use Strand Chucks), the full ultimate strength of the strand was reached in every instance (Table 6.7). This premature failure affected the results for the Alberta splice assembly and the first specimen of the Grab-It™ splice.

Additional tests were also performed on the modified swages used for the dual strand swaged splice. Three static tests were performed to determine the most likely mode of failure for the swaged tendon for the case when the swage was subjected to bearing pressure rather than tension through the threads of a bolted connection. The main reason that these tests were performed was to substantiate the results for the static load tests of the dual strand splice; only two splices were evaluated and quite different results were obtained for each.

Table 6- 7	Strand-in-Air (No Splices) Ultimate Strength Tests		
Test	H	Tu	Comments
1	55 in. (140 cm)	39.1 kips (174 kN)	New Strand Grips (95 % Ultimate)
2	55 in. (140 cm)	39.0 kips (173 kN)	New Strand Grips (94 % Ultimate)
3	54.31 in. (138 cm)	42.0 kips (187 kN)	Old Strand Grips (102 % Ultimate)
4	33.63 in. (85.4 cm)	41.9 kips (186 kN)	Old Strand Grips (101 % Ultimate)
5	33.625 (85.4 cm)	41.8 kips (186 kN)	Old Strand Grips (101 % Ultimate)
6	33.69 in. (85.6 cm)	39.0 kips (173 kN)	New Strand Grips (94 % Ultimate)

Discussion of Ultimate Strength Test Results. The two tests performed on the dual strand swaged splice resulted in different modes of failure. One strand of the first specimen failed within the swage as expected. The failure occurred at 91 % of the ultimate strength of the strand; the manufacturer rates the swaged tendon for 90 % of the ultimate

137

Table 6- 8   Strand-in-Air Static Tensile Strength of Modified Swage Anchorage in Bearing

Test	H	Tu	Comments
1	55.63 in. (142 cm)	36.9 kips (164 kN)	Break of Strand Inside Swage (89 % Ultimate)
2	55.69 in. (141 cm)	37.5 kips (167 kN)	Break of Strand Inside Swage (91 % Ultimate)
3	55.69 (141 cm)	34.6 kips (154 kN)	Break of Strand Inside Swage (84 % Ultimate)

Table 6- 9   Strand-in-Air Tensile Strength of Dual Strand Swaged Splice

Test	A	B	H	Tu	Comments
1	7.125 in. (18 cm)	7.75 in. (19.7 cm)	54.63 in. (138 cm)	74.9 kips (333 kN)	Break of Strand Inside Swage
2	5.5in. (14 cm)	4.5 in. (11.4 cm)	49.25 in. (125 cm)	66.7 kips (297 kN)	Failure of Threads on Bolt

Figure 6- 62   Tensile test setup for dual strand swaged splice assemblies

138

Figure 6- 63   Tensile test setup for Grab-It^{TM} cable splice assemblies

Table 6- 10	Strand-in-Air Tensile Strength Tests of Grab-It^{TM} Cable Splice				
Test	A	B	H	Tu	Comments
1	10.5 in. (26.7 cm)	9.5 in. (24.1 cm)	56 in. (142 cm)	37.7 kips (168 kN)	Break of strand in End Wedge Anchorage
2	9.5 in. (24.1 cm)	10 in. (25.4 cm)	54.8 in. (139 cm)	33.4 kips (149 kN)	Break of strand in Splice Wedge Anchorage

139

Figure 6- 64   Tensile test setup for Alberta splice assemblies

Table 6- 11   Strand-in-Air Static Tensile Strength Tests of Alberta Splice Assemblies

Test	A	B	H	Tu	Comments
1	10 in. (25.4 cm)	5.1 in. (13 cm)	55 in. (140 cm)	38.9 kips (173 kN)	Break of strand in End Wedge Anchorage
2	12.5 in. (31.8 cm)	6.25 in. (15.9 cm)	55.6 in. (141 cm)	39.5 kips (176 kN)	Break of strand in End Wedge Anchorage
3	12 in. (30.5 cm)	6 in. (15.2 cm)	55.9 in. (142 cm)	38.5 kips (171 kN)	Break of strand in End Wedge Anchorage

Figure 6- 65   Tensile test setup for multi-bolt swaged splice assemblies

Table 6- 12   Tensile Strength Tests of Multi-Bolt Swaged Splice

Test	A	B	H	Tu	Comments
1	4.6 in. (11.8 cm)	4 in. (10.2 cm)	39.6 in (101 cm)	36.1 kips (161 kN)	Break through Threaded Portion of Swage
2	4.6 in. (11.8 cm)	4 (10.2 cm)	34.6 (87.9 cm)	36 in. (161 kN)	Break through Threaded Portion of Swage
3	1.5 in. (3.8 cm)	1 (2.54 cm)	30.9 in. (78.4 cm)	35.5 kips (158 kN)	Break through Threaded Portion of Swage
4	1 in (2.54 cm)	1 (2.54 cm)	30.4 in. (77.2 cm)	35.5 kips (158 kN)	Break through Threaded Portion of Swage

strength of the strand due to the swaging process. The second specimen, however, failed through the threads of the bolt. Some problems were encountered while fabricating the some of the turnbuckles for the dual strand splices. In some instances the threads within the turnbuckle were not cut to full depth through the entire length of the turnbuckle. With less than the full depth of threads there is less area to resist the load as it is transferred from the bolt to the turnbuckle and failure through the threads would be likely in this instance. It appeared that the second specimen failed through the threads due to fabrication errors. Although it was not immediately apparent upon inspection of the second specimen tested, two other assemblies were not tested due to improper thread depth. It is very likely that improper depth of the threads within the turnbuckle lead to premature failure of the second specimen which reached only 81 % of the ultimate strength of the strand. The expected mode of failure for this splice was substantiated by further tests of the swaged portion of the splice in bearing (Table 6.8) where each of the three tests resulted in failure of the strand within the swage.

For the first of two specimens tested using the Grab-It™ Cable Splice failure occurred within the strand inside of the wedge anchorage holding the strand at the top of the testing machine. The maximum strength achieved was 91 % of the strand ultimate strength. As previously discussed, this low strength was due to strand notching effects within the wedge anchorage. Onset of strand yielding did occur; however, premature failure resulted within the anchorage. On the other hand, the second test resulted in failure of the strand at the wedge grips within the splice resulting in a strength at failure of 81 % of the strand ultimate strength. It appears that this was the result of the quality of the strand grips supplied with the Grab-It™ Cable Splice.

The ultimate strength of the three specimens using the Alberta splice performed very well. Although the ultimate strength of the strand was not reached, premature failure in each case was caused by notching effects within the anchorages. This was substantiated by tests performed on strands held in the test machine with two different types of anchorages, American and Supreme multi-use strand grips. The grips used for the Alberta tests were all American multi-use strand grips which caused premature failure in every case of strand only tests. Onset of yielding occurred in all three cases, and the ultimate strength of the splice assemblies was between 93% and 96% of the ultimate strength of the strand.

Four ultimate strength tests were performed using the multi-bolt swaged splice. In each case the strand did not break, but failure occurred through the threaded portion of the swage. None of the four splices reached the rated value of 90 % of the ultimate strength of the strand. Two of the specimens reached 86 % and two reached 87 % of the strand ultimate strength. It appears that when the swage is placed in tension the failure occurs within the swage, and when the swage is placed in compression, as used in the dual strand splice, failure occurs within the strand inside of the swage.

6.6 FINAL PHASE OF GIRDER REPAIR - CONCRETE AND STRAND REPAIR

6.6.1 Description and Observations During Repair

The final repair of Steck girder consisted of combining the techniques of preloading prior to concrete patching, strand splicing, and cast-in-place concrete repair. The final concrete repair consisted of patching the concrete that was removed from the bottom flange for the strand splice investigations using a cast-in-place method. Prior to placing the formwork for repair, the four damaged strands were spliced using the Grab-It™ splice mechanism. Identical procedures were followed in stressing the Grab-It™ splices as before, therefore, description of the splice installation will be omitted here.

A schematic of the forms used for the repair is shown in Figure 6.66. The patch material was placed into the forms through openings in the top as shown schematically. A photograph of the bottom portion of the forms in place along with installed splices is shown in Figure 6.67. Once the forms were in place, preload was applied to the girder using the hydraulic rams as before. After preloading, the patch material was placed, allowed to cure, and the forms were removed the next day; however the preload was maintained for three days after the patching was performed.

The stages of the final repair are summarized below:

- Surface preparation
- Apply preload
- Installation of strand splices
- Placement of forms
- Placement of patch material
- Form removal at age of 24 hours
- Removal of preload at age of three days

The material chosen for the concrete repair was a rapid-setting concrete patch material, 928 Fast Patch, manufactured by Burke Concrete Products. The material was extended 60 % by weight using 3/8-in. (9.5-mm) river gravel as was done with earlier cast-in-place repairs (Chapter 5). The material was batched in a drum mixer. Consolidation of the patch material was accomplished using mechanical vibration. Figure 6.68 shows the cast-in-place operation being performed.

Placement of the 928 Fast Patch was similar to the Patchroc 10-61. Some of the difficulties associated with repairing impact damage were not encountered with this repair. Specifically, the shape of the repair area was not as narrow as with previous repairs, and, therefore, consolidation of the patch in this case presented no difficulty whatsoever. The forms were removed within one day and 4-in. by 8-in. (10-cm by 20-cm) cylinders were tested for compressive strength at an age of 1 day and again at 3 days. The average 1-day strength, when forms were removed, was 3530 psi (24.3

Figure 6- 66   *Schematic of formwork for cast-in-place repair of Steck girder — final phase*

Figure 6- 67   *Placement of forms and installed strand splices — final phse of repair — Steck girder*

Figure 6- 68   Placement of 928 Fast Patch — final phaseof repair — Steck girder

Figure 6- 69   Completed repair — final phase — Steck girder

MPa), and the average 3-day strength, when the preload was removed, was 4100 psi (28.3 MPa). A photograph after the removal of forms from the repaired area is shown in Figure 6.69.

6.6.2 Girder Instrumentation and Load Test Procedures

Instrumentation of the girder for the final phase of repair (concrete and strand repair) was the same as for prior load tests. Displacements were measured at each load point and at the midspan cross section. Strain gages were placed on individual wires of the repaired strands in order to monitor stressing of the splices, to evaluate changes in tendon strains due to application and removal of preload, and to evaluate the tendon strains due to subsequent applied loading.

The design loading for the Steck bridge was specified as a railroad E-80 live loading. Based on the girder length and spacing in the bridge structure, the additional load due to impact effects of loads on the bridge was determined to be 30 %. Application of loading in the laboratory was meant to reach a live load and live load plus impact moment between the load application points equivalent to the design moment, based on E-80 loading. Assuming that the load was distributed to only the three interior girders, the live load moment for a single girder was found to be 872 kip-ft. (1182 N-m), and the live load plus impact design moment was then 1134 kip-ft. (1537 N-m). Based on the dimensions of the loading frame used in the laboratory, an applied load of approximately 85 kips (378 kN) per load point would produce an equivalent live load moment between the two load points. An applied load of approximately 110 kips (489 kN) would produce a moment between load points equivalent to the design live load plus impact moment for the girder. Therefore, this final phase of load testing of the girder was based on loads which would produce the equivalent live load and live load plus impact moments in the repaired zone.

Figure 6- 70   Load-deflection response of final phase repair — Steck girder — live load cycle 1, live load

Five cycles of equivalent live load static loading were applied to the girder, and then five additional cycles of live load plus impact equivalent static load were applied to produce an equivalent live load plus impact moment in this region.

6.6.3 Interpretation of Test Results

Load-Deflection Response of Repaired Girder. For comparison purposes, the load-deflection response of the girder in the original state (after the top side rail was removed) will be used for the base response in order to evaluate the overall effects of repairing both concrete and prestressing tendons. Shown in Figure 6.70 is the load-deflection response of each instrumented cross section for the first cycle of static loading after the repair was complete. The curves shown are representative in shape of all of the static load testing that was performed after the final phase of repair.

Table 6.13 summarizes the experimentally measured stiffness at each cross section for all load tests performed for the final phase of the repair. In addition, the results for the experimentally measured stiffness for the original condition are shown for comparison (after removing the top railing, but prior to cutting any tendons).

The results shown in Table 6.13 indicate that the combination of preload, strand repair, and concrete repair has resulted in a stiffness of the girder higher than the original condition. The percentages of repaired to original stiffness for the most part are above 100 %. It is also evident, however, that as the number of cycles of loading increase and as impact is included in the applied load (cycle 6 through 10) that the stiffness of the girder degrades as the section begins to exhibit flexural cracking. Perhaps if the preload were increased, less cracking would have been experienced under live load and live load plus impact; however, care should be exercised to not overstress the concrete during preloading.

Strain Response of Repaired Tendons. Results of strain measurements for individual strands were grouped in the same manner as for other strand splice investigations: lower tendons (1, 3, and 5) and upper tendons (2, 4, and 6). For the sake of clarity the measurements taken when applying and removing preload are separated from strain measurements taken during subsequent load testing of the repaired girder. Figures 6.71 and 6.72 show the strain response for the lower and upper strands respectively when the preload was applied and after the concrete repair when the preload was removed. It was observed that not only was there a change in the slope of the response of both the repaired tendons before and after the concrete was patched and preload applied and removed, but the undamaged tendons exhibited a similar, although not as dramatic, change. It is also evident that the effective prestress for both the repaired and undamaged strands increased due to the effects of preload. It may not be apparent as to why the repaired strands experienced higher levels of strain in each case than the undamaged strands. There are two reasons for this to occur. First, the axial stiffness of the repaired strands is higher than the strand itself owing to the larger cross section when the splice is attached. The higher stiffness causes the spliced strands to attract a higher portion of the tension. Second, due to the unsymmetric nature of the cross section and the impact damage to the girder, bending about the weak axis of the member also occurred, although specific displacement and strain measurements were not taken to quantify the extent of the unsymmetric behavior. However, it was observed during all load tests that application of load caused the bottom flange to displace towards the impacted side of the girder. This would cause higher strains in the outer strands. This same unsymmetric behavior was observed during each test conducted for the splice investigations.

Table 6- 13   Experimentally Measured Stiffness of Final Phase of Repair — Steck Girder

Cycle	South Load Point kips/in. (kN/m)	Midspan kips/in. (kN/m)	North Load Point kips/in. (kN/m)	% of Original for South Load Point	% of Original for Midspan	% of Original for North Load Point
1	229 (40,100)	221 (38,700)	240 (42,000)	107	121	105
2	232 (40,600)	185 (32,400)	243 (42,600)	108	101	106
3	228 (39,900)	182 (31,900)	240 (42,000)	107	100	104
4	231 (40,500)	183 (32,000)	242 (42,400)	108	100	105
5	233 (40,800)	185 (32,400)	243 (42,600)	109	101	106
6	226 (39,600)	176 (30,800)	235 (41,200)	106	96	103
7	223 (39,100)	175 (30,600)	234 (41,000)	104	96	102
8	223 (39,100)	175 (30,600)	235 (41,200)	104	96	102
9	215 (37,700)	171 (29,900)	229 (40,100)	101	94	100
10	220 (38,500)	171 (29,900)	229 (40,100)	103	94	100
Original State (after removal of railing; prior to severing strands)	214 (37,500)	183 (32,000)	230 (40,300)	100	100	100

Figure 6-71   Strain response of bottom instrumented tendons — final phase of repair — Steck girder

Figure 6-72   Strain response of instrumented tendons during first load cycle — final phase of repair — Steck girder

148

Figure 6-73   Strain response of instrumented tendons during sixth load cycle — final phase of repair

When subsequent loading was applied to the girder after the preload was removed, the strain gages on the undamaged strands became unreadable. Several of the gages on the spliced strands also became damaged; however, there were more gages placed on the spliced strands than on the undamaged strands and not all of the gages were damaged, therefore, the results from subsequent load testing will include only measured strains for the spliced strands.

Figure 6.73 shows the strain response of both the lower and upper repaired strands from the first cycle of static loading. Observation of the measured strand strains reveals that at the level of equivalent live load moment applied within the repaired zone no cracking is evident during the first cycle of loading. All of the repaired strands exhibit basically the same behavior: linear strain response up to a level of approximately 500 μstrain.

Figure 6.74 shows the strain response of the repaired tendons during the sixth cycle of loading, the first cycle of equivalent live load plus impact. The main difference between the sixth cycle response and the first cycle response is that flexural cracking of the repaired zone was observed visually and was evident in the measured strain responses. The response of tendon 1, the bottom outside tendon, revealed that flexural cracking within the bottom flange occurred at a load just below the level of preload. The response of tendon 4, the upper inside repaired tendon, revealed that the flexural cracking extended higher and deeper into the flange as the applied load increased to a level approximately 15 kips (67 kN) below the equivalent live load plus impact.

It appears from the results of the first load cycle that the increased prestress due to both strand repair and preloading of the girder prevented cracking of the repaired zone at loads at or below the equivalent live load. When several cycles of equivalent live load were applied and then increased to a level equivalent to live load plus impact the repaired zone experienced some flexural cracking. However, upon removal of the load all flexural cracks closed due to prestressing.

149

Figure 6- 74   *Strain response of instrumented tendons during sixth load cycle — final phase of repair*

6.7 SUMMARY OF STRAND SPLICE EVALUATION

Overall evaluation of each of the strand splices is based on three categories: 1) splice hardware, 2) ease of installation, and 3) splice performance. The first category, splice hardware, evaluates different aspects of each type of splice as described in Tables 6.14, 6.15, and 6.16. Table 6.17 summarizes the strand splice evaluations.

150

Table 6- 14   Evaluation Category — Strand Splice Hardware

Item	Description
location of splice	evaluates the ease with which the splice can be located to provide the proper tightening clearances, the ease of e ither cutting an additional section of strand to be spliced or cu tting the swaged strands to the proper length
fabrication requirements	evaluates the complexity of fabricating the splice comp onents when fabrication is required
relative size of splice	evaluates the cross section of the splice as compared to the strand in order to provide tightening clearances
weight and bulkiness	evaluates the relative weight and bulkiness in terms of handling each splice assembly
ease of assembly	evaluates the relative ease of assembling the splice
availability	stock item or fabrication required

Table 6- 15   Evaluation Category — Ease of Installation

Item	Description
method of stressing	distinguish whether restraint against rotation must be pr ovided
ease of stressing	relative ease or difficulty during stressing to working load of 25 kips (111 kN)
time required for install ation	relative time required to install one strand splice

Table 6- 16   Evaluation Category — Splice Performance

Item	Description
restoration of stiffness	evaluates the percentage of stiffness restored compared to the condition when the girder geometry was changed, but prior to severing of any tendons
increase of stiffness	evaluates the percentage increase in stiffness compared to the condition when all four strands were severed
reduction of strand stresses	evaluates the ability to reduce stresses in the remaining strands
ultimate strength	evaluates ultimate strength of strand and splice assembly with respect to strand ultimate strength (Fpu)
seating losses	evaluates the relative magnitude of anchorage losses due to seating

Table 6- 17   Summary Evaluation of Strand Splice Assemblies

Category	Item	Grab-It™	Multi-Bolt Swage	Alberta Splice	Dual Tendon Swaged Splice
strand hardware	location of splice	straightforward	straightforward	difficult (internal dimensions need to be accounted for)	straightforward
	fabrication requirements	none	factory or field swaging	partial fabrication required (extensive)	factory or field swaging, fabrication of bolts and transfer plates
	relative size of splice	small cross section (requires least amount of room for clearance)	small cross section (requires moderate amount of room for clearance)	large cross section (tight clearance - difficult to fit)	large cross section (tight clearance - difficult to fit)
	weight and bulkiness	lightweight, easily handled	lightweight, easily handled	heavy, moderately difficult to handle	heavy, difficult to handle, bulky
	ease of assembly	few components, simple assembly	few components, simple assembly	many components, moderate assembly	many components, difficult assembly
	availability	stock item easily obtained	non stock item, quick turn around	includes stock items, but requires extensive fabrication	non-stock item (swages), bolts and plates require fabrication (not extensive)
ease of installation	method of stressing	requires restraints at each end, simple to restrain against girder	self-restraining when tightening two bolts at once	requires restraint at one location only, difficult to restrain, strand twists	requires restraint of transfer plates at each end (two locations), difficult to restrain
	ease of stressing	low effort using torque wrench	low effort using universal socket wrenches with pipe extensions	moderate effort using open-ended wrenches with pipe extension	difficult to obtain working load, very difficult to stress
	time required for installation	short	short	moderate	moderate
splice performance	restoration of stiffness	relatively the same magnitude *	relatively the same magnitude *	relatively the same magnitude *	relatively the same magnitude *
	increase of stiffness	relatively the same magnitude *	relatively the same magnitude *	relatively the same magnitude *	relatively the same magnitude *
	reduction of strand stresses	relatively the same magnitude *	relatively the same magnitude *	relatively the same magnitude *	relatively the same magnitude *
	seating losses	relatively the same magnitude *	relatively the same magnitude*	relatively the same magnitude *	relatively the same magnitude *

* For further details concerning the performance of the individual splices in terms of stiffness, stress ranges, and seating losses, refer to the discussion of test results for each splice assembly

152

CHAPTER 7

RAPID INITIAL ASSESSMENT OF DAMAGE

7.1 VISUAL INSPECTION AND PHOTOGRAPHIC DOCUMENTATION

Visual inspection of impact damage is always needed when determining the extent of damage and immediate procedures to be followed after impact damage is reported. A standard damage inspection report could be developed for use by highway agencies in which the size, severity, and location of damage to concrete, normal reinforcement, and prestressing strands could be compiled. Photographic documentation of the resulting damage should accompany any such inspection report, along with photographic documentation of the methods used for repair. Careful visual and photographic assessment can save time when engineering studies are required for in-depth evaluation. A detailed survey of the extent of damage with nondestructive instruments is a time-consuming and labor-intensive operation. By making a preliminary visual assessment, return of the structure to service can be expedited and detailed surveys conducted only when damage is severe enough to warrant further stabilization or long-term replacement.

7.2 RAPID ASSESSMENT OF IMPACT DAMAGE

A rapid assessment method is proposed to aid inspection personnel in making preliminary decisions concerning public safety and potential for repair of the structure. The following material outlines a rapid assessment approach and addresses some of the critical issues that inspection personnel should consider.

Rapid initial assessment of impact damage should address overall observations of the entire structure, as well as specific damage to the concrete, prestressing strands, and normal reinforcement. Items that appear in boldface type are assumed to be critical with respect to closing the structure until further assessment is possible.

7.2.1 Overall Observations

The following items should be assessed:

- **Number and Location of Damaged Girders** — Determine the number of girders that sustained impact damage and their location in the superstructure (interior or exterior girders) (Figure 7.1);

- **Falling Hazards** — Evaluate the possibility of damaged concrete or other appurtenances falling from the structure;

- **Misalignment, Offset, or Rotation of Damaged Girder(s)** — Determine the number of girders affected and type of movement for each caused by the impact (Figure 7.2). Movement that results in translation or rotation of girders from their original position should be carefully examined to assess the consequences of such movement on the integrity of the girder. Lateral movement of a girder or rotation of a girder which results in a deviation of the bottom flange of the girder of more than 5% of the flange width should be studied further;

rotation of a girder which results in a deviation of the bottom flange of the girder of more than 5% of the flange width should be studied further;

- **Change in Profile or Camber** — Note the relative extent of upwards camber caused by the impact (Figure 7.3). Vertical cracks in the upper section of girders would indicate quite severe damage (cracking and crushing) in the bottom flanges of girders;

- Staining or Efflorescence (only if damage was undetected for a long period of time) — Note the location and extent of staining (an indication of corrosion of reinforcement) or efflorescence (an indication of how long cracks may have existed and if water is present).

- **Approximate Location of Impact** — Location of impact near midspan or **near support.**

7.2.2 Observations of Concrete Damage

Classifications of Concrete Damage

- **Spalled Flange** — spalled region of flange, loss of concrete cover from side or below (Figure 7.4)

- **Side Splitting** — occurs when vehicle impacts from below, splits along bottom face of bottom flange (Figure 7.5)

- **Diaphragm Reaction** — occurs when the diaphragm acts as a reaction point for the transverse impact loading (Figure 7.6)

- **Loss of Side Cover** — occurs when vehicle impacts from the side resulting in loss of concrete cover exposing strands from the side (Figure 7.7)

Figure 7- 1   *Schematic of typical bridge cross section differentiating interior from exterior girders*

Figure 7- 2   *Schematic showing different types of girder movement resulting from impact*

Damaged Girder Exhibits Excessive Upwards Camber Due to Loss of Compression Zone

Figure 7- 3   *Schematic showing difference between undamaged girder and damaged girder exhibiting exaggerated upwards camber*

Figure 7- 4   Spalled flange area

Figure 7- 5   Side-splitting concrete damage resulting from vehicle impact

155

Figure 7- 6   *Concrete damage where the diaphragm acts as a reaction for transverse impact loading*

Figure 7- 7   *Typical loss of concrete side cover*

Figure 7- 6   Concrete damage where the diaphragm acts as a reaction for transverse impact loading

Figure 7- 7   Typical loss of concrete side cover

- **Side Impact** — occurs when vehicle impacts the girders from the side resulting in fractured, delaminated, spalled concrete in both the bottom flange and the web. cracking within the web extends to the interface between the top flange and the web. Concrete damage appears as a D-shaped region as shown in Figure 7.8

- **Loss of Concrete Section** — occurs in extreme cases resulting in large volume loss of concrete in the precompressed tensile zone (bottom flange and lower portion of the web) (Figure 7.9)

- **Offset Section** — occurs in extreme cases of side impact resulting in a portion of the concrete remaining intact, yet offset horizontally from the rest of the girder (Figures 7.10 and 7.11). An offset of more than 5% of the girder bottom flange width should be studied in detail and the traffic rerouted until the girder strength can be verified

- **Determine the Location of Damage to Concrete**

  Damage near the end of the girder — Generally, detour of traffic on the bridge will be required until further detailed studies are completed if either moderate or severe damage is observed (Reference 12)

Offset of Portion of Girder

Figure 7- 10 Schematic of concrete damage showing offset portion of damaged girder

  - Consider anchorage and development length for intact and repaired strands

  - Consider damage of the concrete around the beam bearing

  Damage within central portion of the girder or near hold-down points

  - Generally, this is not a problem warranting detour of traffic unless severe concrete damage is observed (Reference 12), more than 10% of the strands are severed or badly damaged, or damage to concrete causes strands to slip from hold-down hardware and lose tension.

  - When damage is located within the central portion of the span, consideration for repair should address the damaged concrete, the tension in the strands, and the flexural capacity of the member.

7.2.3 Observation of Strand Damage

Classification of strand damage (boldface type indicates critical item):

- **Minor Exposure** — exposed prestressing strands. no evidence of damage, no evidence of corrosion (Figure 7.12)

Figure 7- 11   Example of an offset section of the damaged girder

Figure 7- 12   Minor exposure of prestressing tendon

- **Moderate Exposure** — exposed prestressing strands, evidence of damage consisting of nicked or fractured wires, embedded items, corrosion (Figure 7.13)

- **Misalignment** — draped strands become misaligned as a result of impact (Figure 7.14)

- **Severed Strands** — strands become completely severed as a result of impact (Figure 7.14)

If the concrete is so badly damaged that the strand alignment has changed or if the strands are severed or elongated (indicating yielding) in relation to other strands at the section, the bridge should be subjected to a detailed engineering study. In this case traffic should be rerouted unless fewer than 10% of the strands are severed and there is no change in strand alignment

- **Assess the following items:**

  Total number of damaged strands per girder — Fifteen percent of the total number of strands per girder is considered a practical limit of the maximum number of strands that should be considered for repair within a single girder

  Location of strand damage — When the damage occurs near the end of the span, anchorage for the repaired strands should be critical concern. When damage is located within the central portion of the span, consideration for repair should address the damaged and repaired flexural capacity of the member.

Figure 7- 13   Moderate exposure of prestressing strand with an embedded item of unknown origin

Figure 7- 14   Misalignment and complete severing of strands

CHAPTER 8

.

SUMMARY AND CONCLUSIONS

8.1 CONCRETE ASSESSMENT METHODS

8.1.1 Summary of Condition Assessment Methods

Visual Observations and Photographic Documentation. Several methods of evaluating the quality and integrity of damaged and repaired concrete have been studied. The first step in evaluating the degree of impact damage is usually performed by visual observation. The benefits of visual and photographic inspection methods are summarized below:

- Visual inspection was an excellent way to document the location, type, and severity of impact damage.

- Visual inspection allowed identification of areas requiring more detailed examination.

- Visual inspection helped to identify the potential for repair or replacement based on initial observations (size, location, and severity of damage to concrete, normal reinforcement, and prestressing strands).

- Photographic documentation of both impact damage and resulting repair methods provided a permanent record to aid in future evaluation.

Written records of visual observations, especially when supplemented photographically, can provide valuable information for evaluating and repairing impact damage in the future.

Nondestructive Assessment Techniques - Rebound Hammer. The rebound hammer is a very simple tool for rapid determination of the quality or soundness of damaged concrete. It was found that the rebound hammer was an excellent tool for rapid initial assessment, but not for monitoring the quality of concrete repair. The advantages and disadvantages of using the rebound hammer are summarized below.

Advantages of the rebound hammer :

- Provided the capability to detect near surface concrete damage

- Provided the capability to locate delaminated zones

- Could be used to quickly identify areas which require more detailed evaluation

- Trained personnel were not required to use the instrument or interpret the results

- Did not require collection of large amounts of data

A digital rebound hammer:

- Produced more consistent results

- Accounted for the orientation of the instrument

- Provided more consistency between different operators

- Facilitated a global survey of the condition of the concrete for the entire structure by storing test values for later retrieval and processing by computer

Disadvantages of the rebound hammer:

- limited to detecting only near surface damage

- Detailed information pertaining to internal cracks and voids was not provided

- Was not a reliable measure of quality or soundness of concrete repair (the measured rebound numbers after repair did not indicate areas where internal damage still existed)

Nondestructive Assessment Techniques - Impact Echo Method. The impact echo method is a relatively new nondestructive technique. Instrumentation for field application is continually developing as rapid technological advances are made with computer hardware, software and electronic components. The impact echo method is also undergoing refinement in application, measurement techniques, and interpretation of experimental results. The DOCter ™ field impact echo flaw detection system was helpful in assessing the extent of impact damage as well as for monitoring the quality of concrete repairs. The method could be used in several ways: qualitatively or quantitatively, and for local or global assessment.

Used in a qualitative fashion, it was possible to differentiate between sound and unsound material at the surface and between solid or internally damaged concrete. When used in a quantitative fashion, the results of impact echo tests could be used, in certain instances, to determine the thickness of the member or depth to internal damage. However, for the complex geometry of an I-shaped girder, quantitative interpretation of impact echo results was, at best, difficult. Numerical modeling techniques will have to be employed to interpret the results quantitatively for structural shapes that have complex geometry.

The individual amplitude spectra at a sampling location can be evaluated, and the condition at that location can be assessed. When the amplitude spectra from individual locations are combined to form a surface contour of spectral values along the length of the member, global assessment of the entire structure is possible. Used for global assessment, the impact echo method is capable of distinguishing entire zones of internal or surface damage. Although testing and interpretation of impact echo results may be difficult, it was a viable means of delineating between damaged and undamaged regions. The following is a summary of the advantages and disadvantages of impact echo technique as applied to condition assessment for impact damage.

Advantages of the impact echo method:

- Possible to distinguish between sound and unsound concrete

- Possible to detect delaminated zones

- Possible to detect internal flaws in concrete members

- Amount of detail obtained was much more extensive than was possible when using the rebound hammer

- Necessary to have access to one side of a structural member

- Possible to assess concrete damage or quality of repairs in a local or global manner (single location or entire member)

  The impact echo equipment used for this study:

- Was designed for field usage although the instrumentation had to be handled with care (the computer and displacement transducer are both delicate)

- Had the built-in capability through neural network technology to aid in the interpretation of specific test results

Disadvantages of the impact echo method:

- Application of the impact echo method required some training to perform the tests and interpret the results.

- A large quantity of data was obtained even for a single test location. The volume of data was cumbersome to evaluate which made reduction and interpretation both time consuming and difficult.

- Both the instrumentation and the test method are still in the developmental stage.

- The equipment is expensive.

- Complex geometrical shapes require numerical modeling techniques in order to quantitatively assess test results. This requirement makes the method impractical for many evaluation purposes.

Nondestructive Assessment Techniques - Method of Spectral Analysis of Surface Waves (SASW). Similar to impact echo, SASW is a stress wave propagation technique. However, unlike impact echo, SASW evaluates the surface wave velocity, rather than the compression wave velocity of concrete, to provide an indication of the quality of the material at varying depths. SASW was traditionally used for geotechnical engineering applications; however, use of the method has been extended to flaw detection in concrete structures. Since SASW is relatively new, instrumentation has not yet been developed for the rugged conditions encountered in the field. In this study, use of the SASW method was beneficial for assessing the extent of impact damage as well as for monitoring the quality of concrete repairs. Similar to impact echo, the method could be used in different ways: qualitatively or quantitatively, and for local or global assessment.

For a specific location, a dispersion curve showing the variation of surface wave velocity with respect to wavelength (or depth into the member) was generated. The individual dispersion curves could be used qualitatively to distinguish between sound and unsound material based on relative changes in the measured surface wave velocity, or quantitatively to determine the relative depth of damage or depth to an internal flaw. By combining the individual dispersion curves, a contour of surface wave velocity along the length of a member could be used to delineate between damaged and undamaged zones. The global evaluation can then be utilized to determine which areas required more detailed, localized

evaluation. The major advantages and disadvantages for evaluating impact damage and the quality of concrete repairs by the SASW method are summarized below:

Advantages of the SASW method:

- Nearly all the same advantages apply to the SASW technique as for impact echo.

- Unlike the impact echo method, geometric irregularities did not effect results significantly, and, as a result, interpretation of test results for complex geometric shapes was not as difficult as with the impact echo method.

Disadvantages of the SASW method:

- SASW testing required trained personnel to perform the tests and interpret the results.

- A large quantity of data was obtained for each individual test location. The volume of information is very cumbersome to evaluate which makes reduction and interpretation difficult.

- The SASW method and the instrumentation required to perform the tests has not yet been developed for rugged field usage.

- The test setup, measurements, and data reduction were time consuming.

- The instrumentation is very costly.

Nondestructive In-Situ Load Testing of Damaged Structures. One of the evaluation procedures that could be employed to evaluate the effects of damage on the overall serviceability of the structure was in-situ nondestructive load testing. Part of this investigation involved field testing of a damaged bridge structure. Based on the measured deflections of the damaged and undamaged spans, the most important observation was that the reduction in stiffness due to severe concrete damage and damage to only a few tendons in an exterior girder did not have a significant effect on the overall serviceability of the structure. It was concluded that reduction in stiffness due to severe damage did not play a significant role in the overall response of the structure.

8.1.2 Recommendations for Condition Assessment by Nondestructive Methods

Recommendations for Use of the Rebound Hammer. The most advantageous usage of the rebound hammer is for initial damage assessment to distinguish between sound and unsound material. The rebound hammer was shown to be extremely useful for rapid global assessment of a damaged concrete structure. Even though the surface hardness using the rebound hammer is not an accurate means for determining the compressive strength of concrete, the relative values of surface hardness obtained when using a rebound hammer do provide an indication of the soundness of the material being sampled without causing harm to the structure. The use of a digital rebound hammer enhances the ability to rapidly assess a large zone of damaged concrete by comparing relative values of the rebound number. Current practice is to simply assess the soundness of damaged concrete in the case of impact damage by sounding with a hammer. Although this method is simple, quick and relatively reliable, the rebound hammer can quantify relative differences in material quality, where a simple hammer sounding technique cannot. It is suggested that a digital or analog rebound hammer be considered as a tool for rapidly assessing the soundness of damaged concrete.

In terms of condition assessment, the rebound hammer is not recommended for evaluating the quality of concrete repairs. Rebound numbers on both the impacted and nonimpacted faces of the girder following the concrete repair and epoxy injection may not indicate any remaining internal damage. However, it was shown that other nondestructive tests indicated zones of internal damage remained after the repair was completed.

Recommendations for Use of the Impact Echo and SASW Methods. Both the impact echo and SASW methods show more promise for evaluating the quality of concrete repairs than for evaluating the extent of damage incurred by impact. The amount of detail obtained from both of these test methods is not required for estimating the remaining structural capacity of a damaged prestressed bridge girder. Furthermore, the degree of effort involved in performing the tests and interpreting the results is not a cost effective means of damage assessment for the specific case of impact damage. When evaluating impact damage, extremely detailed information is not required for estimation of structural capacity, and, therefore, both methods show more promise for evaluating the quality and consistency of concrete repairs. Both methods are best utilized in a qualitative fashion by making relative comparisons between results from damaged (repaired) and damaged zones of a girder.

While both methods show promise for use as nondestructive evaluation techniques, neither method has been developed to the extent that may be needed for easy use in quality assurance. Both techniques are equally complex in nature, and require trained personnel and expensive equipment to perform the tests and interpret the results. In the case of impact echo, complex geometry causes difficulty in interpreting test results, and, in the case of SASW, instrumentation for field implementation of the method under severe operating conditions has not yet been developed. Provided equipment and experienced personnel are available to perform this type of evaluation, either method could be used for quality assurance purposes.

8.2 CONCRETE REPAIR METHODS

8.2.1 Summary of Repair Methods Investigated

The concrete repair techniques which were evaluated as part of this research were limited to cast-in-place and hand-applied patching materials, combined with low pressure epoxy injection and preloading of the structure prior to repair. The type and extent of damage to a girder removed from service provided an excellent opportunity to evaluate several different classes of commercially available products. It was found that by using a combination of repair techniques, a sound, durable repair could be achieved.

Preloading. It has been shown that the benefits of preloading prior to repair are numerous. First and foremost, by applying preload to a typical impact damaged girder, the profile or shape of the member can be restored. When a large volume of concrete in the bottom flange of a prestressed bridge girder is damaged, a portion of the precompressed tensile zone is lost. With the loss of concrete in the bottom flange, the prestressed concrete member tends to camber upwards. If the camber is large, the top flang of the precast girder and/or the cast-in-place slab above may crack. The resulting excessive upward camber can be reduced by applying preload to the girder, patching the damaged concrete, and then removing the preload. When concrete in the precompressed tensile zone is replaced and the preload removed, the profile of the member is restored to near original shape.

By applying preload to a damaged girder prior to repair in the laboratory, damaged concrete was removed more easily. As the preload was applied, compression in the damaged concrete was relieved which helped to loosen fractured material. At the same time, any existing cracks within the precompressed

tensile zone became wider under preload, and facilitated flushing of debris from the cracks allowing better penetration of injected epoxy.

Perhaps the most important aspect of preloading the structure was observed when measuring the strains of the instrumented prestressing strands within the patched zones. It was shown that the application of preload not only increased the effective prestress of the strands, but upon removal of the preload, precompression of the patched concrete was observed. In order for the patching material to crack under subsequent loading, both the precompression provided by preload and the tensile strength of the patching material had to be overcome. The benefits of preload prior to repair are summarized below:

Benefits of Preloading:

- Possible to restore overall shape to the damaged member

- Facilitated removal of damaged concrete

- Facilitated injection of cracks by opening them wider

- Patches within the bottom flange and portions of the web were compressed which provided a more durable repair by decreasing the likelihood of flexural cracking

- Possible to increase the effective prestress of strands within the damaged areas of the girder

Epoxy Injection. In order to effectively inject epoxy to fill cracks and voids in damaged concrete, it was imperative to build up some pressure on the epoxy. However, when impact occurs, concrete tends to become fractured to such an extent that completely sealing cracks for pressure injection is nearly impossible. For this situation, a slightly different method of injection was developed. By placing internal injection ports within the damaged zones and patching the concrete first, the patching material acted as a seal for the internal voids and cracks. Surface mounted and internal injection ports could then be used to fill both internal and surface damage by normal injection techniques.

Some problems did arise when using the prepackaged, low pressure injection system. Specifically, inadequate mixing of the resin and hardener caused problems with curing of the epoxy. When following the recommendations of the manufacturer for mixing the two components, adequate mixing did not always result, and in several areas the epoxy did not cure properly. Some of the one-way injection valves did not function properly, and backpressure caused leakage of injected epoxy at several locations. The use of premeasured cartridges of resin and hardener alleviated problems with improper proportioning, however, bulk materials are much less expensive. Alternatively, high pressure injection systems can be used. Evaluation of depth of penetration using high versus low pressure systems was not performed, however, higher injection pressures may take less time to reach a given level of penetration. In summary, the benefits and problems associated with epoxy injection for repairing impact damaged concrete are:

- The low pressure injection system used was subject to insufficient mixing which caused problems with curing of the epoxy

- A combination of internal and surface-mounted injection ports allows effective injection of highly fractured zones

- It may be less costly and time consuming to use high pressure injection and bulk materials rather than prepackaged, low pressure injection systems

Large Volume Concrete Replacement - Cast-in-Place Repairs. Three different prepackaged, cast-in-place repair materials were evaluated as part of this investigation. For the initial repair a magnesium phosphate-based patching material, SET 45 HW, and a silica fume modified, cementitious, rapid-setting patching material, Patchroc 10-61, were used. For the final repair, which consisted of replacing the portion of the bottom flange that was removed for strand splice investigations, a rapid-setting, cementitious patching material, Burke Fast Patch 928, was used. In each case the materials were extended 60% by weight with 3/8 in. (9.5 mm) river gravel, mixed in a drum mixer, and placed into forms from above.

An advantage of using prepackaged concrete patching materials is that prior knowledge of mix proportioning was not required. Specially trained personnel or equipment are not needed to mix or place the materials, and, therefore, repairs in remote locations are possible. Furthermore, prepackaged materials are proportioned to enhance certain performance characteristics such as increased adhesion, rapid strength gain, and improved durability, but they are much more costly than ready-mixed concrete. Care should be taken to choose a patching material that has qualities as close as possible to the original concrete including, but not limited to:

- similar color and texture

- similar compressive and tensile strengths

- similar modulus of elasticity

- similar thermal expansion and contraction characteristics

When using prepackaged patching materials, much care should be taken when purchasing from a supplier rather than obtaining the material directly from the manufacturer. Material suppliers stockpile products which, in many instances, are kept for long periods of time until they are sold. When this occurs, the materials become outdated and will no longer perform as intended.

Consolidation of the repair materials into the void spaces appeared to be the most frequent problem associated with cast-in-place methods for repairing impact damage. The size and shape of voids that can result from impact damage are irregularly shaped and the void spaces were quite narrow which made complete filling of the voids difficult. It was found that relying on mechanical vibration and hydrostatic pressure did not force the patching materials completely into the void spaces, and portions of the damaged areas remained after removal of the forms. These remaining voids had to be patched using hand-packed materials.

With regard to the specific materials that were evaluated, the Set 45 HW was not particularly suited to this type of repair. Several factors lead to this conclusion. The working time of Set 45 and Set 45 HW is extremely short, on the order of 10 minutes. The short working time did not allow for placement of large volumes of material. The high heat of hydration could possibly contribute to poor durability by causing microcracks to develop in large patches as the material cools. As the material cured it exhibited a very strong and objectionable odor of ammonia, and the color of the final repair was much darker than the original concrete. Set 45 had a flowable characteristic and mechanical vibration did not consolidate the material. Instead, form vibration was required, but the material still did not completely fill the voids.

On the other hand, the Patchroc 10-61 was much easier to place, mainly due to a longer working time and the ability to use mechanical vibration. The Patchroc did not set as quickly as the Set 45, however, sufficient strength was gained within about one hour that forms could be removed. Like the Set 45, the

169

Patchroc 10-61 could not be consolidated enough to completely fill the internal voids. In comparison to the Set 45, however, the color and texture of the Patchroc appeared very similar to the original concrete.

For the final concrete repair, Burke 928 Fast Patch was used. Placement and consolidation were very similar to the Patchroc. The material was easy to work with and could be consolidated using mechanical vibration. Color and texture of the final repair were very similar to the original concrete. Problems with consolidation did not arise because the shape of the patch was not representative of typical impact damage. Remember that concrete was removed in the bottom flange to expose six prestressing strands for splice investigations, and the resulting void did not become narrow at the ends as was typically the case with impact damage. This material appeared to be effective for cast-in-place large volume concrete patches.

Shallow-Depth Concrete Repairs. There are many different types of prepackaged mortars available for concrete repair. The non-sag properties of some of the polymer and polymer-modified mortars offered an effective means of repairing shallow depth damage in concrete without the use of forms. Typically, impact results in damage on the vertical face of the web of a girder, or on the vertical and overhead surfaces of the bottom flange. When the size and depth of this type of damage is limited, a non-sag repair mortar is an obvious choice for the repair.

It was observed during the course of this research that there are practical limitations on the depth of repairs that can be performed using a hand-applied mortar. Most of the mortars evaluated could be placed no thicker than 1 to 1-1/2 in. (25 to 38 mm) in a single lift. If the damaged area was deeper, most of the mortars had to be placed in multiple lifts. However, multi-lift application requires curing between each lift. If the structure is to be placed into service as quickly as possible, then multi-lift application of a mortar is not a very practical alternative. If the patch is in excess of about 4 in. (100 mm), the use of hand-applied mortar is not recommended. A cast-in-place patching material should be used.

Observations of the different classes of patching mortars evaluated during this investigation showed that the two-component latex-modified mortars (Burke V/O and Fosroc Renderoc HB2) performed much better than the single-component latex-modified mortar (Burke Acrylic Patch). The consistency of the two-component materials was very cohesive and allowed a much higher build than was possible with the single-component material. Furthermore, the two-component materials were self-curing. The silica fume, fiber reinforced, cementitious mortar, EMACO S88, worked very well. Even though the material was difficult to finish and exhibited extensive shrinkage cracking (due to difficulty with curing a vertical surface), it was very easy to mix and place.

8.2.2 Recommendations for Concrete Repair

Preloading. Preloading a damaged prestressed girder is an effective means of providing a durable repair. Preload will increase effective prestress, places patches into compression, and also restores shape to severely damaged members. It is highly recommended that a preload be applied to a structure in order to obtain a durable repair; however, care should be taken not to overstress the repaired girder or other portions of the structure upon preload application or removal. Preload can be most easily realized by placing dead load (loaded vehicles) on the structure above or near the damaged regions.

Epoxy Injection. The recommended method to adequately seal cracked concrete is by epoxy injection. In the case of impact damage, the approach to epoxy injection requires the use of internal and external injection ports. The internal ports should be placed after removal of loose, damaged, and delaminated concrete. The damaged concrete should be patched to seal internal voids and cracks, and then the epoxy

should be injected. If injection is attempted on highly fractured concrete, it will be nearly impossible to seal all of the cracks. Failure to completely seal the cracks prior to injection leads to pressure loss and poor epoxy penetration.

For very small repairs, prepackaged epoxy injection systems are attractive, however they are very costly, and proper mixing of the resin and hardener can prove difficult. Bulk materials and high pressure injection may be used to advantage. Higher injection pressures may speed up the repair work, and bulk materials should be less expensive. It is also recommended that the personnel performing the injection have prior experience with this type of work (either on previous jobs or by some qualification procedure) and that they understand material hazards and injection safety procedures. Once the injection process starts, it cannot be interrupted. If injection work is stopped further injection will not be possible.

Large Volume Concrete Repair. It is possible to use cast-in-place techniques for large volume replacement of damaged concrete. The size and shape of the voids that must be repaired create difficulties when trying to consolidate material to completely fill the void spaces. However, when combined with internal epoxy injection and application of hand-placed mortars to fill remaining voids, a cast-in-place method of repair appears to be a viable method of repairing large volumes of damaged concrete. It is not necessary to use prepackaged repair materials, and ready mixed cast-in-place concrete could be used for repairs of this nature.

If personnel are available with experience in pressure grouting techniques, preplacing aggregate into the void spaces and pressure grouting the repairs may eliminate the difficulties associated with consolidation. A grout material with the correct physical characteristics must be chosen for this procedure. Many polymer-modified grouts are available but their modulus and thermal properties may be quite different from the surrounding concrete.

Another method of repairing both small and large volume damage to concrete that was not investigated, but could prove highly effective, is low or high pressure sprayed concrete. This method seems to have excellent potential for vertical and/or overhead application. Difficulties could arise, however, with placement in congested areas where material rebound and air pockets behind reinforcement are likely. If adequate quality assurance measures are taken, such as trial placement of sprayed concrete under field conditions, this method could be a very effective means of repairing impact damage.

8.3 PRESTRESSING STRAND SPLICE INVESTIGATIONS

8.3.1 Summary of Strand Repair Techniques

In the past, several methods of restoring structural integrity to prestressed concrete beams containing damaged prestressing strands have been investigated including external post-tensioning with strands or high strength bars, metal splice sleeves, and metal cover plates, to name a few. However, the investigations herein were limited to internal strand splice techniques. Both commercially available products as well as specially fabricated hardware were included in this study. Four different splices were evaluated:

- Alberta Splice Sleeve - Designed by the Alberta Transportation and Utilities Department

- Multi-Bolt Splice - Manufactured by Bar Splice Incorporated

- Grab-It™ Cable Splice - Distributed by Prestress Supply Incorporated

- Dual Strand Splice - Partial fabrication by Bar Splice Incorporated

Each of the above splices are capable of inducing tension into the spliced strand at the splice location through either a turnbuckle assembly or by advancing other types of threaded components.

The splice investigations consisted of two phases. During the first phase, each splice assembly was installed on intentionally severed strands in a prestressed concrete girder. Splice performance was based on ease of installation, measured load-deflection response of the damaged and repaired girder, and strain response of repaired and undamaged strands. The second phase of the investigation consisted of testing each splice and strand assembly to failure in direct tension evaluating the ultimate strength and the critical components of each assembly.

In addition to evaluating the performance of each splice, several different methods of monitoring the strand stress levels were investigated. Monitoring of the stressing operations were carried out using strain gages on individual wires of spliced strands, by measuring the applied torque, by measuring average strand elongations using a mechanical dial gage assembly, and by evaluating the lateral stiffness of a stressed strand. It was found that the most consistent and reliable monitoring method was by lateral strand stiffness.

Internal Strand Splices. In terms of installation, there were problems associated with all four splices. The most evident observation for all of the splices was that extreme care was needed to ensure that all threaded components were free of defects, and were thoroughly cleaned and lubricated prior to use. If the threaded components were dirty or damaged in any way, the effort required to torque the splice to reach the desired tension was greatly increased. In some cases, damaged, dirty, or flawed threads prevented the full working tension from being reached. All of the splice assemblies exhibited anchorage seating losses of approximately the same magnitude. The seating losses occurred within the wedge grip assemblies of each splice. Even those splices that used swaged anchorages exhibited seating losses, not within the swage, but within the coupling components.

In terms of structural performance, each type of splice exhibited similar performance. The load-deflection response of the repaired girders was virtually the same with each splice. It was observed that when 2 of the 4 severed strands out of 28 total were spliced, very little difference was observed in the load-deflection response of the girder. In other words, the loss of 2 out of 28 total strands had very little effect on the serviceability of the girder. When all four strands were spliced there was an increase in girder stiffness.

It was also observed that splicing the damaged strands had an effect on the levels of strain experienced by both repaired and undamaged strands. When the severed strands were spliced, the undamaged strands experienced lower levels of stress because the tension induced by external loading was shared by the spliced strands. It was also observed that the levels of strain were higher for the spliced strands than for the undamaged strands. Higher strains in the spliced strand could be attributed to higher axial stiffness of the repaired strands as reported by other researchers.

During the final phase of girder repair, a combination of repair techniques was used. Preload was applied to the girder, the four severed strands were spliced using the Grab-It™ Cable Splice, and the concrete was repaired using a cast-in-place method. Most importantly, it was shown that the combination of repair techniques were effective in restoring the girder to a serviceable condition.

The advantages and disadvantages of internal strand splice techniques are summarized below:

172

<u>Advantages:</u>

- Internal strand splices restored prestress internally. When combined with preload, prestress was restored internally as well as externally.

- Internal strand splices provided a means to stress strands at the location of damage.

- Use of internal strand splices restored a damaged structure to serviceable condition.

- Use of internal strand splices reduced stress levels in undamaged strands.

- Internal strand splices increased the stiffness and strength of a damaged girder.

- Internal repair methods resulted in a neater, cleaner appearance than is possible with external repair methods reported in the literature.

<u>Disadvantages:</u>

- Due to increased axial stiffness of a repaired strand, more load was attracted to the splice than to undamaged strands.

- All of the splices contained wedge anchorages which are locations of stress concentration. Combined with increased axial stiffness, the wedge details could be sources for fatigue-related strand failures.

8.3.2 Strand Repair Techniques - Recommendations

Evaluation of the remaining structural capacity of the damaged girder should take into account number and location of severed strands. If the ultimate flexural strength of the girder with remaining undamaged strands is greater than the factored design moment, then repair by internal strand splices could be used to reduce the level of stress imposed on remaining strands. If the remaining service life of the structure is such that fatigue is not a major concern, internal splice methods could be used to restore ultimate flexural strength to a damaged girder.

Another consideration that should be taken into account is the location of the girder within the structure and the likelihood that the girder would experience the full design load. Yet, in this case, it may not be necessary to repair the strands, but simply to patch the damaged concrete. In any case repair of more than 10 to 15 % of the total number of strands within a single girder is not recommended.

8.4 RECOMMENDATIONS FOR FUTURE RESEARCH

There are several research areas that would benefit from an extension of the work presented in this report. The following subsections describe a direction for future research relating to condition assessment, repair, strengthening, and rehabilitation of damaged or deteriorated structures.

Nondestructive Condition Assessment. Further development of the state-of-the-art in nondestructive assessment is an area where much work is needed. Future research in nondestructive evaluation of concrete structures should concentrate not only on the development of new techniques, but also on refining existing methods for field use.

Repair, Rehabilitation, and Strengthening of Damaged or Deteriorated Structures. With respect to repair and strengthening methods for damaged or deteriorated structures, emphasis in future research

should not only be placed on the use of new materials and methods of repair, but also on developing tools to help inspectors and engineers in making the decisions regarding repair. This could take the form of an expert system to suggest the most appropriate materials and methods of repair, or development of an analytical load rating systems for damaged and repaired structures.

Development of a database for documenting the long-term performance of repaired structures would provide valuable information for future generations of engineers. Included in such a system would be information pertaining to the methods used to evaluate the initial condition of the structure, the methods used to repair or strengthen the structure, as well as information pertaining to the difficulties or benefits associated with the choice of materials and methods used.
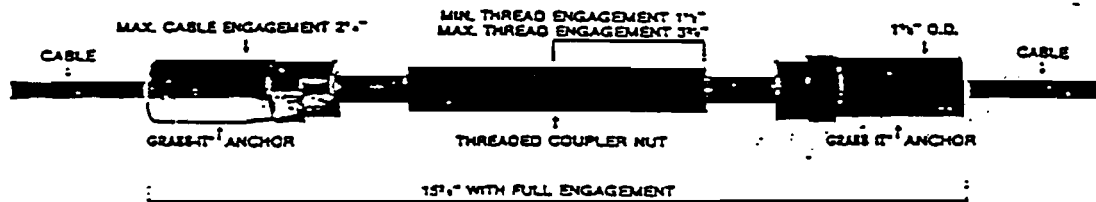
APPENDIX A

SPLICE DETAILS

Tested for Dependability
GRABB-IT* Cable Splice
(Patented)

Let the GRABB-IT* Cable Splice be the solution to your cable repair problems.

The GRABB-IT* Cable Splice will splice and retension broken or damaged P.C. strand in both bonded and unbonded conditions.
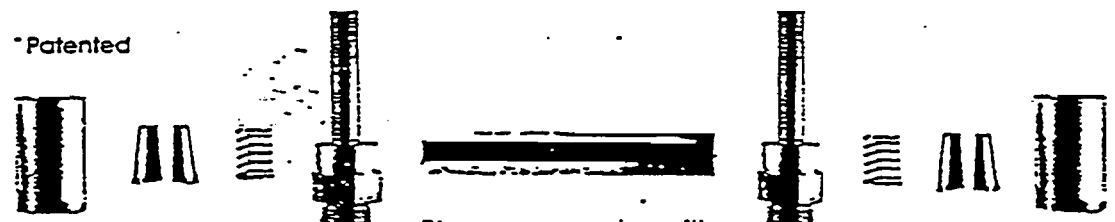
Applying tension to the cables is accomplished by screwing the two GRABB-IT* cable anchors together after they have been locked on to the strand.

The force introduced in the strand can be measured by either a strain gauge or torque wrench.

With a minimum of 1½" thread engagement, the GRABB-IT* Cable Splice will meet and exceed the design strength of the strand. (Laboratory Test results available.)

All GRABB-IT* Cable Splice units are zinc chromate plated to ASTM B-633 type 3 to provide corrosion resistance.

GRABB-IT* Cable Splice is available in most standard sizes — 3/8", 7/16", 1/2".

*Patented

Place your order with:

PRESTRESS SUPPLY INC.

1804 West Lake Parker Drive   Lakeland, Florida 33805   (813) 683-4492, 683-4111
Toll Free Lines 1-800-328-8036 • In Florida 1-800-282-7321
FAX No. (813) 683-2886

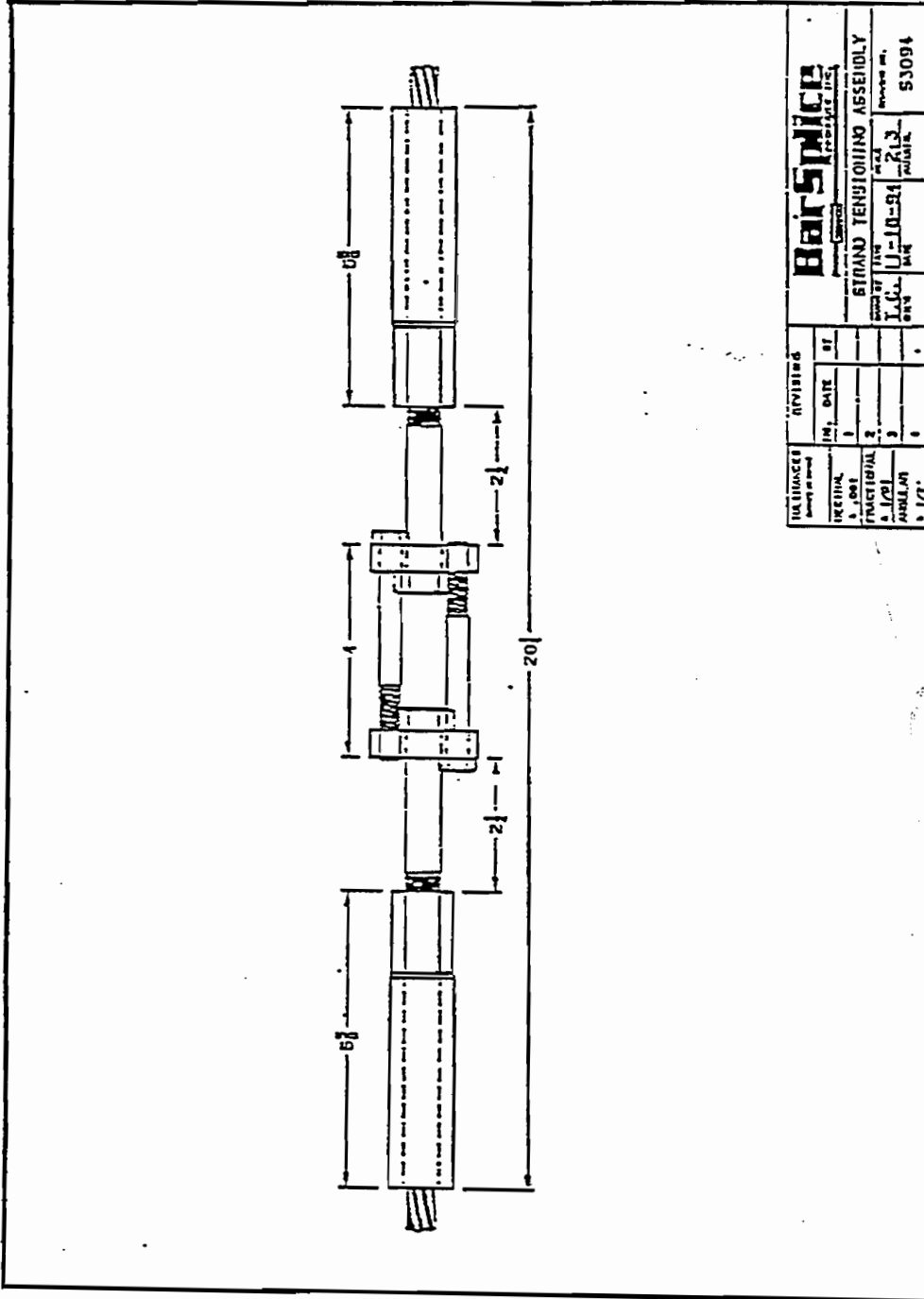*Figure A-1   Manufacturer information on Grab-It^{TM} cable splice*

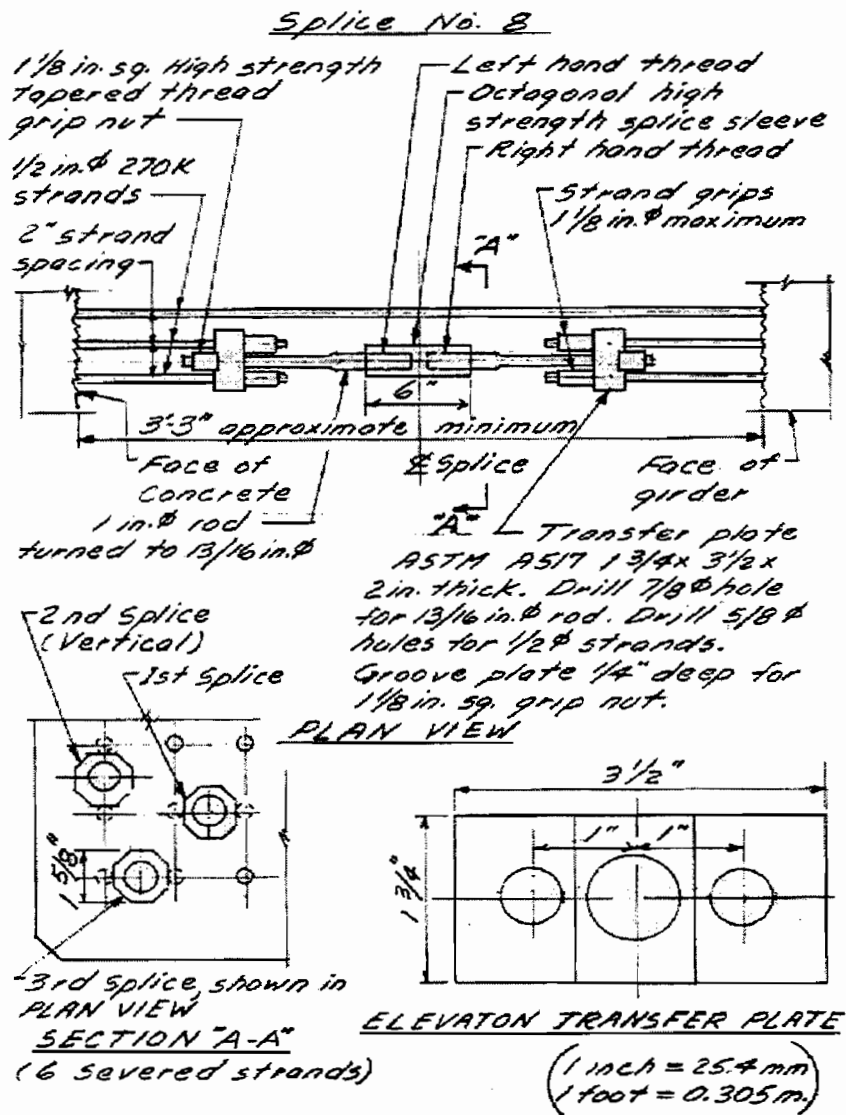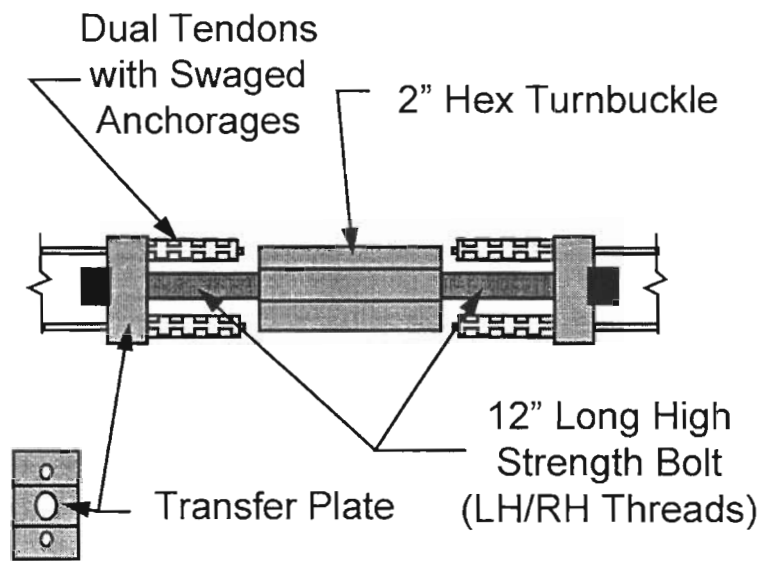Figure A-2   Detail of multi-bolt swaged splice (supplied by Bar-Splice Incorporated)

177

Splice No. 8

1 1/8 in. sq. High strength Tapered thread grip nut
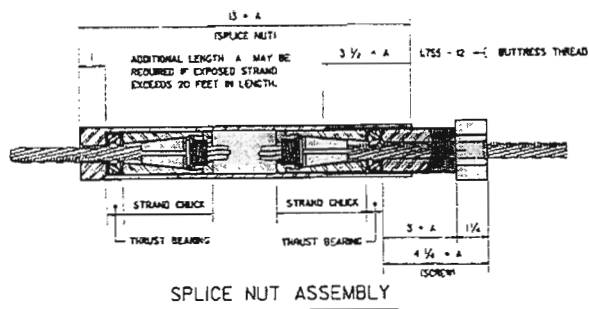
Left hand thread

Octagonal high strength splice sleeve

Right hand thread

1/2 in. ⌀ 270K strands

2" strand spacing

Strand grips 1 1/8 in. ⌀ maximum

"A"

3'-3" approximate minimum

6"

Face of Concrete

℄ Splice

Face of girder

1 in. ⌀ rod turned to 13/16 in. ⌀

"A"

Transfer plate ASTM A517 1 3/4 x 3 1/2 x 2 in. thick. Drill 7/8 ⌀ hole for 13/16 in. ⌀ rod. Drill 5/8 ⌀ holes for 1/2 ⌀ strands. Groove plate 1/4" deep for 1 1/8 in. sq. grip nut.

PLAN VIEW

2nd Splice (Vertical)

1st Splice

5/8"

3rd Splice, shown in PLAN VIEW

SECTION "A-A"
(6 severed strands)

3 1/2"

1" 1"

1 3/4"

ELEVATON TRANSFER PLATE

(1 inch = 25.4 mm
1 foot = 0.305 m.)

Figure A-3   Detailed drawing of dual strand splice taken from Reference 27

178

Dual Tendons with Swaged Anchorages

2" Hex Turnbuckle

12" Long High Strength Bolt (LH/RH Threads)

Transfer Plate

The modifications made to the dual strand splice design from Project 12-21consisted of using swaged anchorages and prefabricated 12 inch long high strength bolts, rather than standard wedge anchorages and a machined down threaded rod. The transfer plate was not modified.

Figure A- 4   *Schematic of modified dual strand splice using swaged anchorages and 2-in. diameter high strength bolts*

Figure A- 5   Schematic of Alberta Transportation Utilities Department strand splice sleeve

APPENDIX B

BRIDGE STRUCTURE DETAILS

Figure B- 1   Plan View of Mopac Structure over Steck Avenue in Austin, Texas

Existing ballast to be removed and falsework constructed beneath the cross ties in such a fashion to provide for continued use of the track during construction. This work will be performed by others and will not be a part of this contract.
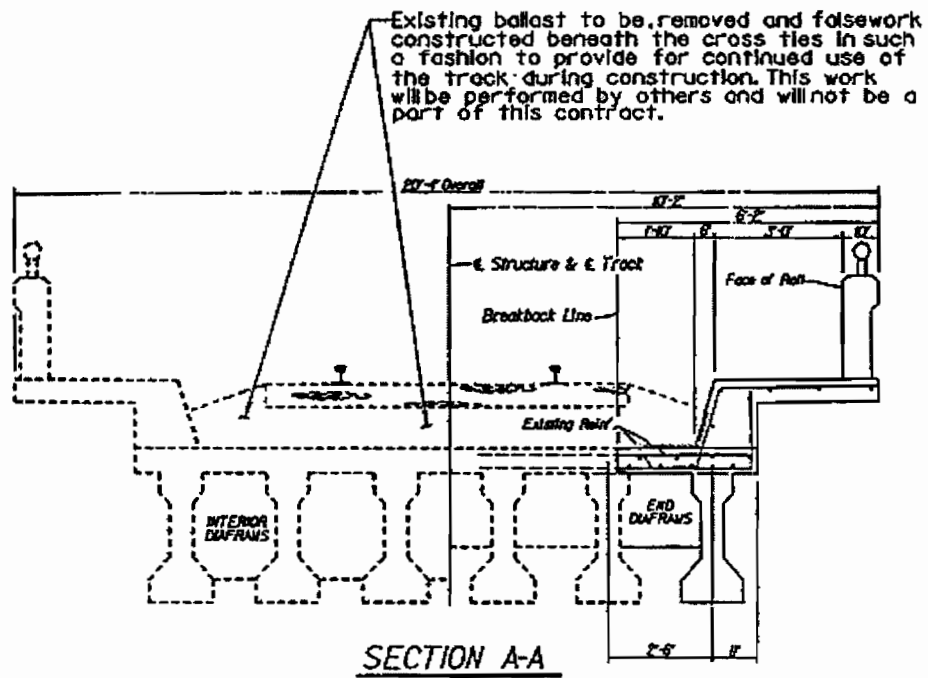
SECTION A-A

Figure B- 2   Cross Section of Mopac Bridge Superstructure

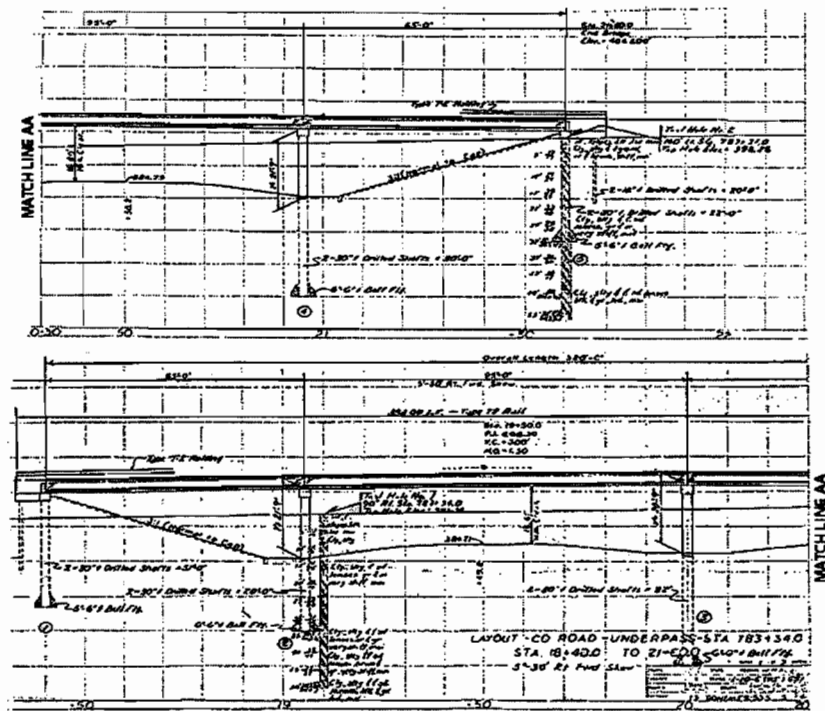*Figure B- 3   Elevation of Bridge Structure over Interstate 10 at Waelder,*
Texas

184

Figure B- 4   Plan View of Waelder Bridge Superstructure

PLAN ~ 65'-0" & 95'-0" SPANS

Figure B- 5   Transverse Section of Waelder Bridge

186

3' - 8"

e = 20.13"

5 sp. @ 2" = 10"

e = 10.92"

Midspan Section   **Endspan Section**

26 - 1/2 " - 270 ksi Strands @ 28.91 kips each

Figure B- 6   Strand Arrangement for Waelder Bridge Girders

187

REFERENCES

1. ACI Committee 201, "Guide for Making a Condition Survey of Concrete in Service," ACI Report No. 201.1R-92, American Concrete Institute, Detroit, 1992.

2. ACI Committee 546, "Guide for Repair of Concrete Bridge Superstructures," ACI 546.1R-80 (88), American Concrete Institute, Detroit, 1988.

3. ACI Committee 548, "Guide for the Use of Polymers in Concrete," ACI 548, 1R-92, American Concrete Institute, Detroit, 1992.

4. Amon, J.A., Snell, L.M., "The Use of Pulse Velocity Techniques to Monitor and Evaluate Epoxy Grout Repair to Concrete," Concrete International, December 1979, pp. 41-44.

5. ASTM, Standardization Basics, Philadelphia: American Society of Testing of Materials.

6. ATU, Restressing Broken Strand, Alberta Transportation and Utilities Department, unpublished.

7. Bay, J.A., Stokoe, K.H., II, "Field Determination of Stiffness and Integrity of PCC Slabs Using the SASW Method," *Conference on Nondestructive Evaluation of Civil Structures and Materials Proceedings*, University of Colorado at Boulder, 1990, p. 75.

8. Bullock, R.E., "Factors Influencing Concrete Repair Materials," Concrete International, September 1980, pp. 67-68.

9. Civjan, S.A., "Method to Evaluate Remaining Prestress in Damaged Prestressed Bridge Girders," Thesis, The University of Texas at Austin, May 1995.

10. Czarnecki, Lech, "The Status of Polymer Concrete," Concrete International, July 1985, pp. 47-53.

11. "Diagnosis and Assessment of Concrete Structures, State of the Art Report," Comite Euro-International Du Beton, Bulletin D;Information No. 192, January 1989.

12. Feldman, L.R., "Current Practice in the Repair of Impact-Damaged Prestressed Bridge Girders," Thesis, The University of Texas at Austin, December 1993.

13. Kalinski, M.E., Stokoe, K.H., II, Jirsa, J.O., Roesset, J.M., "Nondestructive Identification of Internally Damaged Areas of a Concrete Beam Using the SASW Method," *Proceedings of the 1994 Annual Meeting of the Transportation Research Board*, Washington, D.C.

14. Kuhlman, L.A., "Latex Modified Concrete for the Repair and Rehabilitation of Bridges," *The International Journal of Cement Composites and Lightweight Concrete*, Vol. 7, No. 4, November 1985, pp. 241-246.

15. Kuhlman, L.A., "Styrene Butadiene Latex Modified Concrete: The Ideal Repair Material?" Concrete International, October 1990, pp. 59-65.

16. Lichtenstein, A.G., "Bridge Rating Through Nondestructive Load Testing," National Cooperative Highway Research Program, Washington, D.C., National Research Council, June 1993.

17. "Manual for Railway Engineering," American Railway Engineering Association, Washington, D.C., 1991.

18. "Manual for the Condition Evaluation of Bridges," American Association of State Highway and Transportation Officials, 1994.

19. McGovern, Martin S., "Cementitious Patching Materials," Concrete Repair Digest, October/November 1991, pp. 139-142.

20. Moses, F., and Verma D., "Load Capacity Evaluation of Existing Bridges," National Cooperative Highway Research Program Report 301, Washington, D.C., National Research Council, November 1980, December 1987.

21. Olsen, L.D., and Wright, C.C., "Nondestructive Testing for Repair and Rehabilitation," ACI SCM-27 (93), pp. 50-56, American Concrete Institute, Detroit, 1993.

22. Olsen, S.A., French, C.W., and Leon, R.T., "Reusability and Impact Damage Repair of Twenty-Year-Old AASHTO Type III Girders," University of Minnesota Research Report No. 93-04, May 1992.

23. Rizzo, E.M., and Sobelman, M.B., "Selection Criteria for Concrete Repair Materials," Concrete International, September 1989, pp. 46-49.

24. Sansalone, M., and Carino, N.J., "Impact Echo: A Method for Flaw Detection in Concrete Using Transient Stress Waves," National Bureau of Standards, NBSIR No. 86-3452, September 1986.

25. Sansalone, M., and Pratt, D.G., "Theory and Operation Manual for the Impact-Echo Field System," Cornell University Structural Engineering Report No. 92-2, Volume 1, January 1993.

26. Shanafelt, G.O., and Horn, W.B., "Damage Evaluation and Repair Methods for Prestressed Concrete Bridge Members," National Cooperative Highway Research Program Report 226, Washington, D.C., National Research Council, November 1980.

27. Shanafelt, G.O., and Horn, W.B., "Damage Evaluation and Repair Methods for Prestressed Concrete Bridge Members," National Cooperative Highway Research Program Report 280, Washington, D.C., National Research Council, December 1995.

28. Specifications for Highway Bridges, American Association of State Highway and Transportation Officials, 1994.

29. Tracy, R.G., and Fling, R.S., "Rehabilitation Strategies," Concrete International, September 1989, pp. 41-45.

30. Unknown, "Epoxies for Concrete Repair and Restoration," Anon., Concrete Construction, March 1979, pp. 169-174.

31. Unknown, "Latex Modified Concrete and Mortar for Repair," Concrete Construction, Vol. 29, No. 10, October 1984.

32. Unknown, "Patching Concrete with Rapid-Setting Materials: A Guide to Their Choice and Use," Concrete Construction, Vol. 29, No. 3, March 1979, pp. 177-180.

33. Unknown, 'Repair Techniques and Materials: A Guide to the Selection of the Right Methods and Materials for the Job," Concrete Construction, Vol. 26, No. 1, January 1981, pp. 31-47.

34. Walters, G.D., "Latex Hydraulic Cement Additives," Session 195, Transportation Research Board, Washington, D.C., January 1988.

35. Walters, G.D., "What are Latexes?" <u>Concrete International</u>, December 1987, pp. 44-47.

36. Warner, J., "Selecting Repair Materials: Some Important Material Properties that Should be Considered," <u>Concrete Construction</u>, Vol. 29, No. 10, October 1984, pp. 865-871.